THE REPUBLIC OF TURKEY
MUĞLA SITKI KOÇMAN UNIVERSITY
GRADUATE SCHOOL OF NATURAL AND APPLIED SCIENCES

DEPARTMENT OF GEOLOGICAL ENGINEERING

DEVELOPMENT OF A LOCAL GROUNDWATER FLOW MODEL FOR THE LİWA AQUIFER (SCHEME A), UAE

MASTER THESIS

GONCA AVŞAR

SEPTEMBER 2017
MUĞLA

G. AVŞAR DEPARTMENT OF GEOLOGICAL ENGINEERING MASTER THESIS MUĞLA 2017

THE REPUBLIC OF TURKEY
MUĞLA SITKI KOÇMAN UNIVERSITY
GRADUATE SCHOOL OF NATURAL AND APPLIED SCIENCES

DEPARTMENT OF GEOLOGICAL ENGINEERING

DEVELOPMENT OF A LOCAL GROUNDWATER FLOW MODEL FOR THE LİWA AQUIFER (SCHEME A), UAE

MASTER THESIS

GONCA AVŞAR

SEPTEMBER 2017
MUĞLA

MUGLA SITKI KOCMAN UNIVERSITY

Graduate School of Natural and Applied Sciences

THESIS CONFIRMATION

The thesis, prepared by **GONCA AVŞAR,** titled as **"DEVELOPMENT OF A LOCAL GROUNDWATER FLOW MODEL FOR THE LİWA AQUIFER (SCHEME A), UAE"** has been accepted unanimously/majority by the jury listed below that fulfils the necessary conditions for master degree of Department of Geological Engineering at 20/09/2017.

THESIS DEFENCE JURY

Prof. Dr. Moumtaz RAZACK **(Head of Jury)**
Department of Geosciences,
University of Poitiers, Poitiers, France
Signature:

Asst. Prof. Dr. Bedri KURTULUŞ **(Supervisor)**
Department of Geological Engineering,
Mugla Sitki Kocman University, Muğla
Signature:

Asst. Prof. Dr. Özgür AVŞAR **(Member)**
Department of Geological Engineering,
Mugla Sitki Kocman University, Muğla
Signature:

Asst. Prof. Dr. Gilles POREL **(Member)**
Department of Geosciences,
University of Poitiers, Poitiers, France
Signature:

Asst. Prof. Dr. Jacques BODIN **(Member)**
Department of Geosciences,
University of Poitiers, Poitiers, France
Signature:

Asst. Prof. Dr. Aude NAVEAU **(Member)**
Department of Geosciences,
University of Poitiers, Poitiers, France
Signature:

Asst. Prof. Dr. Mustafa Can Canoğlu **(Member)**
Department of Environmental Engineering
Sinop University, Sinop
Signature:

Date of Defence: 20/09/2017

MUGLA SITKI KOCMAN UNIVERSITY

Graduate School of Natural and Applied Sciences

THESIS CONFIRMATION

The thesis, prepared by **GONCA AVŞAR,** titled as **"DEVELOPMENT OF A LOCAL GROUNDWATER FLOW MODEL FOR THE LİWA AQUIFER (SCHEME A), UAE"** has been accepted unanimously/majority by the jury listed below that fulfils the necessary conditions for master degree of Department of Geological Engineering at 20/09/2017.

DEPARTMENT CONFIRMATION

Asst. Prof. Dr. Bedri KURTULUŞ

Head of Department of Geological Engineering,
Mugla Sitki Kocman University, Muğla

Signature:

Asst. Prof. Dr. Bedri KURTULUŞ

Supervisor, Department of Geological Engineering,
Mugla Sitki Kocman University, Muğla

Signature:

Date of Defence: 20/09/2017

I hereby declare that all information in this document has been obtained and presented in accordance with academic rules and ethical conduct. I also declare that, as required by these rules and conduct, I have fully cited and referenced all material and results that are not original to this work.

Gonca Avşar

20/09/2017

(imza)

ÖZET

LİWA AKİFERİ'NİN BÖLGESEL YERALTI SUYU AKIŞ MODELİNİN GELİŞTİRİLMESİ (ŞEMA A), BAE

Gonca AVŞAR

Yüksek Lisans Tezi

Fen Bilimleri Enstitüsü

Jeoloji Mühendisliği Bölümü

Danışman: Yrd. Doç. Dr. Bedri KURTULUŞ

Eylül 2017, 67 sayfa

Tatlı su kurak ortamlarda sınırlı yağış ve sıcak iklim nedeniyle değerli bir kaynaktır. Arap Yarımadası'nda bulunan Birleşik Arap Emirlikleri (BAE) kurak bir iklime sahiptir ve su kaynakları sınırlıdır. Bu bölgede ana su kaynağı yeraltı sularıdır. Bununla birlikte son yıllardaki nüfus, tarım ve endüstriyel faaliyetlerdeki artış su talebinin artmasına neden olmuştur. Bu artan su talebini karşılamak adına, özellikle güvenli içme suyu için, BAE deniz suyunu, çoğunlukla Abu Dabi kıyılarında, tatlı suya dönüştüren deniz suyu arıtma tesisleri kurdu. Bu arıtma tesisleriyle büyük ölçülerde tatlı su üretimi gerçekleştirilmesine rağmen depolama olanaklarının acil durumlar için yetersiz kaldığı sonucuna varılmıştır. Bu sebeple, tatlı su depolamak üzere güvenilir bir yeraltı rezervuarı oluşturmak için Liwa Akiferi Depolama ve İyileştirme (ADİ) Projesi, 2008 yılında Abu Dhabi'nin Liwa bölgesinde geliştirildi. Bu proje kapsamında Liwa Vahası'nın kuzeyinde birçok pompalama ve gözlem kuyusu inşa edildi. Proje boyunca birçok pompa testi yapıldı. Bu testlerden elde edilen verilerle, Liwa Akiferi'nin hidrolik özelliklerini belirlemek adına birçok analiz ve çalışma gerçekleştirildi. Bu tezin amacı, hidrolik özelliklerin tahmin edilmesi için bu proje kapsamındaki A Şeması'ndaki pompalama testlerinden elde edilen verileri kullanarak Liwa Akiferi'nin 2 boyutlu geçici bir yeraltı suyu akışı modelini geliştirmektir.

Anahtar Kelimeler: Yeraltı Suyu Akış Modeli, Liwa Akiferi, Liwa ADİ Projesi, MODFLOW

ABSTRACT

DEVELOPMENT OF A LOCAL GROUNDWATER FLOW MODEL FOR THE LİWA AQUIFER (SCHEME A), UAE

Gonca AVŞAR

Master of Science (M.Sc.)

Graduate School of Natural and Applied Sciences

Department of Geological Engineering

Supervisor: Asst. Prof. Dr. Bedri KURTULUŞ

September 2017, 67 pages

In arid environments, fresh water is a precious resource because of the limited rainfall and hot climate. The United Arab Emirates (UAE) has an arid environment, and so suffers from a lack of water sources on the Arabian Peninsula. The main source of water in the UAE is groundwater. However, an increase in population, agriculture and industrial activities in recent years has resulted in an increasing demand for water. In order to meet this increased demand for water, especially for safe drinking water, the UAE has constructed several desalination plants to convert seawater into fresh water, mostly along the coast of Abu Dhabi. Despite the huge volume of fresh water which can be produced by these plants, storage facilities would be inadequate in an emergency situation. Thus, the Liwa Aquifer Storage and Recovery (ASR) Project was developed in order to establish a reliable underground reservoir to store and recharge fresh water in the Liwa area, Abu Dhabi in 2008. Within the scope of the project, several pumping and observation wells were constructed in the North of the Liwa Oasis. During the project, pumping tests were conducted and many analysis and studies were performed in order to determine the hydraulic characteristics of the Liwa aquifer. The purpose of the current study is to develop a 2-D transient groundwater flow model of the Liwa Aquifer using data obtained from pumping tests in Scheme A to predict hydraulic properties with code MODFLOW in Groundwater Vistas.

Keywords: Groundwater Flow Model, Liwa Aquifer, Liwa ASR Project, MODFLOW

To the memory of my father

ACKNOWLEDGEMENT

I want to express, first and foremost, the deepest appreciation to my supervisor, Asst. Prof. Dr. Bedri KURTULUŞ for providing me with the opportunity to conduct this thesis.

I would like to express my special thanks to Nesrin TÜFEKÇİ AVŞAR for her guidance.

I am also thankful to Asst. Prof. Dr. Jacques BODIN, who generously shared his professional experience, for his precious support.

I would like to express my thanks to Prof. Dr. Moumtaz RAZACK for his guidance.

I am deeply grateful to my beloved mother and brothers for their endless support, encourage and patience not only during my master degree but in every aspect of my life.

I would like to thank my friends Çağrı Alperen İNAN and Halil İbrahim GÜLŞEN for their support during my master degree.

TABLE OF CONTENT

ACKNOWLEDGEMENT ..... **vii**
TABLE OF CONTENT ..... **viii**
LIST OF TABLES ..... **x**
LIST OF FIGURES ..... **xi**
1. INTRODUCTION **1**
2. STUDY AREA **2**
2.1. Geography 2
2.2. Climatology 3
2.3. Geology 4
2.4. Water resources 6
2.4.1. Surface water 6
2.4.2. Groundwater 6
2.4.2.1. *Groundwater salinity* 7
2.4.3. Desalinated water 8
2.4.4. Treated wastewater 8
2.5. Hydrogeology 9
2.5.1. Aquifer types 10
3. LIWA AQUIFER STORAGE AND RECOVERY PROJECT (ASR) **12**
4. METHODS **14**
4.1. Data Analysis 14
4.1.1. Static groundwater levels 14
4.1.2. Pumping tests 16
4.2. Modelling 23
4.2.1. Grid design, initial and boundary conditions 23
4.2.2. Targets and stress periods 24
4.2.3. Parameter estimation 27
5. RESULTS **28**
6. DISCUSSION **34**
7. CONCLUSION **36**

REFERENCES **38**
APPENDICES **40**
Appendix A. Observation Wells of RW078 40
Appendix B. Observation Wells of RW103 47
Appendix C. Observation Wells of RW008 54
Appendix D. Observation Wells of RW033 58
CURRICULUM VITAE **66**

LIST OF TABLES

Table 2.1. Groundwater classification schemes used in the Abu Dhabi Emirate (Brook et al, 2006). 7
Table 4.1. Pumping and observation wells used in the transient groundwater flow model. 16
Table 4.2. Start-finish dates and times of the phases. 18
Table 4.3. Total number of observation times in the model. 24
Table 4.4. Stress periods of each pumping well. 26
Table 5.1. Statistics of the model calibration. 29
Table 5.2. Horizontal hydraulic conductivity (K_x) estimations in the locations where targets are located in the model and estimations obtained from project reports. 32
Table 5.3. Specific yield (S_y) estimations in the locations where targets are located in the model and estimations obtained from project reports. 33

LIST OF FIGURES

Figure 2.1. Location map of the study area. (Yellow lines represent the country boundaries.) 2
Figure 2.2. Emirates of the UAE and location of the project area. Scheme A, B and C represents well sites of the project. 3
Figure 2.3. Composite log belonging to the well located in the center of the scheme A (Zetaş/GIZ Report, 2015). 5
Figure 2.4. Percentages of water resources in the Abu Dhabi Emirate in 2012 (International Water Management Institute (IWMI), 2016). 7
Figure 2.5. Groundwater salinity in the shallow aquifers in the Abu Dhabi Emirate .. 8
Figure 2.6. Hydraulic head map and flow directions in the UAE (Rizk and Alsharhan, 2003). 9
Figure 2.7. Recharge and discharge areas in the Abu Dhabi Emirate (Elmahdy and Mohamed, 2015). 10
Figure 2.8. Main aquifers in the United Arab Emirates (Al Hammadi, 2003). 11
Figure 3.1. Scheme A, B and C each constituting 105 wells. 13
Figure 4.1. Contour map of static groundwater levels which were measured from 31 observation wells in Scheme A during December in 2013. 15
Figure 4.2. Contour map of static groundwater levels which were measured from 11 observation wells in Scheme A during October in 2013. 15
Figure 4.3. Pumping rates during SDT and CDT phases. 18
Figure 4.4. Locations of the pumping well RW078 and its observation wells (Zetaş/GIZ Reports, 2015). 19
Figure 4.5. Drawdowns measured in the observation wells of the pumping well RW078 with time during the phases. 19
Figure 4.6. Locations of the pumping well RW103 and its observation wells (Zetaş/GIZ Reports, 2015). 20
Figure 4.7. Drawdowns measured in the observation wells of the pumping well RW103 with time during the phases. 20

Figure 4.8. Locations of the pumping well RW008 and its observation wells (Zetaş/GIZ Reports, 2015). 21
Figure 4.9. Drawdowns measured in the observation wells of the pumping well RW008 with time during the phases. 21
Figure 4.10. Locations of the pumping well RW033 and its observation wells (Zetaş/GIZ Reports, 2015). 22
Figure 4.11. Drawdowns measured in the observation wells of the pumping well RW033 with time during the phases. 22
Figure 4.12. Grid design, boundary conditions and locations of 4 pumping wells. Blue columns at the north and south represent the constant head boundaries. 24
Figure 4.13. Pumping wells (RW078, RW103, RW008 and RW033) and their observation wells as targets. 25
Figure 4.14. Locations of pilot points. 27
Figure 5.1. Calibration plot representing observed and computed drawdown values. 28
Figure 5.2. Observed vs Computed drawdown plot from one of the 49 observations well data. This observation well belongs to the first pumping period when RW078 is pumped. Each green rectangle in the plot indicates the pumping wells. 29
Figure 5.3. Drawdown contours after the calibration. 30
Figure 5.4. Horizontal hydraulic conductivity (m/h) distribution after the calibration. 31
Figure 5.5. Comparison of K_x estimations obtained from the model and the project reports. 32
Figure 5.6. Comparison of S_y estimations obtained from the model and the project reports. 33
Figure A.1. Observed vs Computed drawdown plot of RW101. 40
Figure A.2. Observed vs Computed drawdown plot of RW088. 40
Figure A.3. Observed vs Computed drawdown plot of RW079. 41
Figure A.4. Observed vs Computed drawdown plot of RW087. 41
Figure A.5. Observed vs Computed drawdown plot of RW066. 42
Figure A.6. Observed vs Computed drawdown plot of RW051. 42
Figure A.7. Observed vs Computed drawdown plot of RW036. 43

Figure A.8. Observed vs Computed drawdown plot of RW095. 43
Figure A.9. Observed vs Computed drawdown plot of RW035. 44
Figure A.10. Observed vs Computed drawdown plot of RW077. 44
Figure A.11. Observed vs Computed drawdown plot of RW006. 45
Figure A.12. Observed vs Computed drawdown plot of RW003. 45
Figure A.13. Observed vs Computed drawdown plot of RW012. 46
Figure B.1. Observed vs Computed drawdown plot of RW089. 47
Figure B.2. Observed vs Computed drawdown plot of RW080. 47
Figure B.3. Observed vs Computed drawdown plot of RW090. 48
Figure B.4. Observed vs Computed drawdown plot of RW081. 48
Figure B.5. Observed vs Computed drawdown plot of RW068. 49
Figure B.6. Observed vs Computed drawdown plot of RW069. 49
Figure B.7. Observed vs Computed drawdown plot of RW096. 50
Figure B.8. Observed vs Computed drawdown plot of RW097. 50
Figure B.9. Observed vs Computed drawdown plot of RW070. 51
Figure B.10. Observed vs Computed drawdown plot of RW056. 51
Figure B.11. Observed vs Computed drawdown plot of RW095. 52
Figure B.12. Observed vs Computed drawdown plot of RW071. 52
Figure B.13. Observed vs Computed drawdown plot of RW094. 53
Figure C.1. Observed vs Computed drawdown plot of RW022. 54
Figure C.2. Observed vs Computed drawdown plot of RW023. 54
Figure C.3. Observed vs Computed drawdown plot of RW038. 55
Figure C.4. Observed vs Computed drawdown plot of RW054. 55
Figure C.5. Observed vs Computed drawdown plot of RW007. 56
Figure C.6. Observed vs Computed drawdown plot of RW009. 56
Figure C.7. Observed vs Computed drawdown plot of RW024. 57
Figure C.8. Observed vs Computed drawdown plot of RW081. 57
Figure D.1. Observed vs Computed drawdown plot of RW064. 58
Figure D.2. Observed vs Computed drawdown plot of RW049. 58
Figure D.3. Observed vs Computed drawdown plot of RW019. 59
Figure D.4. Observed vs Computed drawdown plot of RW063. 59
Figure D.5. Observed vs Computed drawdown plot of RW018. 60

Figure D.6. Observed vs Computed drawdown plot of RW002. 60
Figure D.7. Observed vs Computed drawdown plot of RW048. 61
Figure D.8. Observed vs Computed drawdown plot of RW001. 61
Figure D.9. Observed vs Computed drawdown plot of RW077. 62
Figure D.10. Observed vs Computed drawdown plot of RW015. 62
Figure D.11. Observed vs Computed drawdown plot of RW016. 63
Figure D.12. Observed vs Computed drawdown plot of RW030. 63
Figure D.13. Observed vs Computed drawdown plot of RW044. 64
Figure D.14. Observed vs Computed drawdown plot of RW074. 64
Figure D.15. Observed vs Computed drawdown plot of RW024. 65

1. INTRODUCTION

The aim of this study is to estimate hydraulic characteristics of the Liwa Aquifer such as horizontal hydraulic conductivity and specific yield by constructing a 2-D transient groundwater flow model using MODFLOW in Groundwater Vistas. In this study, the data, which was used in the transient groundwater flow model, was obtained from the Liwa Aquifer Storage and Recovery (ASR) Project. Drawdown measurements from observation wells during the pumping periods were used in order to calibrate the model.

In this report, firstly, geographical, climatological, geological, hydrogeological characteristics and water resources of the study area are mentioned. Afterwards, the Liwa (ASR) Project, methods used in the study, the model and the results are covered. At the end, results are evaluated and discussed in order to understand how the model is realistic and what can be done to develop it. Furthermore, hydraulic conductivity and specific yield results obtained from the model are compared with the results obtained from the reports of the project.

2. STUDY AREA

2.1.Geography

The United Arab Emirates (UAE) is located in the southeastern part of the Arabian Peninsula. It is bordered by Oman to the east, the Kingdom of Saudi Arabia to the South and West, and the Persian Gulf to the North. In the east, the Al-Hajar Mountains fall within the borders of Dubai Emirate in the north and in Oman. It is the highest mountain range in the Eastern Arabian Peninsula. The Liwa area is situated in the Emirate of Abu Dhabi covering about 80% of the total area of the UAE. It is a part of Rub 'al Khali Desert and about 145 km southwest of the city of Abu Dhabi (Figure 2.1).

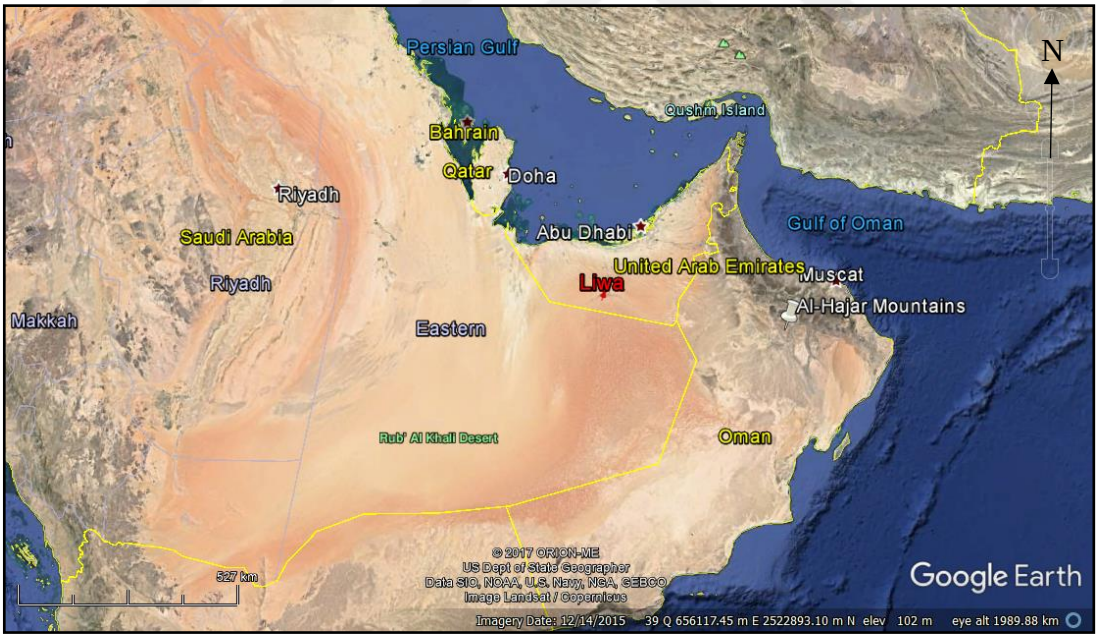

Figure 2.1. Location map of the study area. (Yellow lines represent the country boundaries.)

Liwa has a crescent-shaped oasis, which is an isolated area of vegetation in a desert. It stretches about 110 km in an east-westerly direction. Several villages and agricultural

areas exist throughout the oasis. The project area with Scheme A, B and C, where all tests were conducted, is located to the North of the Liwa Oasis. In this study, Scheme A was the focus and only the data obtained from Scheme A was used for the groundwater flow modeling. The center of Scheme A is represented by a red point, whose coordinates are 763204.31 E and 2580103.04 N (Figure 2.2).

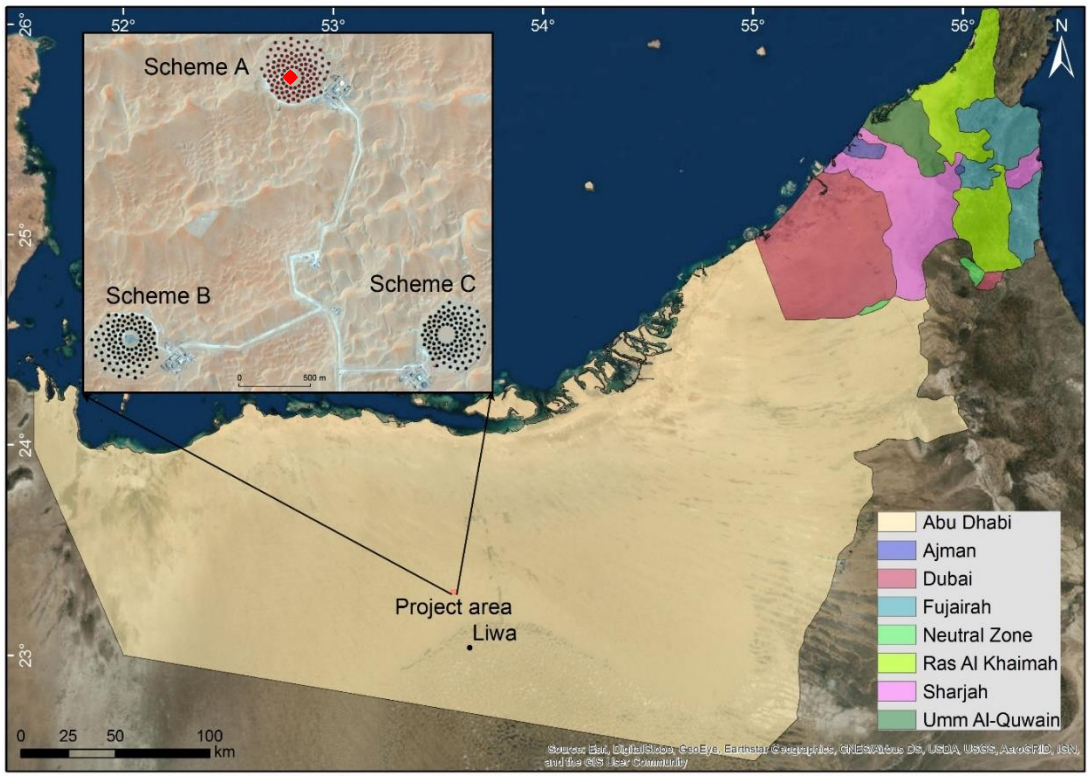

Figure 2.2. Emirates of the UAE and location of the project area. Scheme A, B and C represents well sites of the project.

2.2.Climatology

The Emirate of Abu Dhabi has an arid and hot climate, with less than 100 mm/year average rainfall and a very high rate of evaporation (2-3 m/year) (Brook et al., 2006). Most of the rainfall occurs during winter between October and March. Besides, the spatial and temporal distribution of the rainfall is highly variable. For instance, in 2003, the mean rainfall per month was about 2.9 mm in January, 0.2 mm in February,

3.9 mm in March, and 44.7 mm in April, while there was no precipitation in the remaining months (Al-Katheeri et al., 2009). It can be said that heavy and short rainfalls provide the best opportunities for aquifer recharge.

2.3.Geology

In the Abu Dhabi, desert environment is dominant. The coastal region consists of tidal flats and sabkha deposits. Towards the inland area, most of the Emirate is covered by aeolian sand dunes, which have resulted from wind patterns in the desert (Symonds et al, 2005). Large barchan sand dunes, especially, are characteristic structures in the South of the Liwa Oasis. Interdunal sabkha deposits can also be observed in this area.

The Liwa area/aquifer has two main stratigraphic units which are Tertiary (older) and Quaternary (younger) units. The Tertiary unit (a thickness of over 350 m) is composed of mudstones, evaporites and clastics of Miocene age, whereas the Quaternary unit (a thickness between 100 and 150 m) consists of fine to medium sands and interdunal sandstone deposits (Al-Katheeri et al., 2009).

In addition, according to the well composite logs obtained from the ASR project area in Liwa, there are three main lithological units. Sand unit at the top, sandstone deposites (with intercalation of siltstone, mudstone, marl, thin sand lenses) and carbonates-evaporites at the bottom of the site, observed through the vertical section (Figure 2.3).

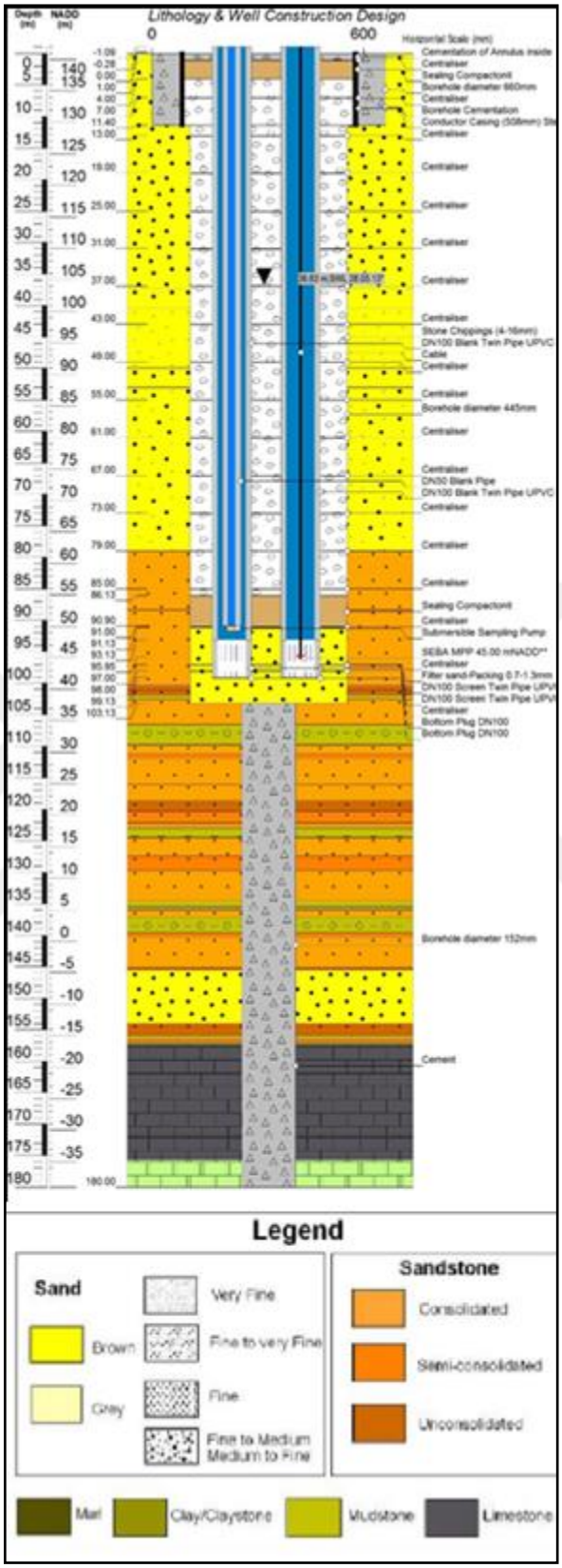

Figure 2.3. Composite log belonging to the well located in the center of the scheme A (Zetaş/GIZ Report, 2015).

2.4.Water resources

Water sources are deficient due to the arid and hot climate in the Emirate of Abu Dhabi. They can be classified into conventional and non-conventional sources. Conventional water sources are natural, depending on the amount of rainfall in the environment resulting in surface water and groundwater. However, non-conventional water sources are generated by human using technology. Desalinated water and treated wastewater are examples of the non-conventional water sources used in Abu Dhabi.

2.4.1. Surface water

Surface water is limited and temporary, because of low rainfall, high evaporation rates, the flat nature of the land and high porosity-permeability of dune-forming sands (Rizk and Alsharhan, 2003). Therefore, perennial rivers and lakes cannot be observed in the Emirate of Abu Dhabi. However, both onshore and offshore fresh water springs are found along the coastal belt of the Emirate (Brook and Dawoud, 2005).

2.4.2. Groundwater

Groundwater is the main water source in Abu Dhabi (Figure 2.4). Shallow sand aquifers are classified as renewable water sources, whereas deep aquifers are non-renewable (Al-Rashed and Sherif, 2000). Because of the increasing population, agricultural and industrial activities in recent years, water demand has increased and over pumping occurs.

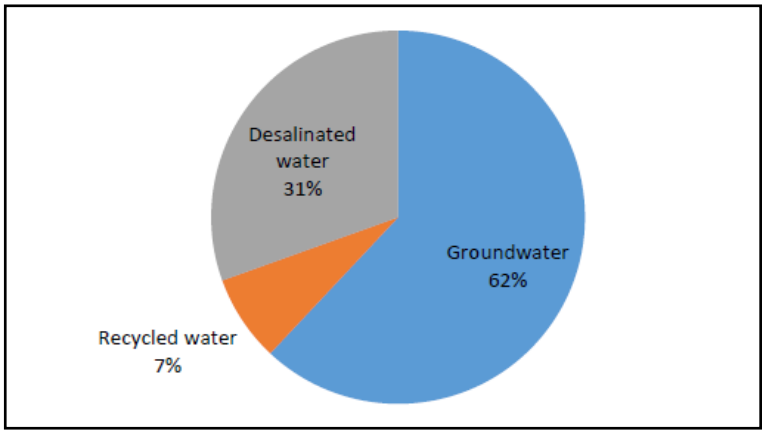

Figure 2.4. Percentages of water resources in the Abu Dhabi Emirate in 2012 (International Water Management Institute (IWMI), 2016).

2.4.2.1. Groundwater salinity

The salinity of the groundwater can be examined and classified using TDS (total dissolved solids) values (Table 2.1). In the Emirate of Abu Dhabi, high salinity can be observed throughout the coastal region because of salt-water intrusion from the sea and coastal sabkha deposits. Further inland, groundwater is becoming brackish and then fresh in the middle of the Emirate where the Liwa aquifer is located (Figure 2.5). Fresh water can be also observed in the north-east, near mountainous areas. However, south of the Liwa Oasis it is highly saline due to inland sabkha deposits.

Table 2.1. Groundwater classification schemes used in the Abu Dhabi Emirate (Brook et al, 2006).

Source	TDS Range (mg/l)	Classification
ERWDA (2003)	0-1500	Fresh
	1500-8000	Low Brackish
	8000-15000	High Brackish
	15000-35000	Saline
	>35000	Hypersaline
GTZ et al (2005)-German Standards	0-1500	Fresh
	1500-4000	Slightly Brackish
	4000-7000	Medium Brackish
	7000-10000	Strongly Brackish
	10000-25000	Sligthly Saline
	25000-50000	Medium Saline
	50000-100000	Strongly Saline
	>100000	Brine

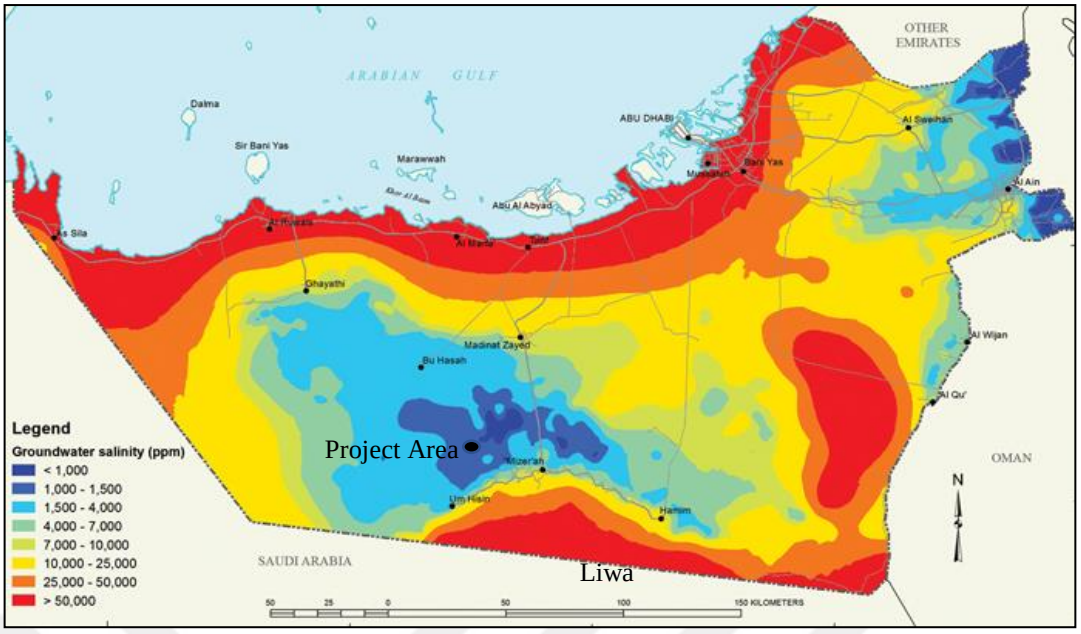

Figure 2.5. Groundwater salinity in the shallow aquifers in the Abu Dhabi Emirate

2.4.3. Desalinated water

As previously mentioned, water demand has been increasing in recent years. In order to meet this increased demand, especially for drinking water, the UAE has constructed several desalination plants, and has one of the most developed desalination production and distribution systems in the world. The first desalination plant was installed in Abu Dhabi in 1960 with a total capacity of 250 m^3/day (Brook et al, 2006).

2.4.4. Treated wastewater

As a substitute for fresh water in agriculture and industry, treated wastewater also has a significant role in water resource management. However, it is critical to make periodical analyses and field studies to promote the safe use of treated sewage water.

2.5. Hydrogeology

Heavy and short-term rainfalls over Al-Hajar Mountains, located in the east of the UAE, are the main groundwater source for the aquifers of the UAE. After rain falls over the mountains, water flows down through wadis, which are impermanent streams in the desert environments, and dry most of the time expect after rain. Water gathers in the piedmont plains, quickly infiltrates and recharges into the shallow alluvial gravel aquifers. Thereafter, groundwater flows from the east (Al-Hajar Mountains) towards the west, northwest and southwest (Figure 2.6 & 2.7).

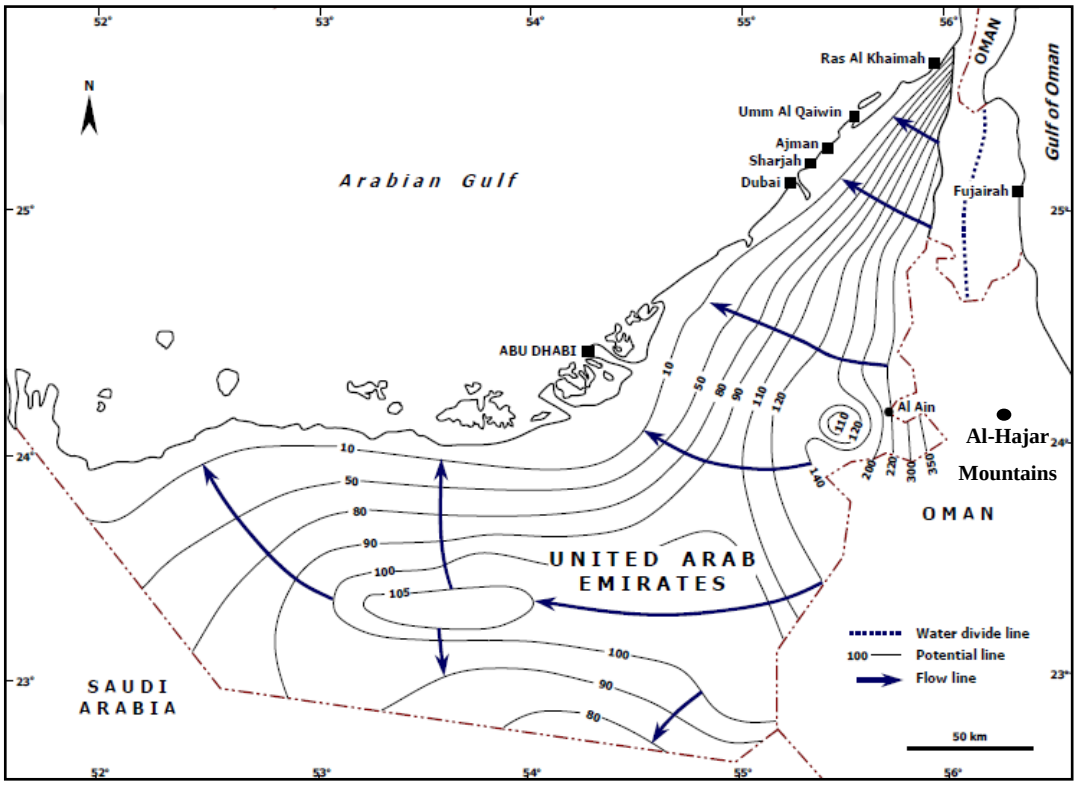

Figure 2.6. Hydraulic head map and flow directions in the UAE (Rizk and Alsharhan, 2003).

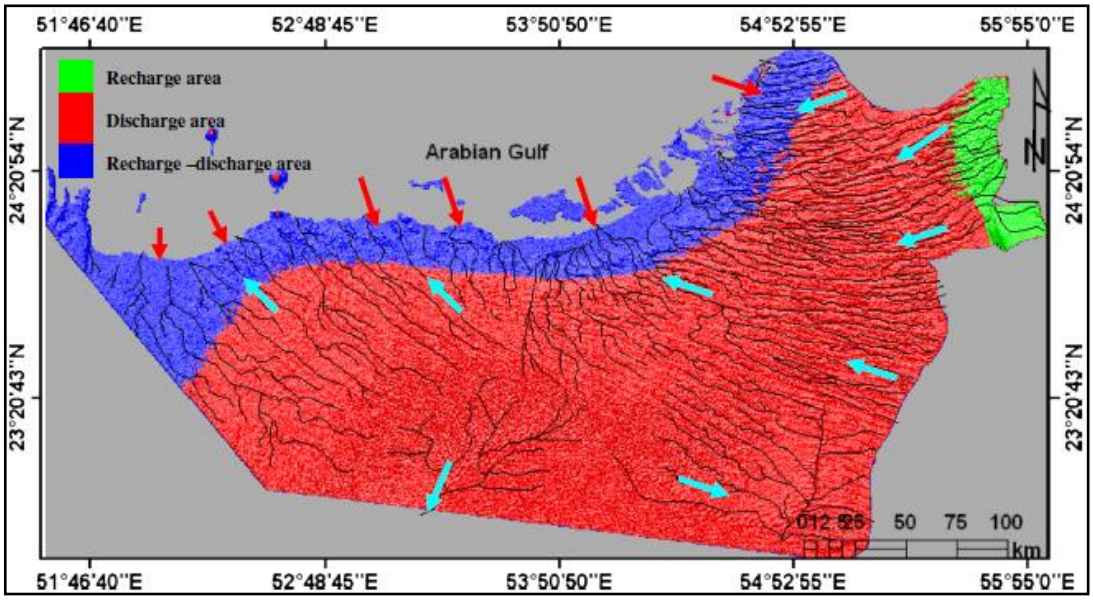

Figure 2.7. Recharge and discharge areas in the Abu Dhabi Emirate (Elmahdy and Mohamed, 2015).

2.5.1. Aquifer types

Different types of aquifers occur within the borders of the UAE (Figure 2.8). Sand dune aquifer in the middle, gravel aquifer located throughout the piedmont plains of Al-Hajar Mountains in the east, coastal sabkha aquifer which is uneconomic, and carbonate aquifer in the north-east are observed and classified as shallow and unconsolidated aquifers. Deep aquifers also occur throughout Abu Dhabi, and are largely carbonate deposits. However, shallow aquifers are more productive (Brook et al., 2006). Moreover, Brook and Dawoud (2005) categorize groundwater formations in the UAE into two types, which are the Tertiary sediments consisting of loosely cemented, calcareous sandstones, sandy limestone, silty chalk, and gypsum layers, and the Quaternary unconsolidated clastic sediments covering most of the country. Liwa aquifer is formed by sand dune deposits belonging to the Quaternary period.

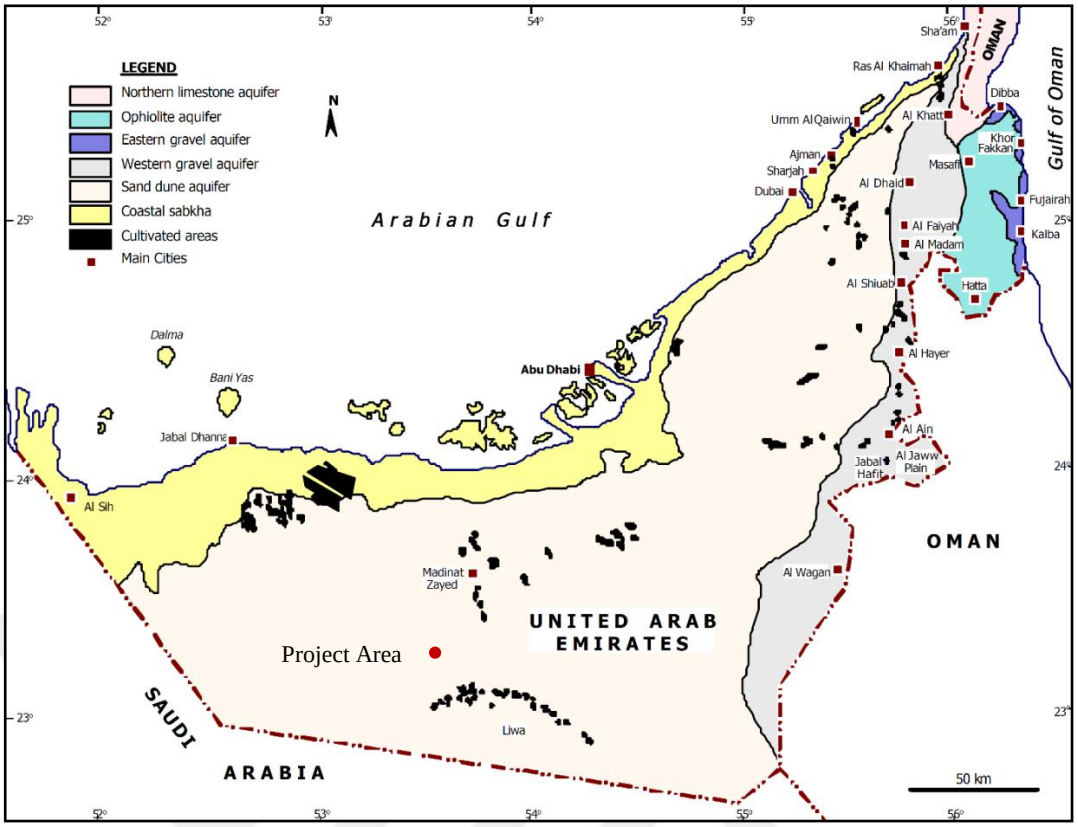

Figure 2.8. Main aquifers in the United Arab Emirates (Al Hammadi, 2003).

3. LIWA AQUIFER STORAGE AND RECOVERY PROJECT (ASR)

As mentioned previously, desalinated water makes up a significant percentage of available water in the arid environment of the UAE. Although there are plenty of desalination plants along the coast of the UAE, which produce huge volumes of drinking water, a secure water supply is not guaranteed due to a lack of storage facilities for the desalinated/fresh water in a case of emergency, and demand for drinking water can only be met for a short period. In this case, the UAE needs to increase the storage facilities for fresh water. Therefore, the Liwa ASR Project was developed in order to establish a reliable and sustainable underground reservoir to store and recharge fresh water in the Liwa area. The project was conducted between 2008 and 2015 with the consultants Zetaş-GIZ.

Within the scope of the project, 315 wells were constructed as 3 schemes: scheme A, B and C (Figure 3.1), in order to determine the hydraulic properties of the Liwa aquifer.

In this study, only data belonging to Scheme A was used.

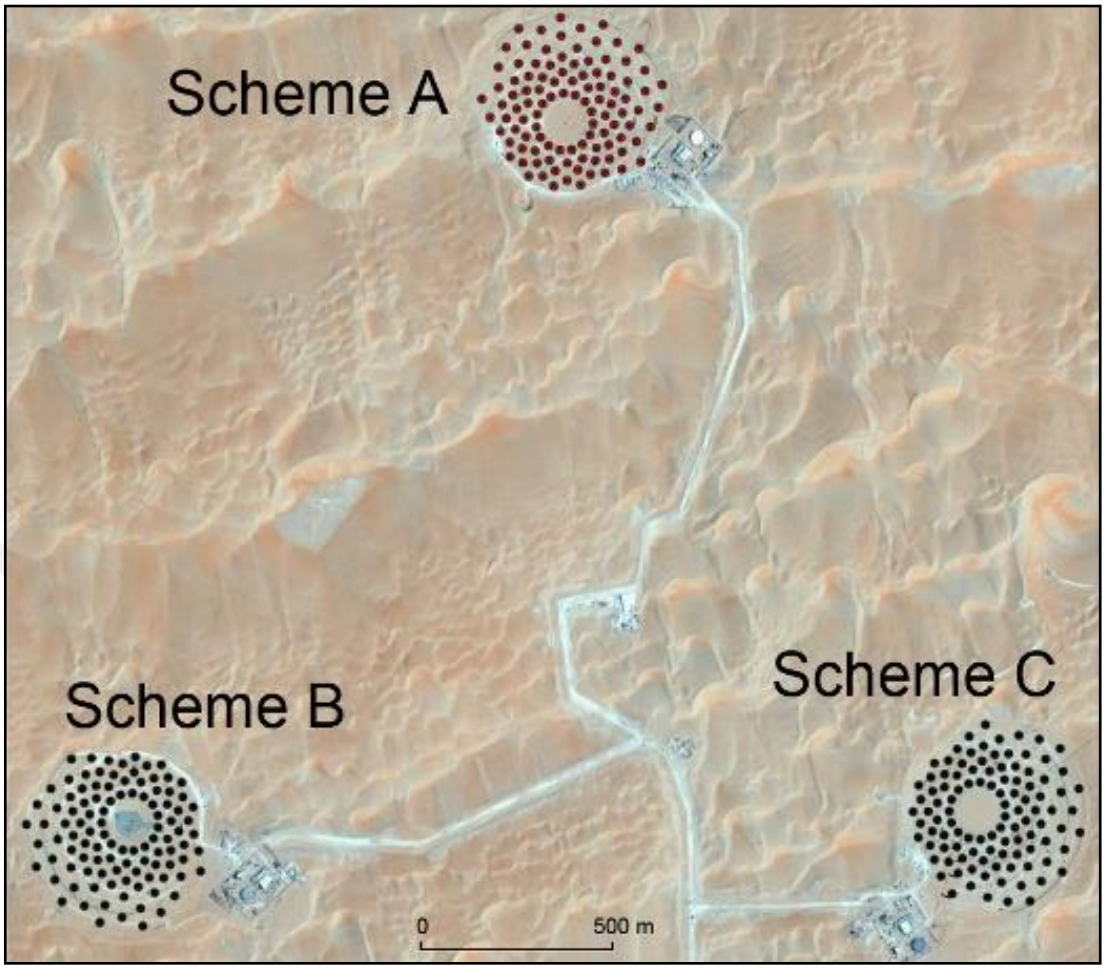

Figure 3.1. Scheme A, B and C each constituting 105 wells.

4. METHODS

The study began with a literature survey in order to understand climatological, geological and hydrogeological characteristics of the study area. After data analysis, the modelling phase was started.

4.1.Data Analysis

Dataset of scheme A was gathered, analyzed and regulated to import Groundwater Vistas. Firstly, static groundwater levels were examined in order to construct a steady state groundwater flow of the area. Secondly, drawdown data, obtained during pumping phases, was assessed to construct a transient groundwater flow of the area.

Furthermore, horizontal hydraulic conductivity and specific yield values, which were determined by experts in this branch, were gathered from the project reports written by Zetaş (consultant firm in Turkey) and confirmed by GIZ (consultant firm in Germany).

4.1.1. Static groundwater levels

When static groundwater levels were mapped by Surfer 8, depressions were observed on the contour map (Figure 4.1 and 4.2). A piezometric map, which exhibits the flow pattern of the area, could not be obtained. The reason may be that the aquifer has been pumped for a long time in different periods during the project. Therefore, it was concluded that the aquifer is not in a steady state and it was not possible to construct a steady state groundwater flow model. After this conclusion, it was decided that a transient groundwater flow model would be constructed using drawdown data for calibration.

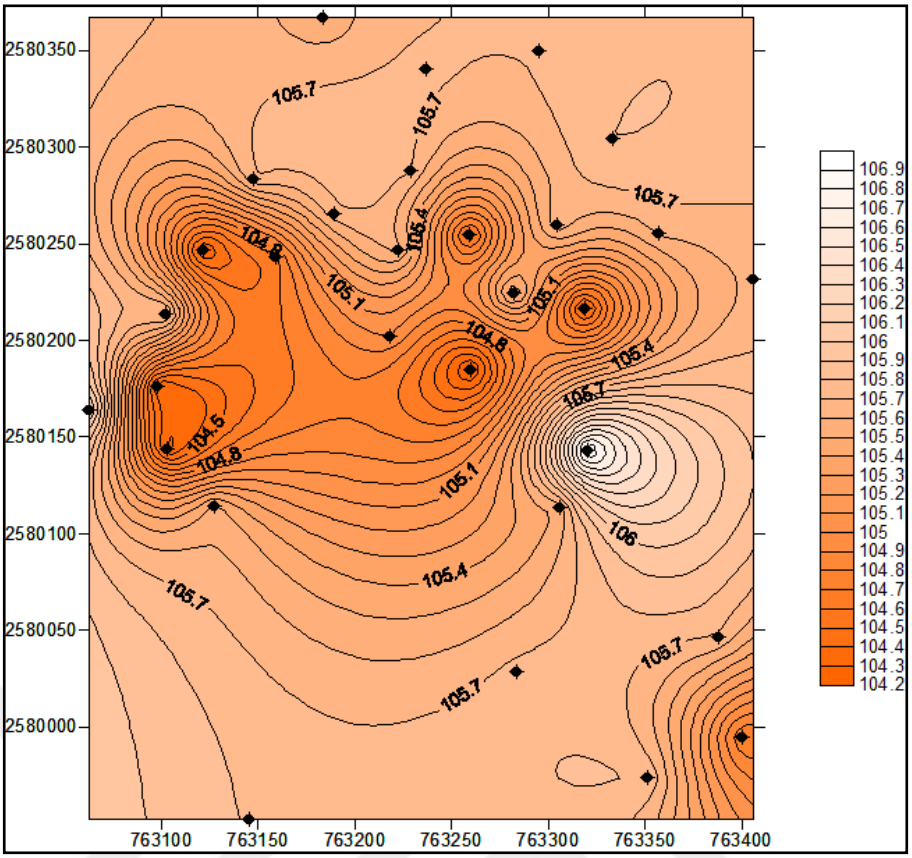

Figure 4.1. Contour map of static groundwater levels which were measured from 31 observation wells in Scheme A during December in 2013.

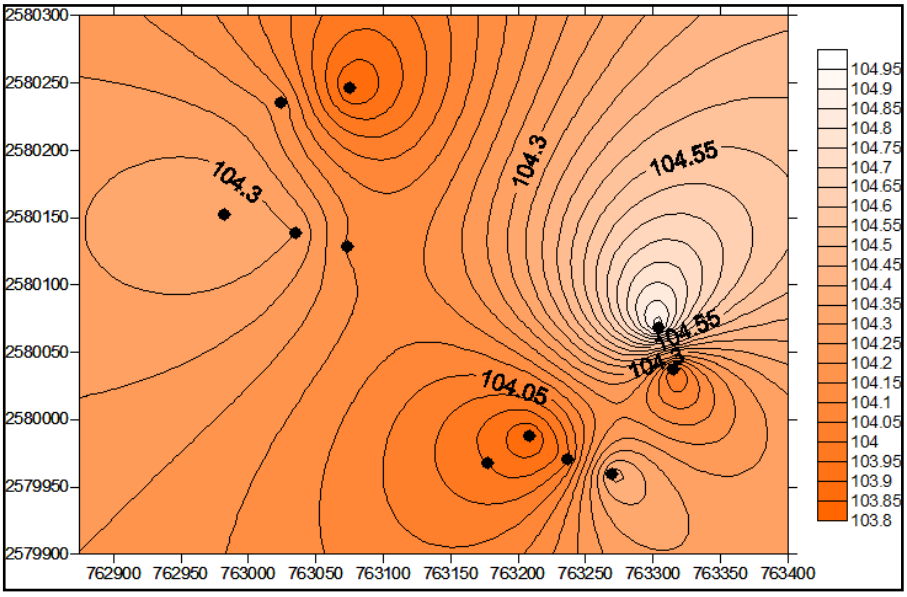

Figure 4.2. Contour map of static groundwater levels which were measured from 11 observation wells in Scheme A during October in 2013.

4.1.2. Pumping tests

During the project, pumping tests were conducted. This study is dealing with four pumping wells RW078, RW103, RW008 and RW033 which are pumped in different times. Each pumping well has its own observation wells where drawdown data was measured (Table 4.1).

Table 4.1. Pumping and observation wells used in the transient groundwater flow model.

Pumping Wells	**RW078**	**RW103**	**RW008**	**RW033**
Observation Wells	RW003	RW056	RW007	RW001
	RW006	RW068	RW009	RW002
	RW012	RW069	RW022	RW015
	RW035	RW070	RW023	RW016
	RW036	RW071	RW024	RW018
	RW051	RW080	RW038	RW019
	RW066	RW081	RW054	RW024
	RW077	RW089	RW081	RW030
	RW079	RW090	-	RW044
	RW087	RW094	-	RW048
	RW088	RW095	-	RW049
	RW095	RW096	-	RW063
	RW101	RW097	-	RW064
	-	-	-	RW074
	-	-	-	RW077

Pumping tests are composed of 4 phases (Figure 4.3) as following for each pumping well:

Phase I. A 5-step drawdown test **(SDT)** at incremental pumping rates of 30, 60, 90, 120, 150 m^3/h during **15 hours** (3 hours for each pumping rate).

Phase II. A **SDT recover**y phase during **48 hours**.

Phase III. A constant discharge test **(CDT)** at a pumping rate of 150 m^3/h during **72 hours**.

Phase IV. A **CDT recovery** phase during **72 hours.**

Start-finish dates and times of the phases for each pumping wells and phases are shown in the Table 4.2.

Besides, locations of each pumping well with its observation wells are demonstrated in Figure 4.4, 4.6, 4.8 and 4.10 whereas graphs of drawdowns, measured in the observation wells with time during the phases for each pumping period, are illustrated in Figure 4.5, 4.7, 4.9 and 4.11.

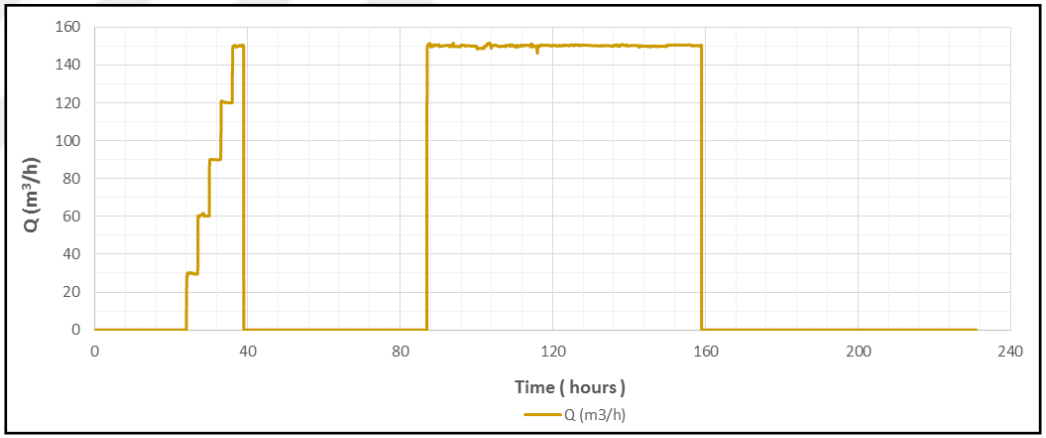

Figure 4.3. Pumping rates during SDT and CDT phases.

Table 4.2. Start-finish dates and times of the phases.

	SDT		Recovery		CDT		Recovery	
Pumping Wells	**Start**	**Finish**	**Start**	**Finish**	**Start**	**Finish**	**Start**	**Finish**
1. RW078	11.10.2013°17:30	12.10.2013°08:30	12.10.2013°08:30	14.10.2013°08:30	14.10.2013°08:30	17.10.2013°08:30	17.10.2013°08:30	20.10.2013°08:30
2. RW103	24.10.2013°17:00	25.10.2013°08:00	25.10.2013°08:00	27.10.2013°08:00	27.10.2013°08:00	30.10.2013°08:00	30.10.2013°08:00	02.11.2013°08:00
3. RW008	03.11.2013°17:00	04.11.2013°08:00	04.11.2013°08:00	06.11.2013°08:00	06.11.2013°08:00	09.11.2013°08:00	09.11.2013°08:00	12.11.2013°08:00
4. RW033	23.11.2013°17:00	24.11.2013°08:00	24.11.2013°08:00	26.11.2013°08:00	26.11.2013°08:00	29.11.2013°08:00	29.11.2013°08:00	02.12.2013°08:00

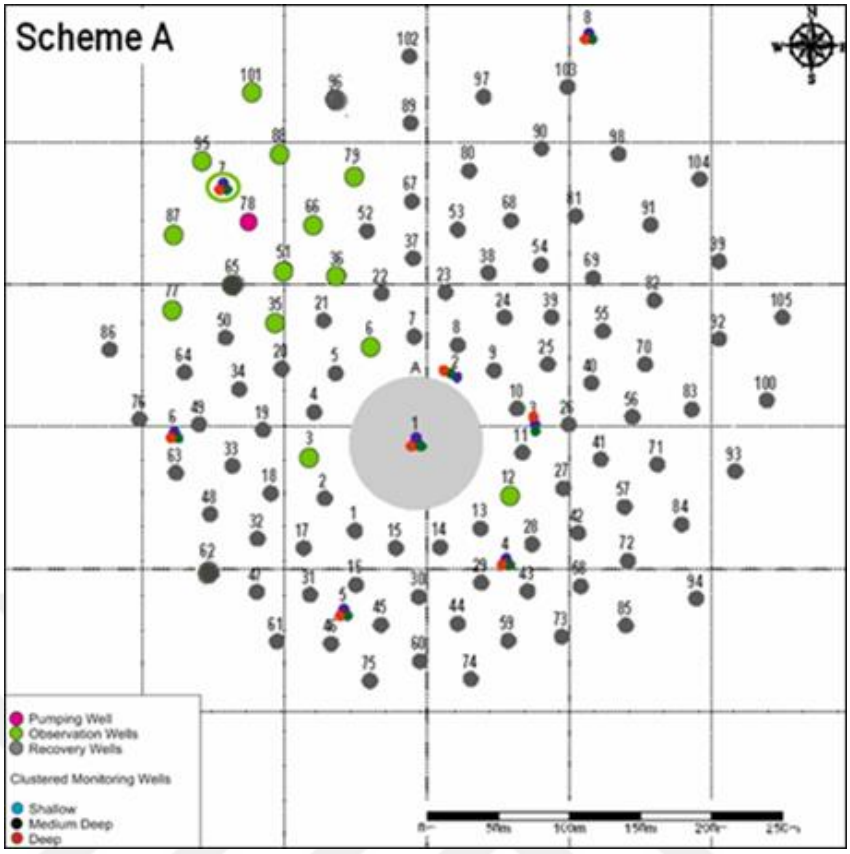

Figure 4.4. Locations of the pumping well RW078 and its observation wells (Zetaş/GIZ Reports, 2015).

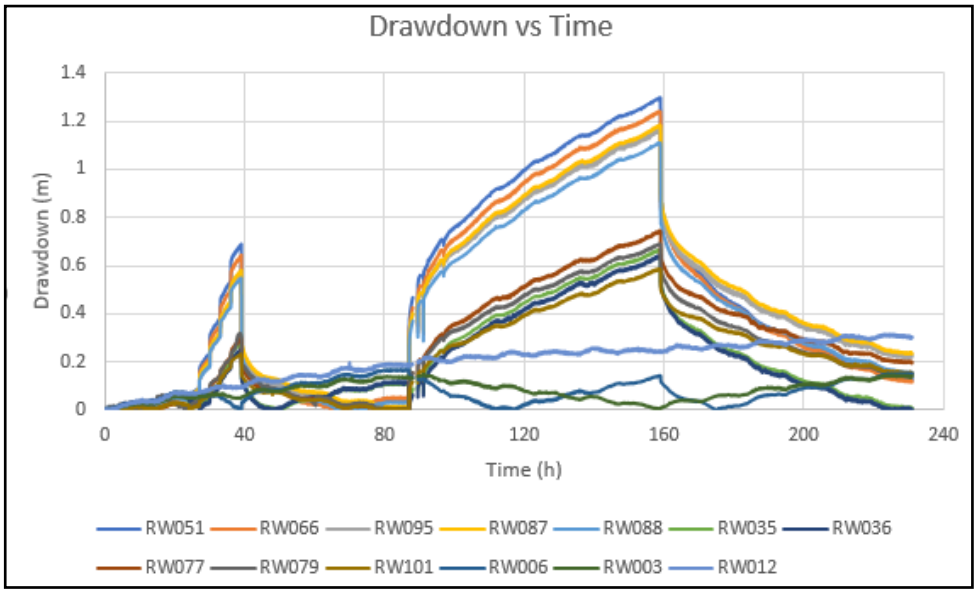

Figure 4.5. Drawdowns measured in the observation wells of the pumping well RW078 with time during the phases.

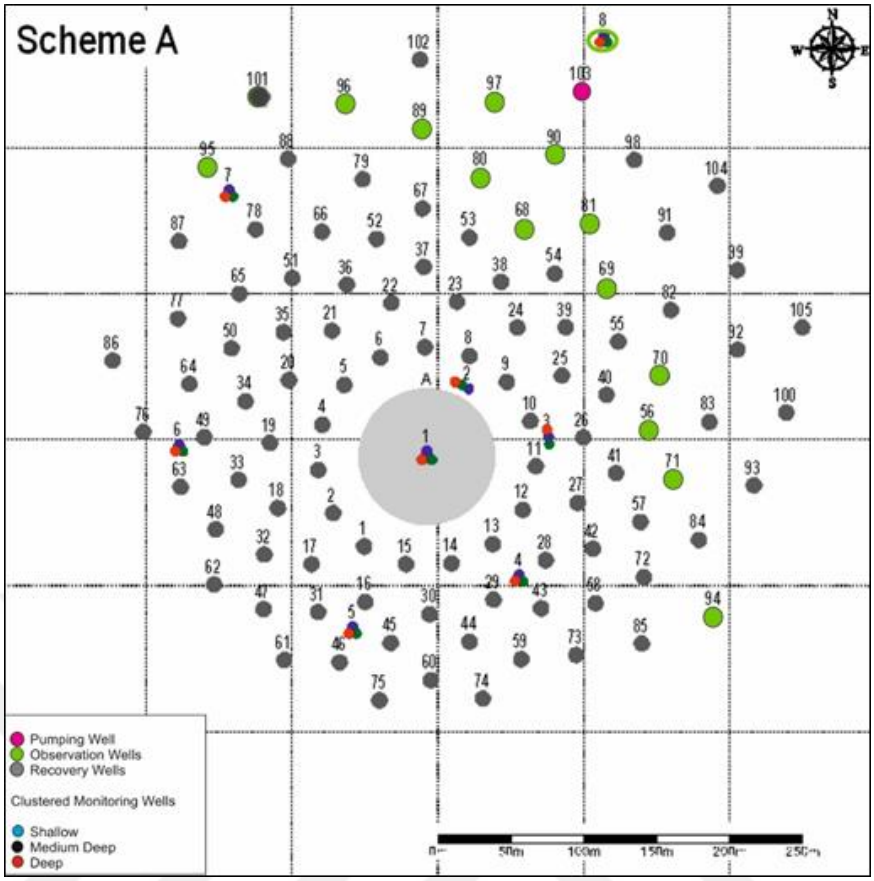

Figure 4.6. Locations of the pumping well RW103 and its observation wells (Zetaş/GIZ Reports, 2015).

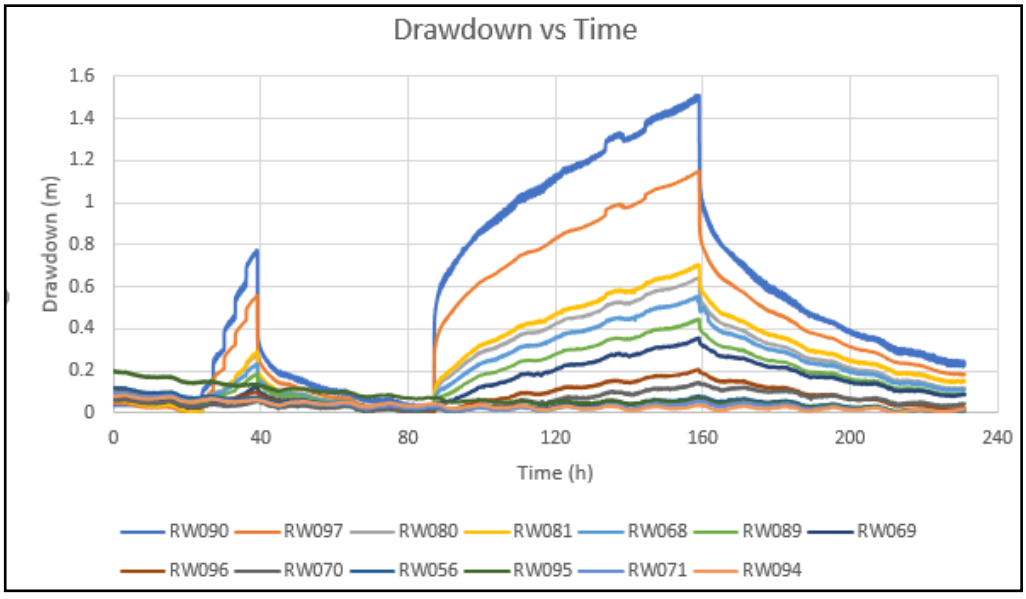

Figure 4.7. Drawdowns measured in the observation wells of the pumping well RW103 with time during the phases.

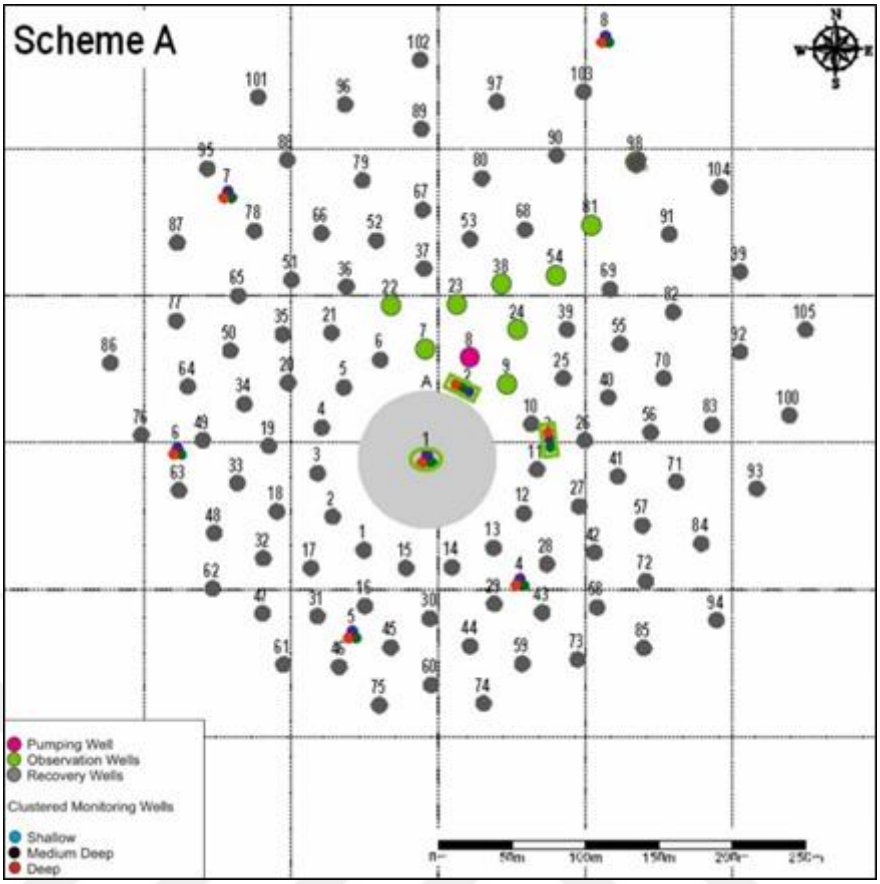

Figure 4.8. Locations of the pumping well RW008 and its observation wells (Zetaş/GIZ Reports, 2015).

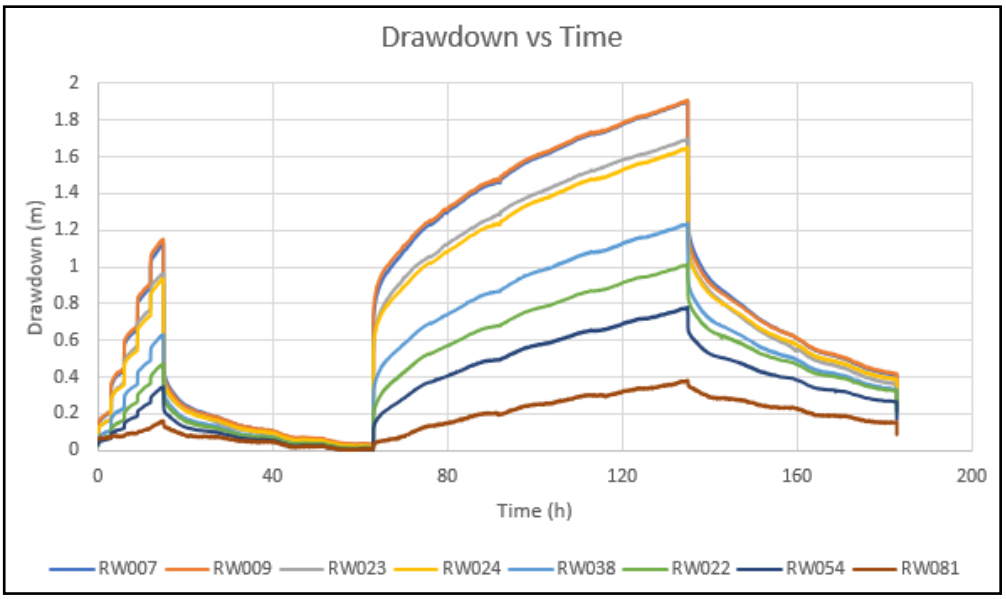

Figure 4.9. Drawdowns measured in the observation wells of the pumping well RW008 with time during the phases.

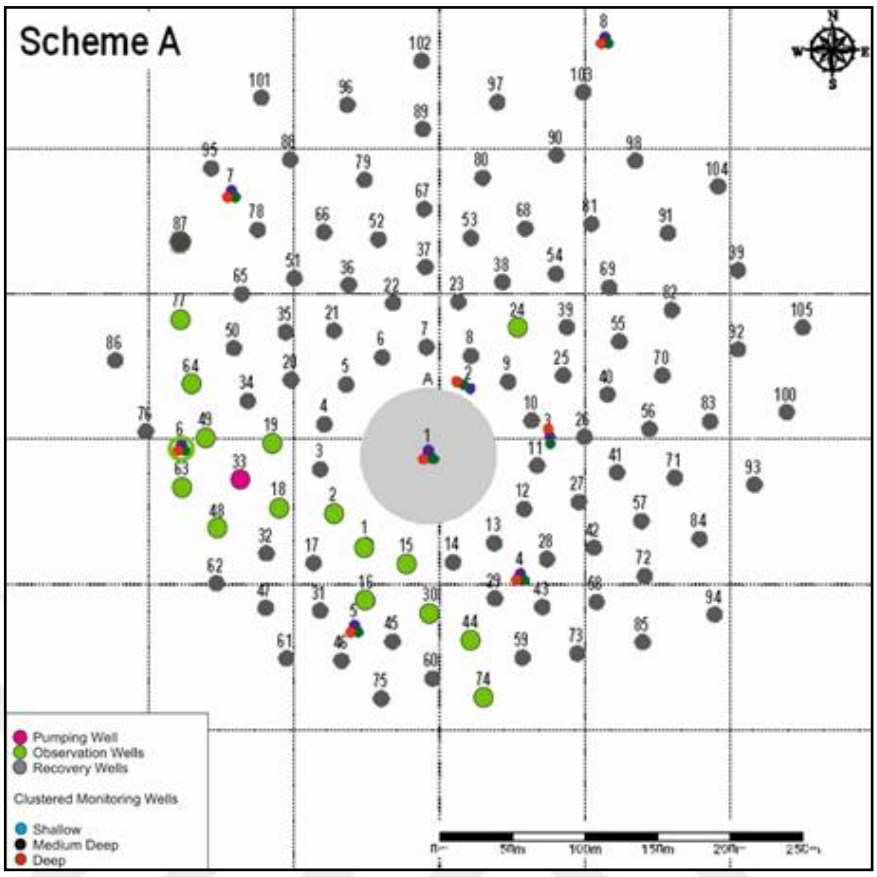

Figure 4.10. Locations of the pumping well RW033 and its observation wells (Zetaş/GIZ Reports, 2015).

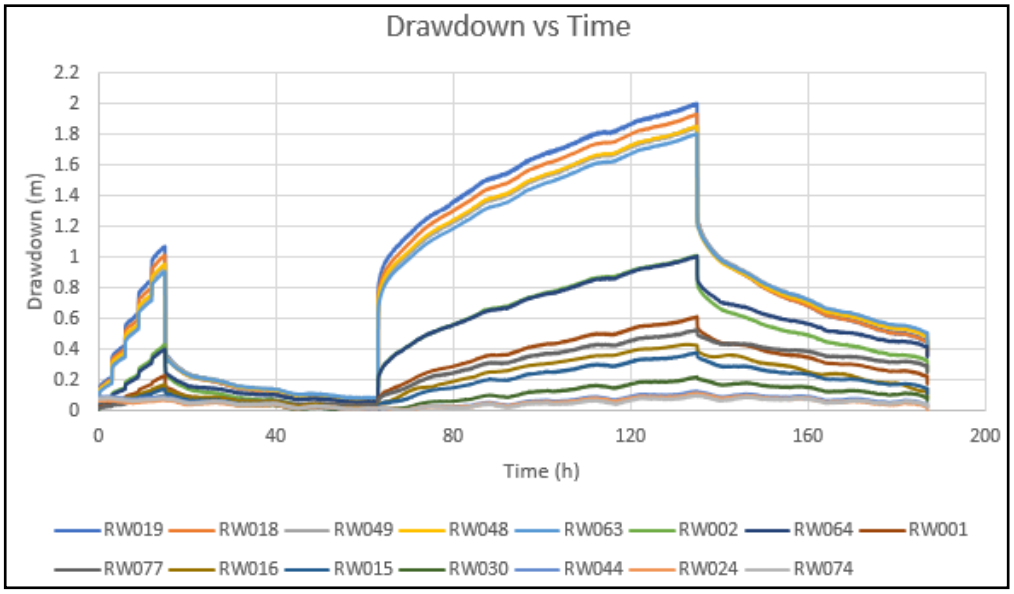

Figure 4.11. Drawdowns measured in the observation wells of the pumping well RW033 with time during the phases.

4.2.Modelling

In order to construct 2-D transient groundwater flow model of the Liwa Aquifer, Groundwater Vistas-MODFLOW was selected.

4.2.1. Grid design, initial and boundary conditions

The 2-D flow model is composed of 40 rows and 36 columns (Figure 4.12). Dimensions are 1500 m in height and 1500 m in width. Grid spacing ranges from 25 m to 100 m in X and Y directions. Rows and columns are denser in the center, where the study area is located, to have more and smaller cells. This means more computation in the area where the targets are denser. At the center of the model grid, cells are square in shape and 25 m in dimension.

The model consists of 1 sand layer with a thickness of 70 m. The bottom elevation is 65 m and the top elevation is 135 m. The bottom elevation corresponds to the bottom of the sand unit, and the bottom of the well screen which is illustrated in Figure 2.3 in the Geology section.

Boundaries were placed as far as possible away from the area of interest in order to minimize the effect of these artificial boundary conditions. Therefore, the distances between boundaries and the outermost targets in the north, south, east and west were determined as 500 m. In the north and south, constant head boundaries are located. The constant heads are 105 m in both north and south boundaries. In the east and west, no flow boundary conditions exist.

Initial conditions such as hydraulic conductivity, specific yield and initial heads were determined and assumed constant and homogenous through the whole model grid according to the data obtained from project reports. Initial head was assumed to be 105 m, since static groundwater levels, which were measured during the project, range between 104 m and 106 m.

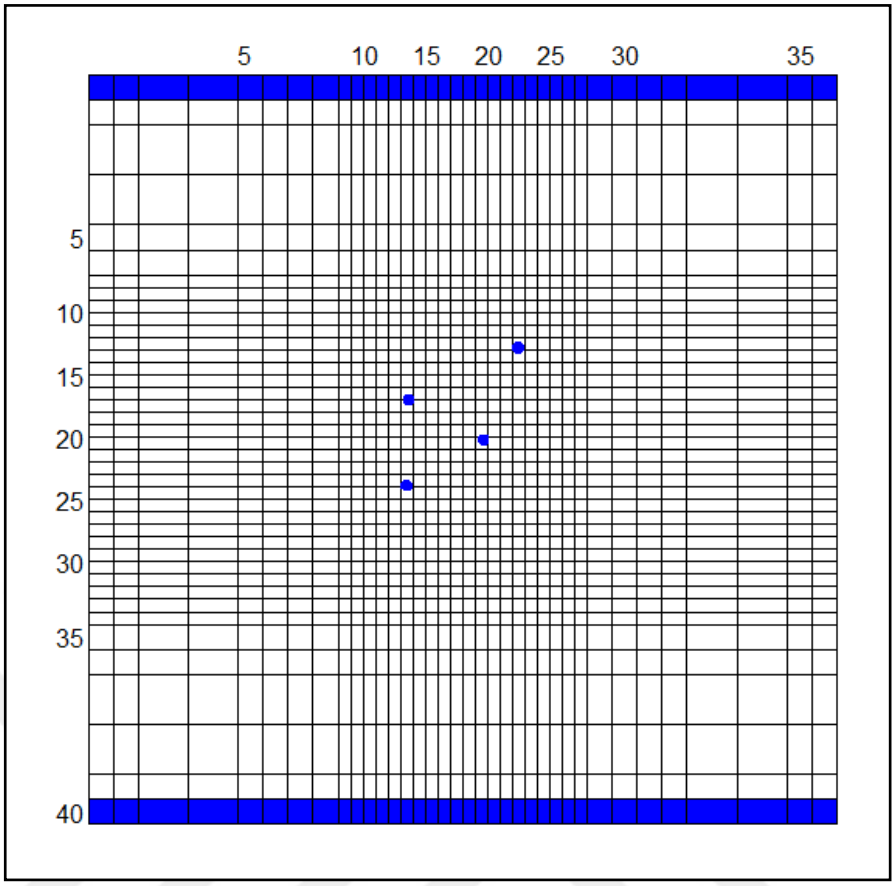

Figure 4.12. Grid design, boundary conditions and locations of 4 pumping wells. Blue columns at the north and south represent the constant head boundaries.

4.2.2. Targets and stress periods

In total, 49 observation well data were imported as targets into the model and target type is drawdown (Table 4.3) (Figure 4.13). 4 observation wells are common and used twice in two pumping wells. Thus, the number of observation wells in total is 45.

Table 4.3. Total number of observation times in the model.

Pumping Wells	Number of Observation Wells	Number of Observation Times for each Observation Well	Number of Observation Times	Total Number of Observation Times
RW078	13	48	13*48 = 624	2337
RW103	13	48	13*48 = 624	
RW008	8	48	8*48 = 384	
RW033	15	47	15*47 = 705	

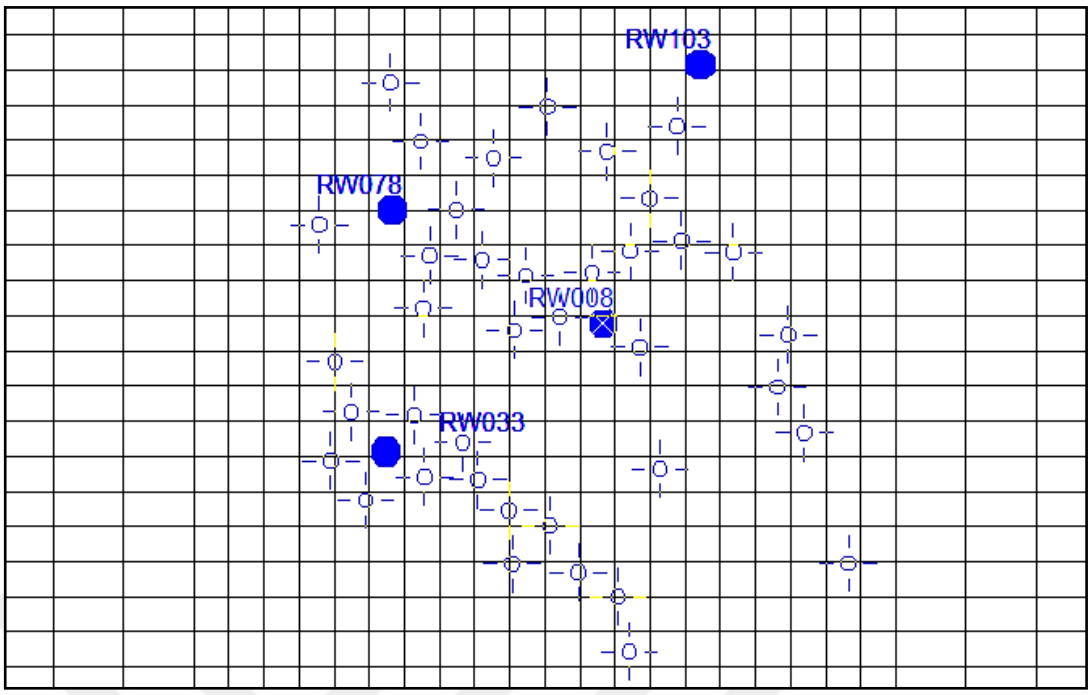

Figure 4.13. Pumping wells (RW078, RW103, RW008 and RW033) and their observation wells as targets.

There are 35 stress periods and total length of stress periods is 1238.5 hours. Hourly drawdown data was used during SDT phase, whereas the drawdown data measured every 6 hours were used during CDT and recovery phases. Time steps were determined according to this criterion. In addition, after the last recovery phases (72 hours), there are time intervals with no drawdown measurement between each pumping well. For instance, the time interval between pumping of RW078 and RW103 is 104.5 hours, between that of RW103 and RW008 is 33 hours and finally, between that of RW008 and RW033 is 273 hours. These time intervals were assigned to one stress periods as steady state type. 1-time step, which represents the last drawdown measurement at the end of the last recovery period, was used for these steady state periods (Table 4.4).

Table 4.4. Stress periods of each pumping well.

Pumping Wells	Stress Periods	Length(h)	Q(m3/h)	Time Steps	Phases
RW078	1	3	30	3	SDT
	2	3	60	3	
	3	3	90	3	
	4	3	120	3	
	5	3	150	3	
	6	48	0	8	Recovery
	7	72	150	12	CDT
	8	72	0	12	Recovery
	9	104.5	0	1	
RW103	10	3	30	3	SDT
	11	3	60	3	
	12	3	90	3	
	13	3	120	3	
	14	3	150	3	
	15	48	0	8	Recovery
	16	72	150	12	CDT
	17	72	0	12	Recovery
	18	33	0	1	
RW008	19	3	30	3	SDT
	20	3	60	3	
	21	3	90	3	
	22	3	120	3	
	23	3	150	3	
	24	48	0	8	Recovery
	25	72	150	12	CDT
	26	72	0	12	Recovery
	27	273	0	1	
RW033	28	3	30	3	SDT
	29	3	60	3	
	30	3	90	3	
	31	3	120	3	
	32	3	150	3	
	33	48	0	8	Recovery
	34	72	150	12	CDT
	35	72	0	12	Recovery

4.2.3. Parameter estimation

Parameter estimation was performed using pilot-points technique and Pest (Figure 4.14). In addition to hydraulic conductivity, specific yield estimation by pilot-points was also performed to achieve a better calibration results. Thus, parameters to be estimated were determined as horizontal hydraulic conductivity and specific yield. Pilot-points for horizontal hydraulic conductivity were located with intervals of 100 m around the whole area whereas pilot-points for specific yield were distributed with intervals of 300m through the whole area. The number of pilot-points for horizontal hydraulic conductivity is 225 and for specific yield is 25.

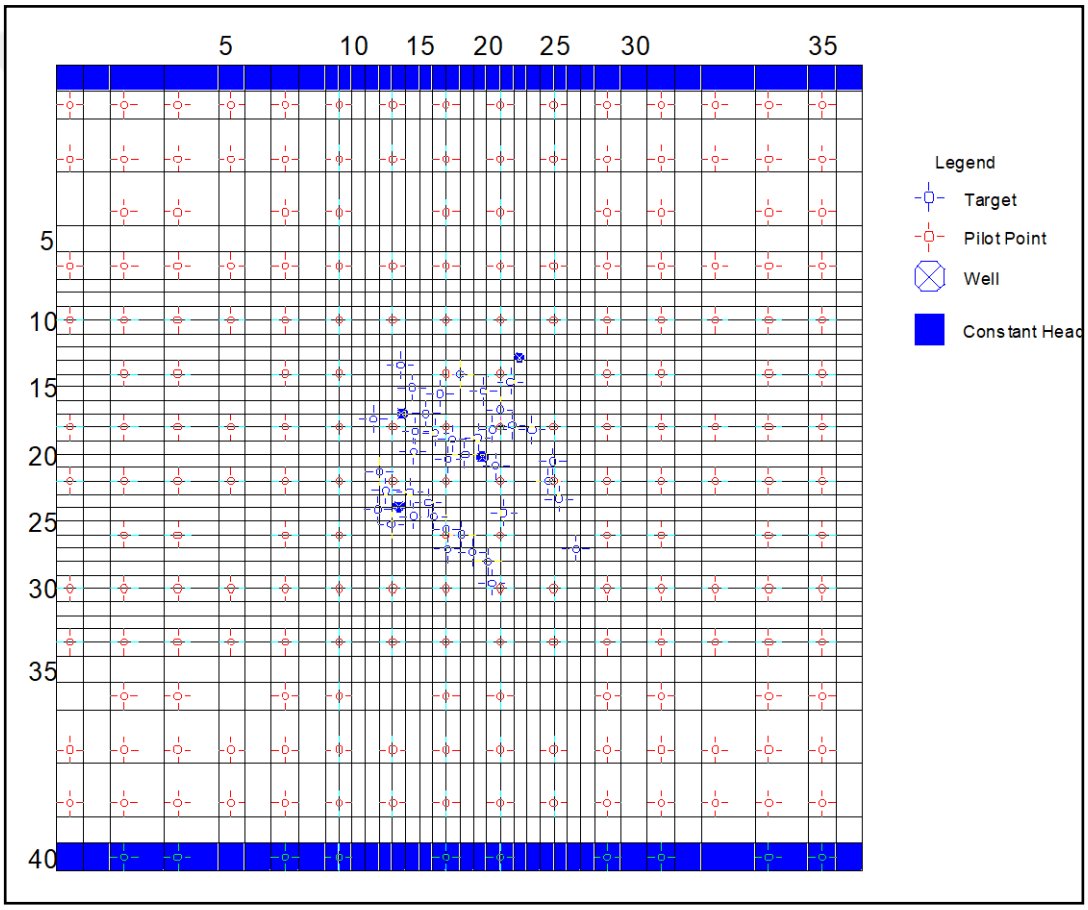

Figure 4.14. Locations of pilot points.

5. RESULTS

After several Pest runs, done in order to decrease the difference between observed and computed drawdown values, the following plot of observed vs computed values was obtained (Figure 5.1). In addition, statistics from the model calibration are illustrated in the Table 5.1.

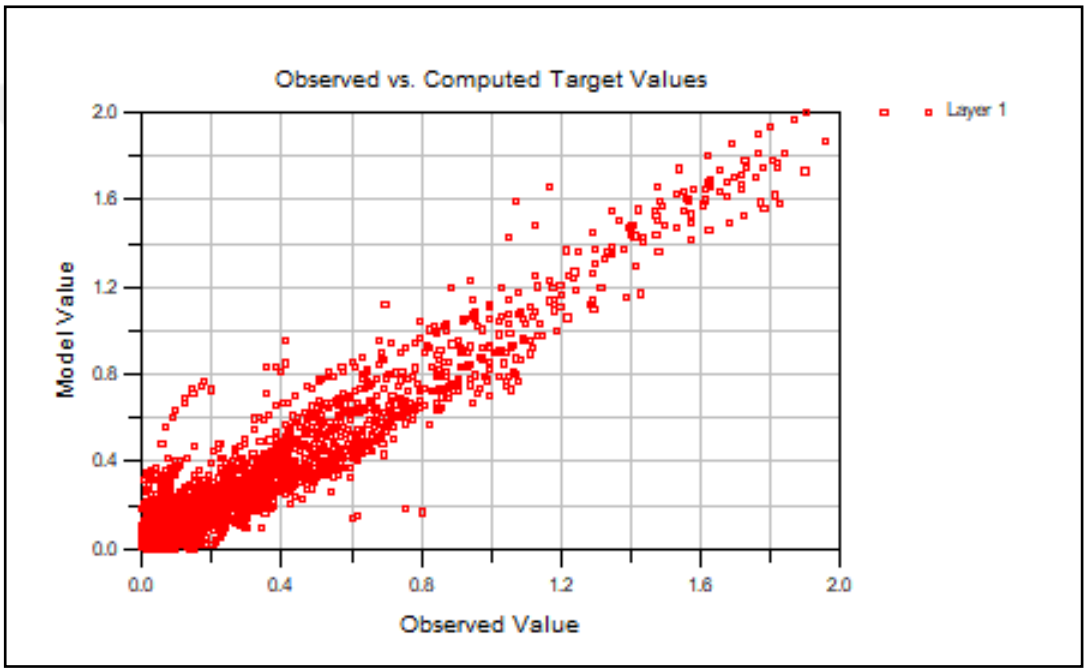

Figure 5.1. Calibration plot representing observed and computed drawdown values.

Table 5.1. Statistics of the model calibration.

Residual Mean	0.00
Residual Standard Dev.	0.11
Absolute Residual Mean	0.08
Residual Sum of Squares	30.30
RMS Error	0.11
Minimum Residual	-0.60
Maximum Residual	0.65
Number of Observations	2337

Observed vs computed drawdown plot from one of the 49 observations well data is illustrated (Figure 5.2).

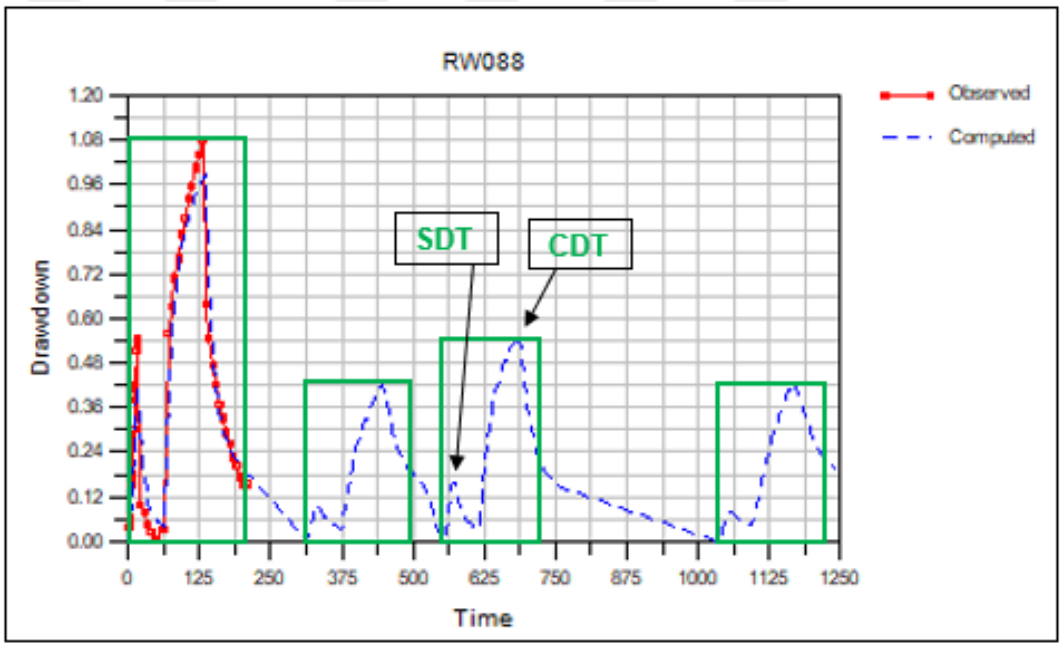

Figure 5.2. Observed vs Computed drawdown plot from one of the 49 observations well data. This observation well belongs to the first pumping period when RW078 is pumped. Each green rectangle in the plot indicates the pumping wells.

Drawdown contour map can be illustrated as following (Figure 5.3).

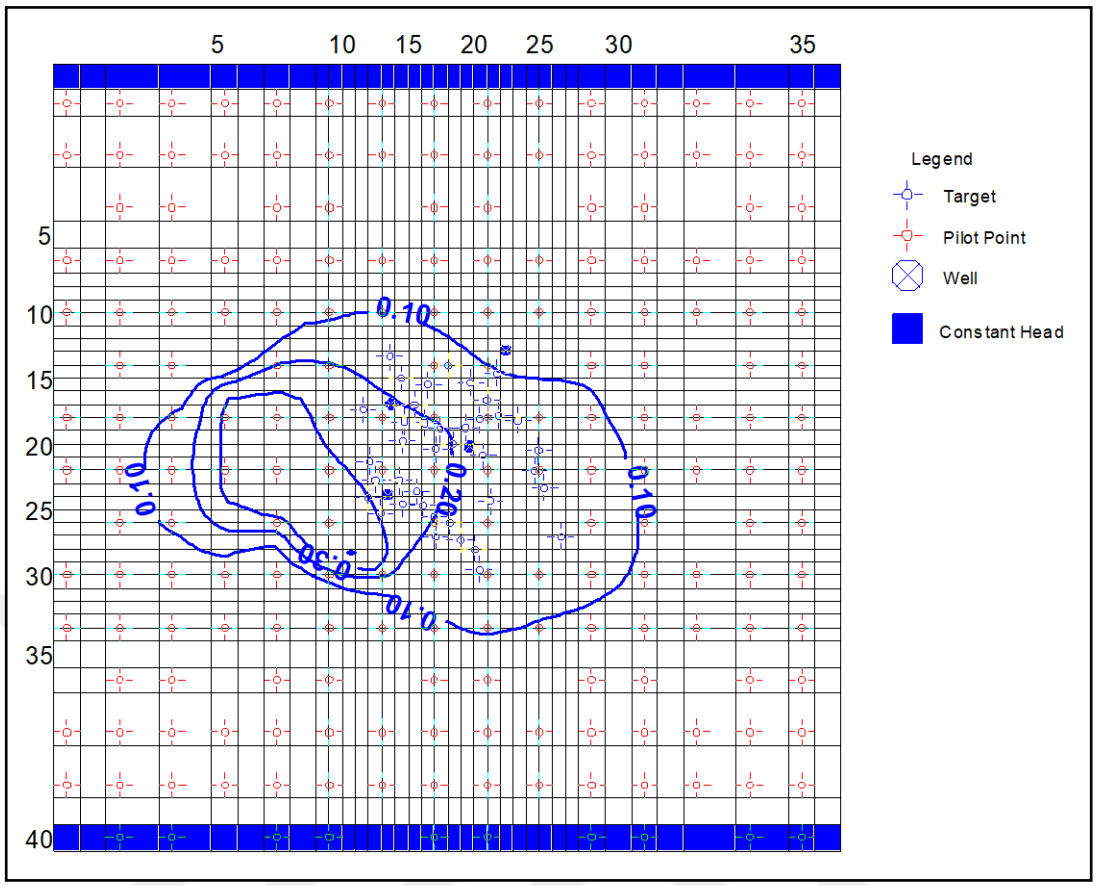

Figure 5.3. Drawdown contours after the calibration.

Horizontal hydraulic conductivity (m/h) distribution after the calibration is shown (Figure 5.4).

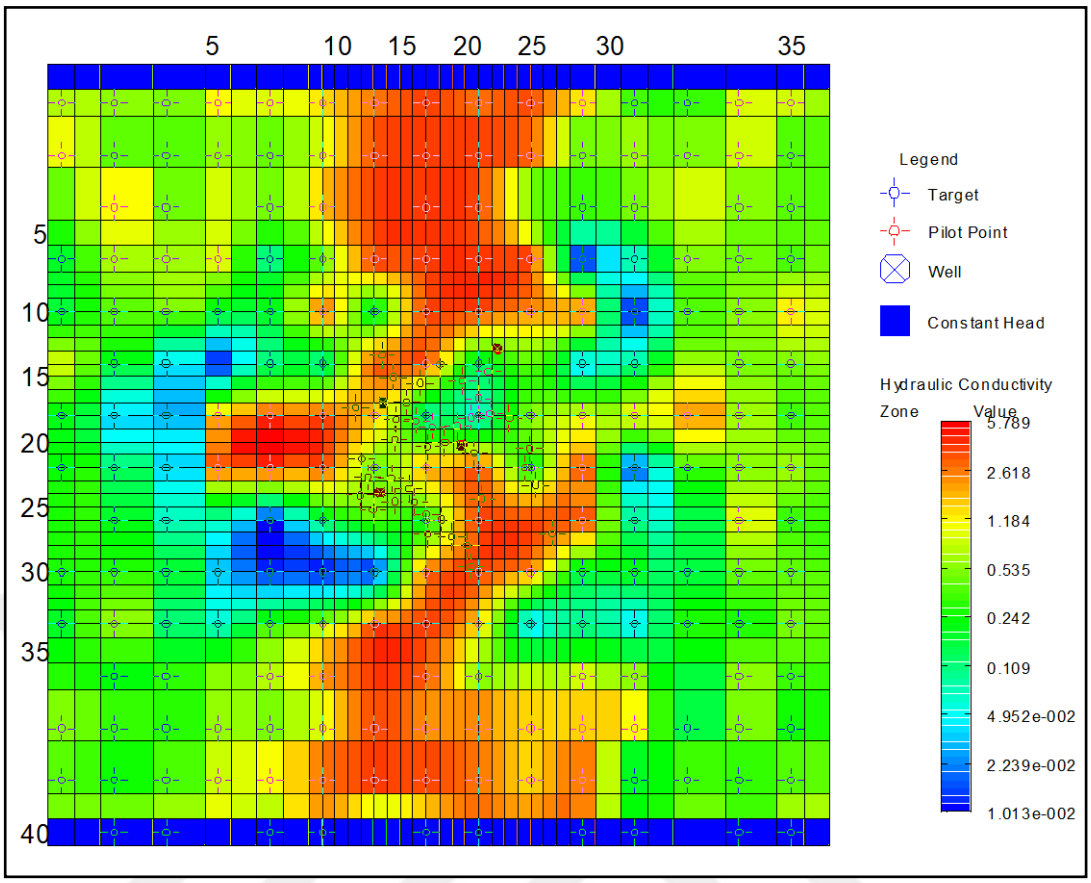

Figure 5.4. Horizontal hydraulic conductivity (m/h) distribution after the calibration.

In Table 5.2 and 5.3, horizontal hydraulic conductivity (Kx) and Specific yield (Sy) estimations in the model and the project are shown. Moreover, these estimations are compared and represented by graphs in Figures 5.5 and 5.6.

Table 5.2. Horizontal hydraulic conductivity (K_x) estimations in the locations where targets are located in the model and estimations obtained from project reports.

	Kx (m/h)			Kx (m/h)	
Targets	**Model**	**Project**	**Targets**	**Model**	**Project**
RW003	0.707	0.354	**RW007**	0.701	0.521
RW006	0.710	0.567	**RW009**	0.777	0.633
RW012	3.211	0.983	**RW022**	0.123	0.425
RW035	0.628	0.313	**RW023**	0.131	0.421
RW036	0.168	0.371	**RW024**	0.272	0.450
RW051	0.698	0.604	**RW038**	0.106	0.438
RW066	0.804	0.038	**RW054**	0.086	0.679
RW079	1.112	0.171	**RW081**	0.147	0.454
RW087	2.085	0.992	**RW001**	0.430	0.338
RW088	2.160	0.596	**RW002**	0.549	0.475
RW101	2.869	0.713	**RW015**	0.973	0.721
RW056	0.398	0.596	**RW016**	0.683	0.533
RW068	0.096	0.996	**RW018**	0.494	0.758
RW069	0.313	0.375	**RW019**	0.642	0.763
RW070	0.342	0.650	**RW030**	1.223	0.425
RW071	1.014	0.483	**RW044**	3.053	0.608
RW080	0.177	0.408	**RW048**	0.478	0.758
RW089	0.711	0.867	**RW049**	0.571	0.617
RW090	0.136	0.367	**RW063**	0.568	1.271
RW094	2.697	0.421	**RW064**	0.641	0.796
RW095	2.158	0.525	**RW074**	3.945	0.429
RW096	0.279	0.358	**RW077**	1.888	0.304
RW097	0.279	0.863	-	-	-

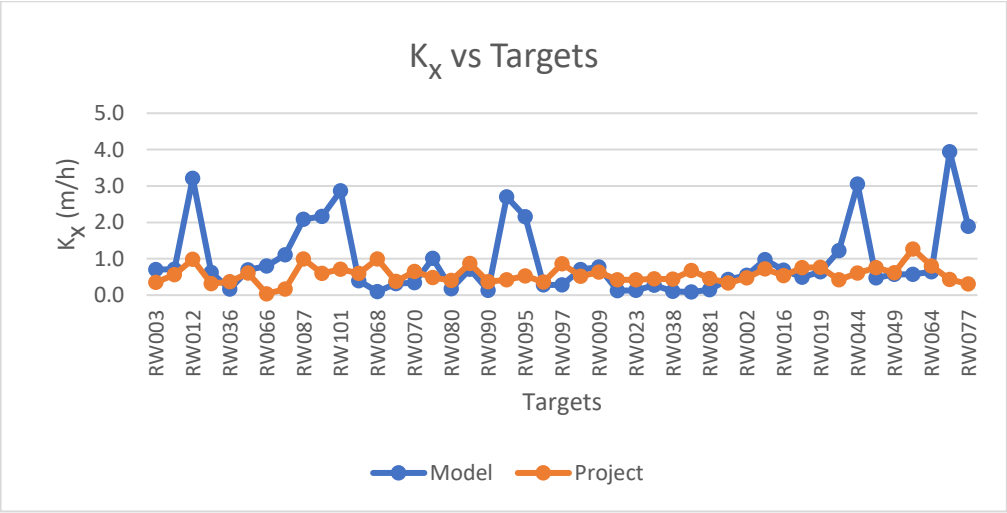

Figure 5.5. Comparison of K_x estimations obtained from the model and the project reports.

Table 5.3. Specific yield (S_y) estimations in the locations where targets are located in the model and estimations obtained from project reports.

	S_y			S_y	
Targets	**Model**	**Project**	**Targets**	**Model**	**Project**
RW003	0.044	0.110	**RW007**	0.035	0.052
RW006	0.036	0.081	**RW009**	0.034	0.029
RW012	0.060	0.031	**RW022**	0.031	0.089
RW035	0.039	0.200	**RW023**	0.028	0.830
RW036	0.032	0.097	**RW024**	0.030	0.100
RW051	0.039	0.037	**RW038**	0.027	0.130
RW066	0.032	0.081	**RW054**	0.023	0.027
RW079	0.031	0.100	**RW081**	0.021	0.100
RW087	0.032	0.084	**RW001**	0.057	0.130
RW088	0.033	0.100	**RW002**	0.050	0.094
RW101	0.038	0.094	**RW015**	0.064	0.024
RW056	0.047	0.037	**RW016**	0.085	0.022
RW068	0.039	0.065	**RW018**	0.045	0.037
RW069	0.026	0.075	**RW019**	0.043	0.037
RW070	0.040	0.078	**RW030**	0.090	0.077
RW071	0.068	0.096	**RW044**	0.097	0.039
RW080	0.025	0.100	**RW048**	0.046	0.047
RW089	0.029	0.080	**RW049**	0.048	0.041
RW090	0.020	0.074	**RW063**	0.051	0.260
RW094	0.103	0.047	**RW064**	0.048	0.090
RW095	0.041	0.098	**RW074**	0.143	0.120
RW096	0.026	0.088	**RW077**	0.053	0.120
RW097	0.026	0.062	-	-	-

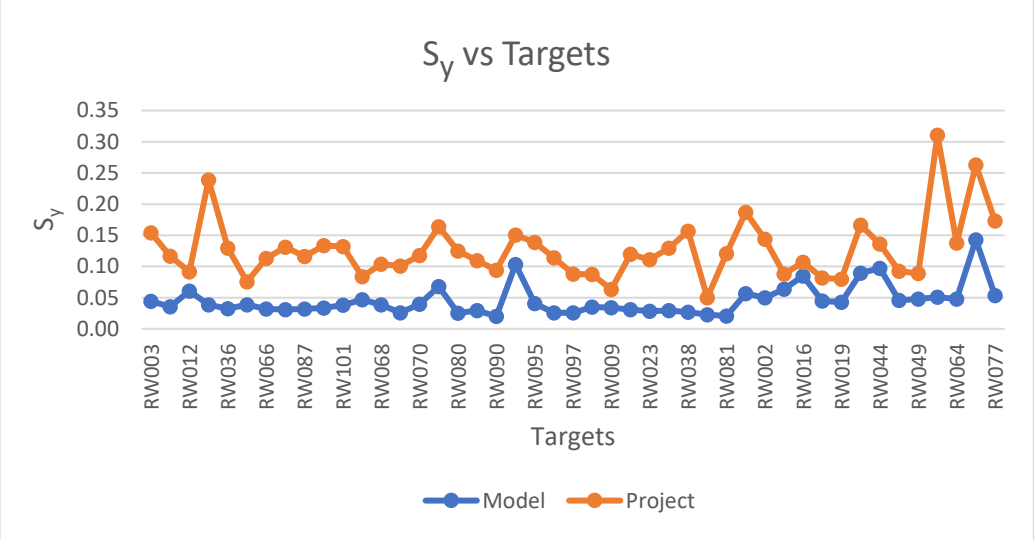

Figure 5.6. Comparison of S_y estimations obtained from the model and the project reports.

6. DISCUSSION

First of all, in the context of this study, the aim was to construct a steady state groundwater flow model of the Liwa aquifer using static groundwater level data of the aquifer at the beginning. However, flow pattern of the study area cannot be found out properly due to some depression observed in the piezometric map according to the available static groundwater level data. This may result from the pumping of the aquifer for a long time in different periods during the project. Thus, it was concluded that the aquifer may not be in a steady state and it may not be possible to construct a steady state groundwater flow model with the available data. In this case, developing a transient groundwater flow model of the aquifer was decided by using drawdown data for the calibration. Thereafter, the transient flow model was tried to be designed as simple and basic as possible at the start of the modelling. The aim was to start and proceed from the simplest model by developing in time.

Moreover, for the parameter estimation and calibration process, pilot-points technique was used with the intention of assigning different and interpolated horizontal hydraulic conductivity and specific yield values and have a better calibration through the whole area rather than zone-based calibration. In addition, the significance of the pilot-points number was understood in calibration and parameter estimation for this model. It was observed that after increase in the pilot-points number of horizontal hydraulic conductivity, calibration became better and the huge differences between hydraulic conductivity estimations in relatively short distances was reduced. Besides, in the beginning, specific yield was assigned as constant through the grid using one pilot-point. In order to understand how specific yield is effective in the calibration, pilot-points numbers of specific yield were increased gradually. Finally, it was observed that it was not necessary to increase as many as that of the horizontal hydraulic conductivity. It may be concluded that the horizontal hydraulic conductivity is more variable with the horizontal distance than the specific yield.

In the model, horizontal hydraulic conductivity values are relatively high in north-west and south-east of the target area (red color in the horizontal hydraulic conductivity map). In these areas, grain size may be relatively larger causing higher K_x estimations. For instance, gravel lenses may occur. However, even if this is the case, these K_x estimations seem so high. Another possibility may be fractures or faults which are striking in these areas. On the other hand, in the middle of the target area, K_x estimations seem more realistic. In addition, when K_x estimations of the model and the project are compared as illustrated with graphs in the results section, it is observed that they are not so far each other, except some high values. Besides, specific yield estimations in the model are underestimated with respect to the values obtained from the project reports. It may be originated from the methods used for estimations in the project reports.

7. CONCLUSION

The objective was to predict hydraulic characteristics of the Liwa Aquifer which are horizontal hydraulic conductivity and specific yield by constructing 2-D transient groundwater flow model using MODFLOW in Groundwater Vistas. Scheme A, including four pumping wells with 45 observation wells in total, was focused within the scope of the study. Drawdown data obtained from observation wells during the pumping periods were used in order to calibrate the model. In the report, geographical, climatological, geological, hydrogeological characteristics and water resources of the study area, Liwa (ASR) Project, methods of the study, the model and the results were covered. At the end of the study, results were evaluated and discussed. Furthermore, hydraulic conductivity and specific yield results obtained from the model were compared with the results obtained from the reports of the project. In brief,

- The horizontal hydraulic conductivity is more variable with the horizontal distance than the specific yield

-The reason of the high horizontal hydraulic conductivity values in north-west and south-east of the target area may be relatively higher grain size such as gravel lenses or fractures or faults in these areas.

- According to comparison of K_x estimations of the model and the project, it is observed that they are not so far each other, except some high values.

-The S_y estimations in the model are underestimated with respect to the values obtained from the project reports. It may be originated from the methods used for estimations in the project reports.

To conclude, it can be said that modelling is an infinite process. In other words, it is possible to develop a model in time in order to approximate it to the real conditions. Thus, as our future perspective, the model in the current study can be developed in

time to have better results by increasing number of cells and pilot points or by additional parameters to be estimated or by changing and trying different boundary conditions or additional field data can be obtained. On the other hand, the other Schemes, which are B and C, may be used for constructing another model.

REFERENCES

Abdelfattah M. A. (2013). Integrated suitability assessment: A way forward for land use planning and sustainable development in Abu Dhabi, United Arab Emirates. *Arid Land Research and Management*, 27: 41-64.

Al-Hammadi M.K. (2003). *Assessment of groundwater resources using remote sensing and GIS*, M.Sc. Thesis. UAE University, UAE, 158p.

Al-Katheeri E. S., Howari F. M. and Murad A. A. (2009). Hydrogeochemistry and pollution assessment of quaternary–tertiary aquifer in the Liwa area, United Arab Emirates. *Environ Earth Science,* 59: 581–592.

Al-Rashed M. F. and Sherif M. M. (2000). Water resources in the GCC countries: An overview. *Water Resource Management,* 14: 59-75.

Brook M. C. and Dawoud M. (2005). Coastal water resources management in the United Arab Emirates. *Integrated coastal zone management in the United Arab Emirates,* 5-8 June 2005, Abu Dhabi.

Brook M. C., Al-Houqani H., Darawsha T., Al-Alawneh M. and Achary S. (2006). Groundwater resources: Development and management in the Emirate of Abu Dhabi, United Arab Emirates, 15-34. Mohamed A. M. O., *Arid land hydrogeology: In search of a solution to a threatened resource*. Taylor & Francis Group, London, 184p.

Elmahdy S. I. and Mohamed M. M. (2015). Groundwater of Abu Dhabi Emirate: a regional assessment by means of remote sensing and geographic information system. *Arabian Journal of Geosciences*, 8: 11279-11292.

Anonym, *Water resources statistics bulletin for Abu Dhabi Emirate – Technical report*, ERWDA, Abu Dhabi, 2003, 43p.

Anonym, G*roundwater assessment project Abu Dhabi – Technical report*, GTZ/Dornier and Consult/ADNOC, Abu Dhabi, 2005, 32p.

McDonnell R. and Fragaszy S., *Groundwater use and policies in Abu Dhabi - Project report, IWMI,* Abu Dhabi, 2016, 83p.

Murad A. A. (2010). An overview of conventional and non-conventional water resources in arid region: assessment and constrains of the United Arab Emirates (UAE). *Journal of Water Resource and Protection,* 2: 181-190.

Rizk Z.S and Alsharan A. S. (2003). Water resources in the United Arab Emirates, 245-264, Alsharhan A. S., and Wood W. W., *Water resources perspectives: evaluation, management and policy*. Elsevier, Amsterdam, 398p.

Symonds R., Robledo A. and Al-Shateri H., *Use of environmental tracers to identify and date recent recharge to the surficial aquifer of northeastern Abu Dhabi Emirate, United Arab Emirates – NDC–USGS Technical series administrative report,* Abu Dhabi, 2005, 24p.

Anonym, *Strategic water storage/recovery project Liwa, UAE – Technical reports,* Zetaş/GIZ, Abu Dhabi, 2015, 145p.

APPENDICES

Appendix A. Observation Wells of RW078

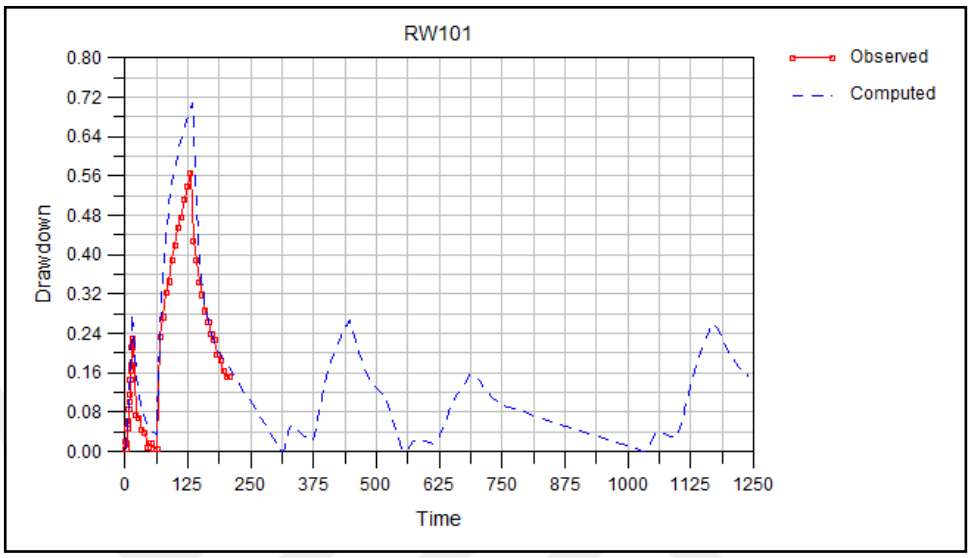

Figure 0.1. Observed vs Computed drawdown plot of RW101.

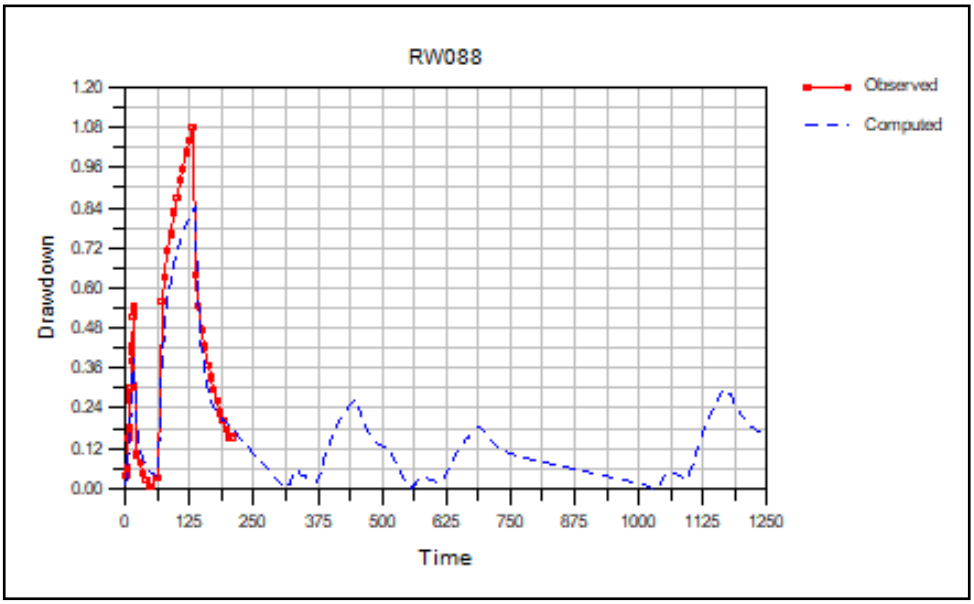

Figure 0.2. Observed vs Computed drawdown plot of RW088.

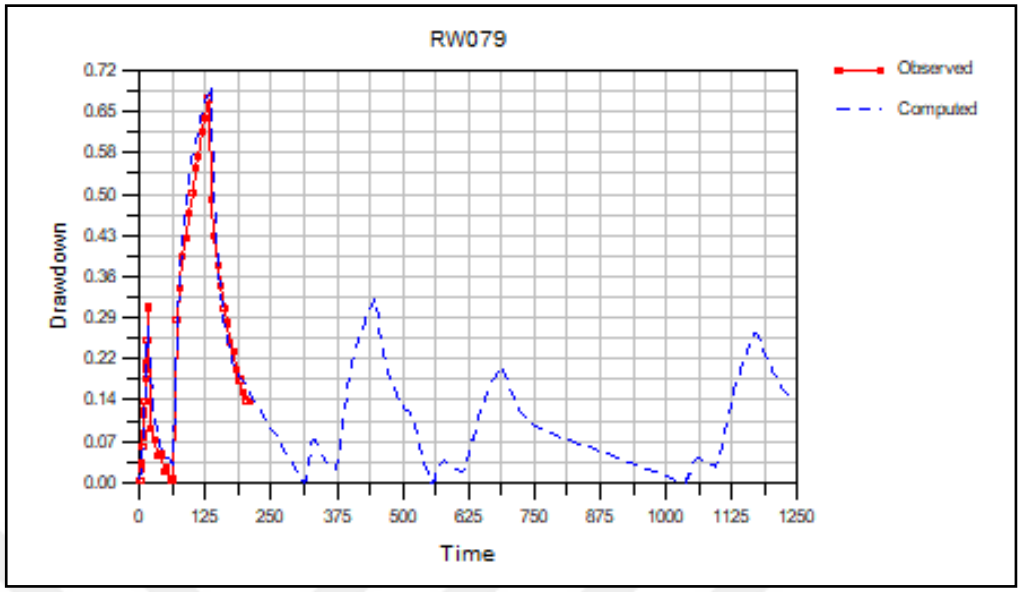

Figure 0.3. Observed vs Computed drawdown plot of RW079.

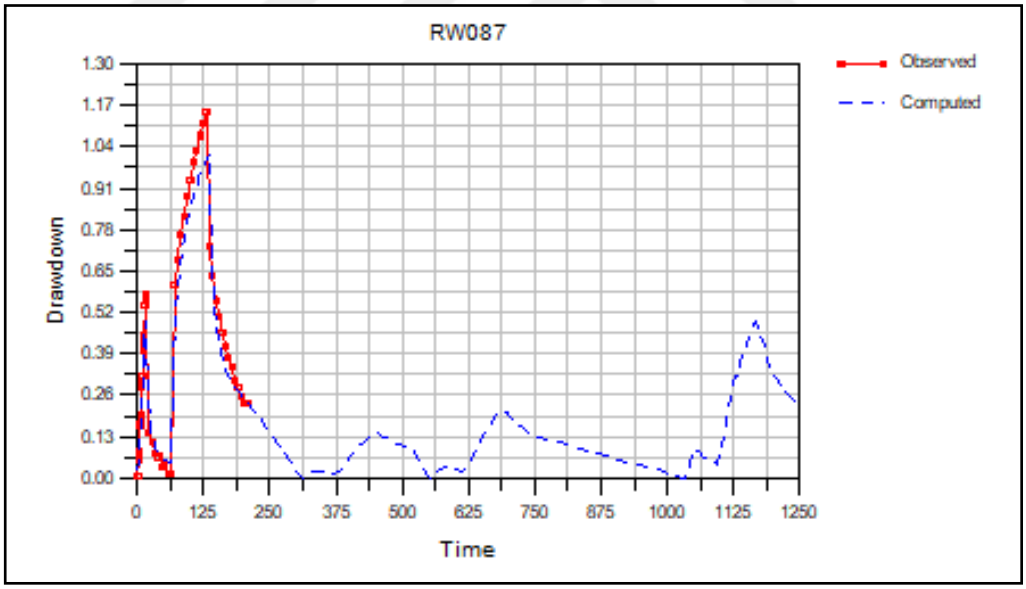

Figure 0.4. Observed vs Computed drawdown plot of RW087.

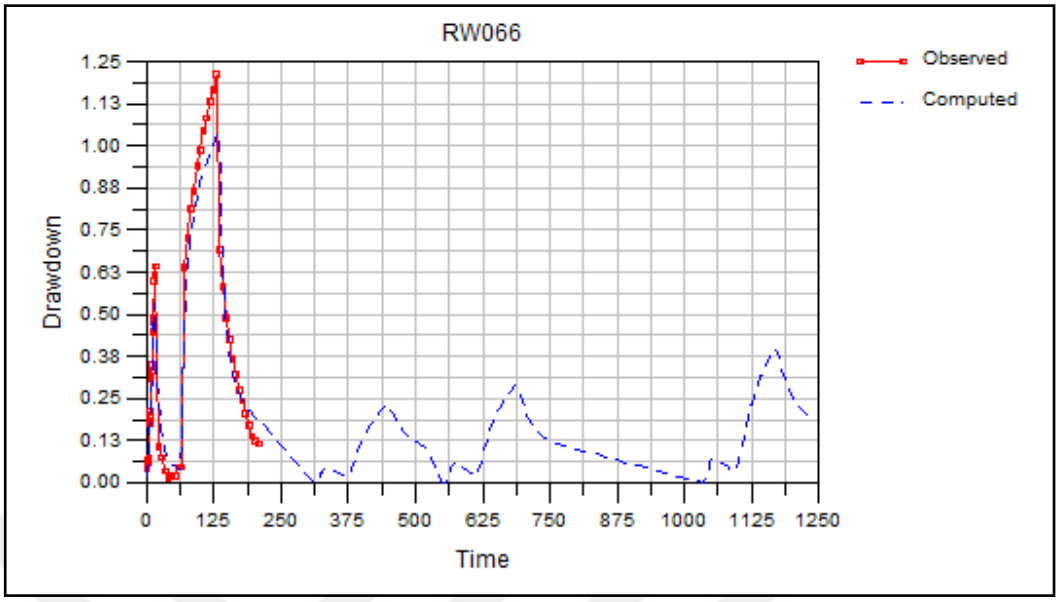

Figure 0.5. Observed vs Computed drawdown plot of RW066.

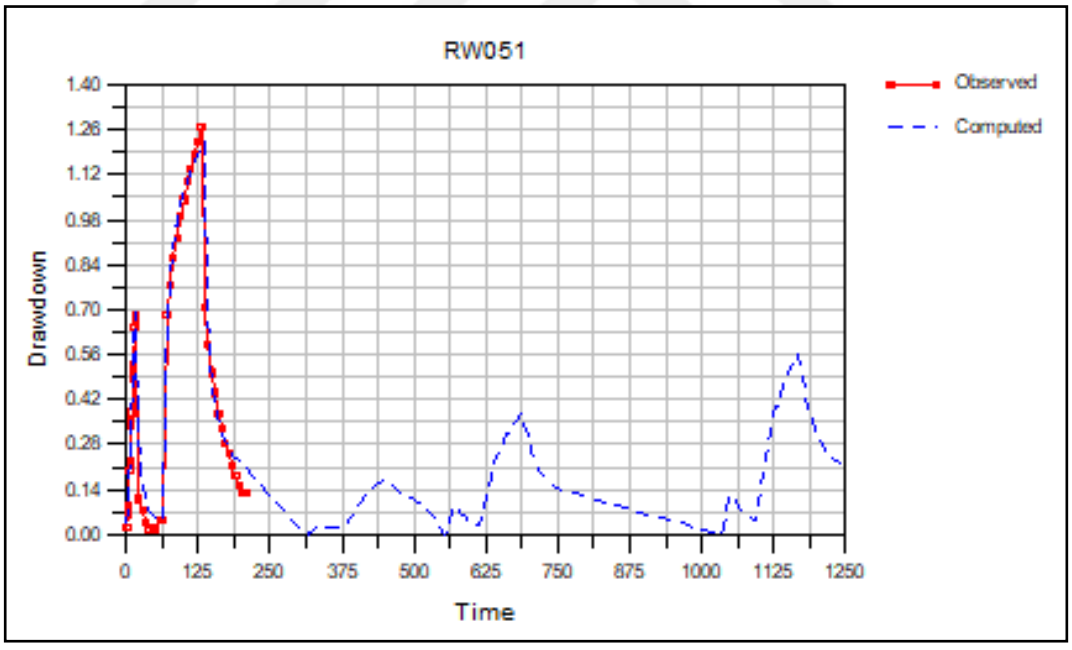

Figure 0.6. Observed vs Computed drawdown plot of RW051.

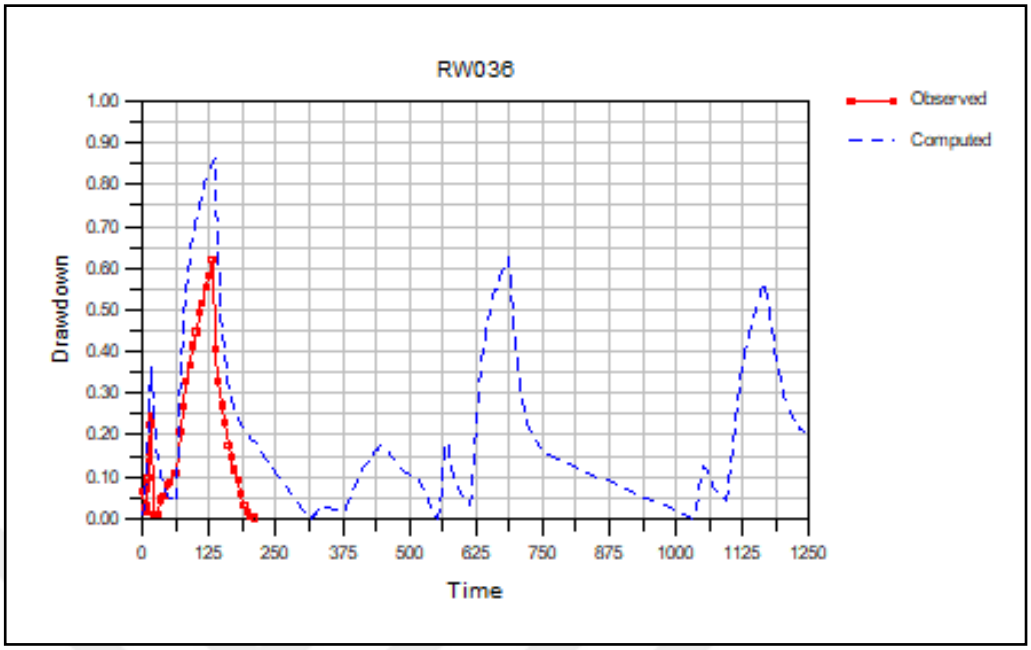

Figure 0.7. Observed vs Computed drawdown plot of RW036.

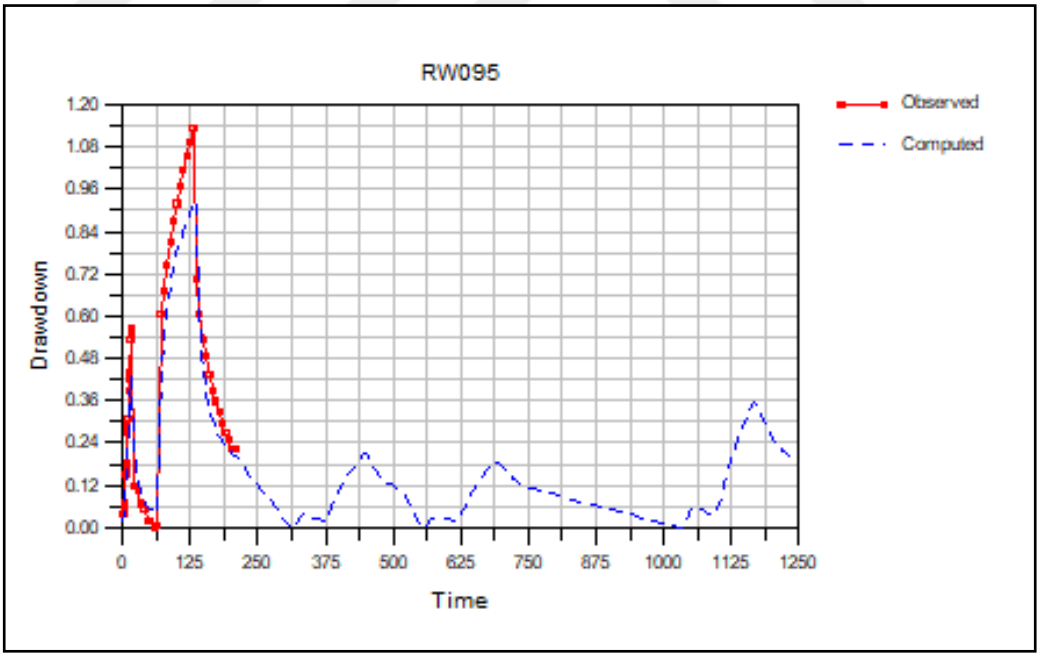

Figure 0.8. Observed vs Computed drawdown plot of RW095.

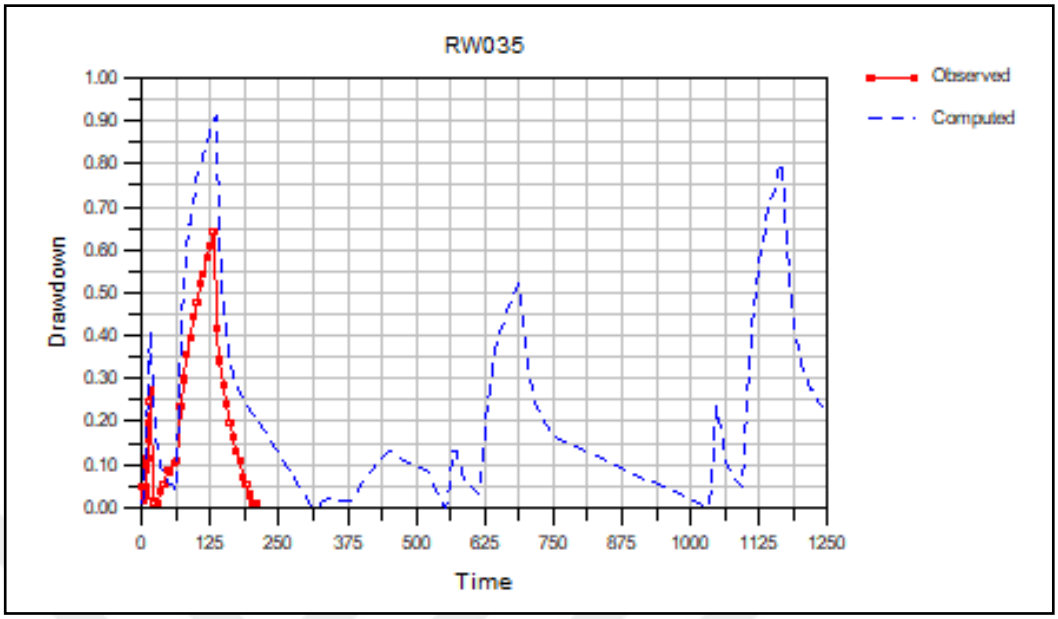

Figure 0.9. Observed vs Computed drawdown plot of RW035.

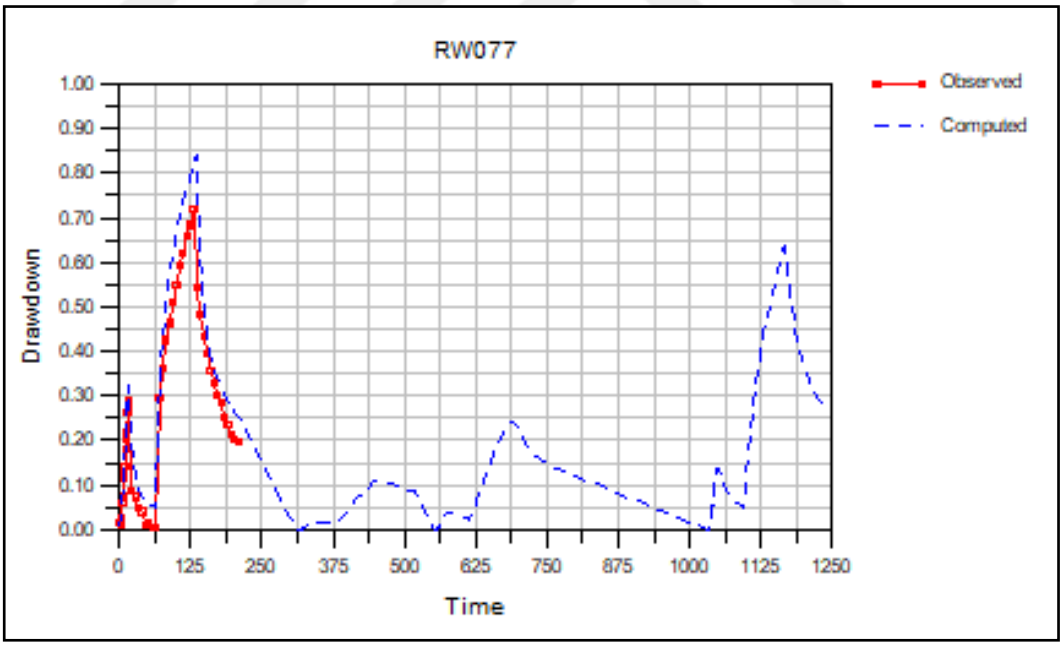

Figure 0.10. Observed vs Computed drawdown plot of RW077.

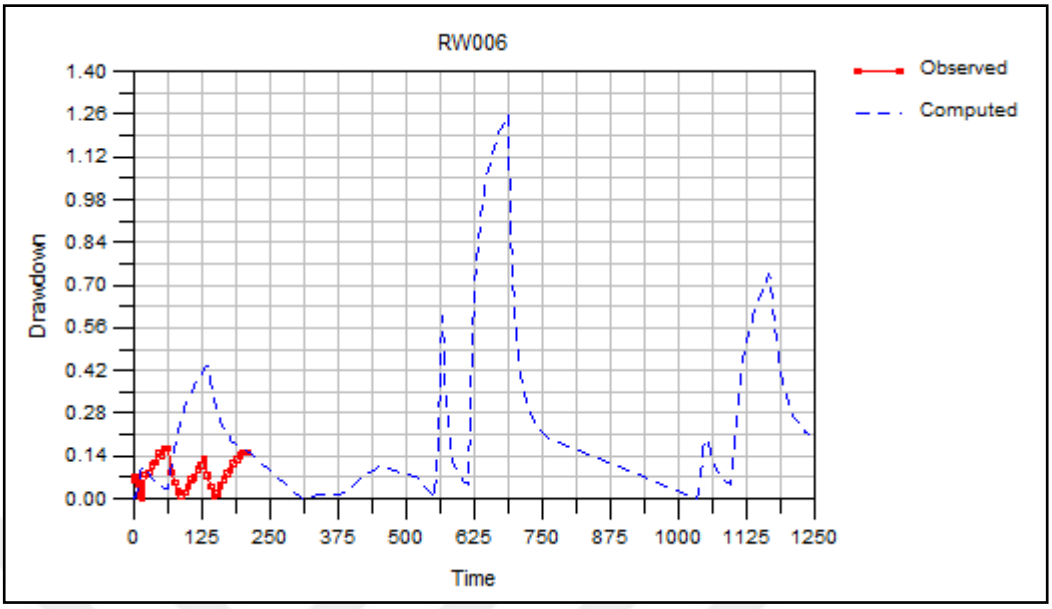

Figure 0.11. Observed vs Computed drawdown plot of RW006.

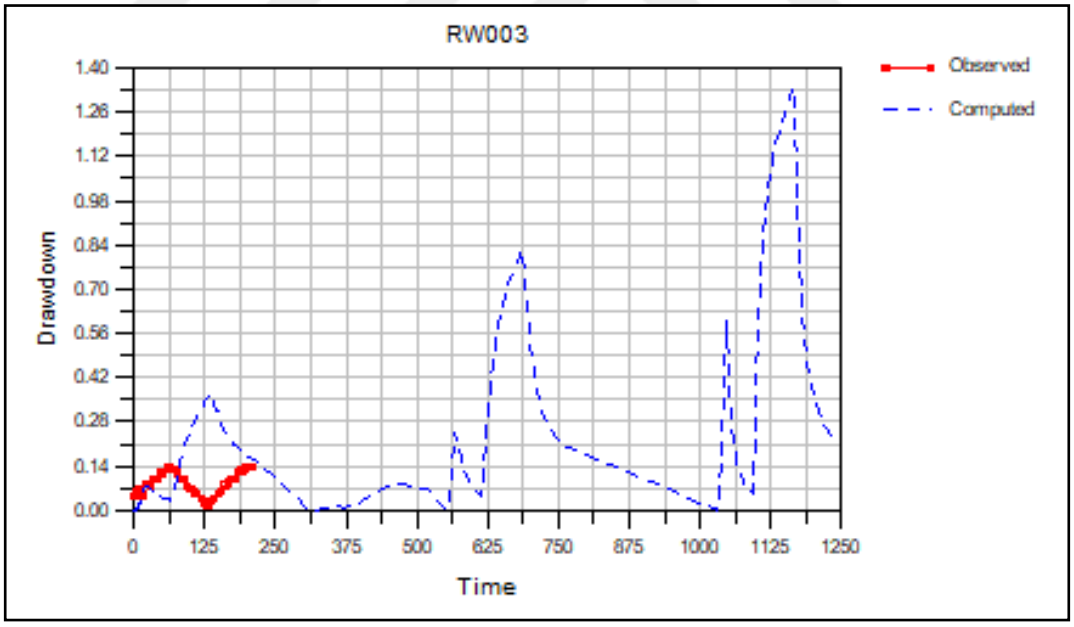

Figure 0.12. Observed vs Computed drawdown plot of RW003.

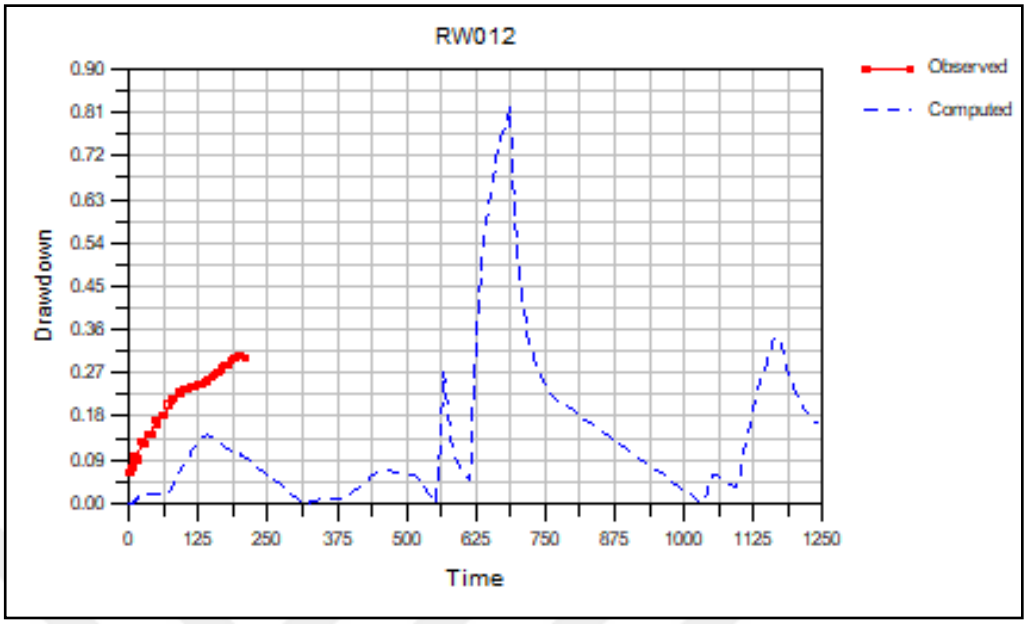

Figure 0.13. Observed vs Computed drawdown plot of RW012.

Appendix B. Observation Wells of RW103

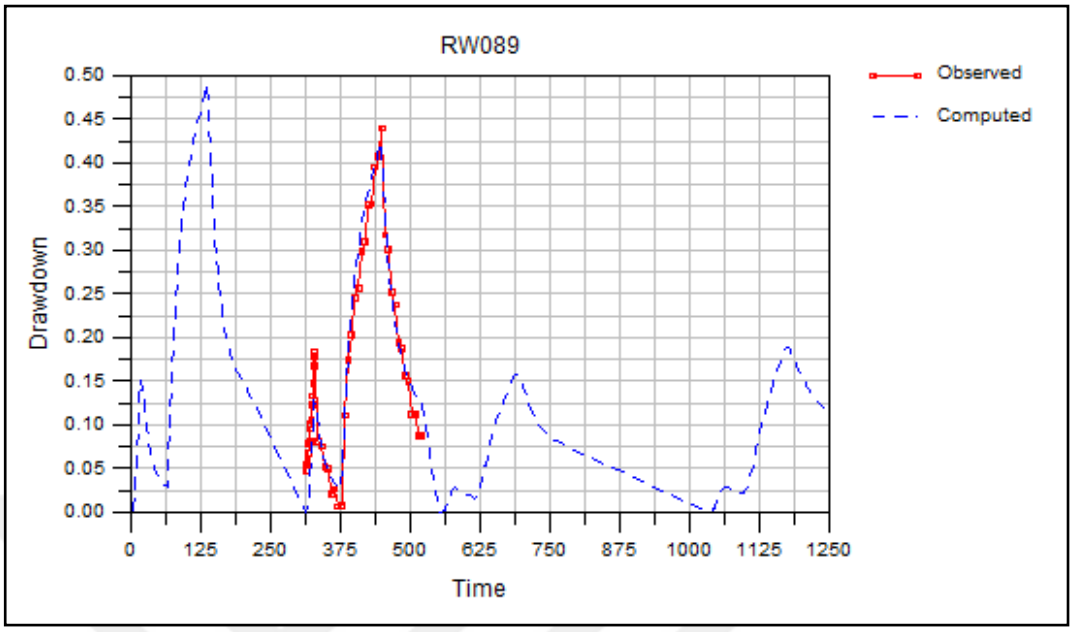

Figure 0.14. Observed vs Computed drawdown plot of RW089.

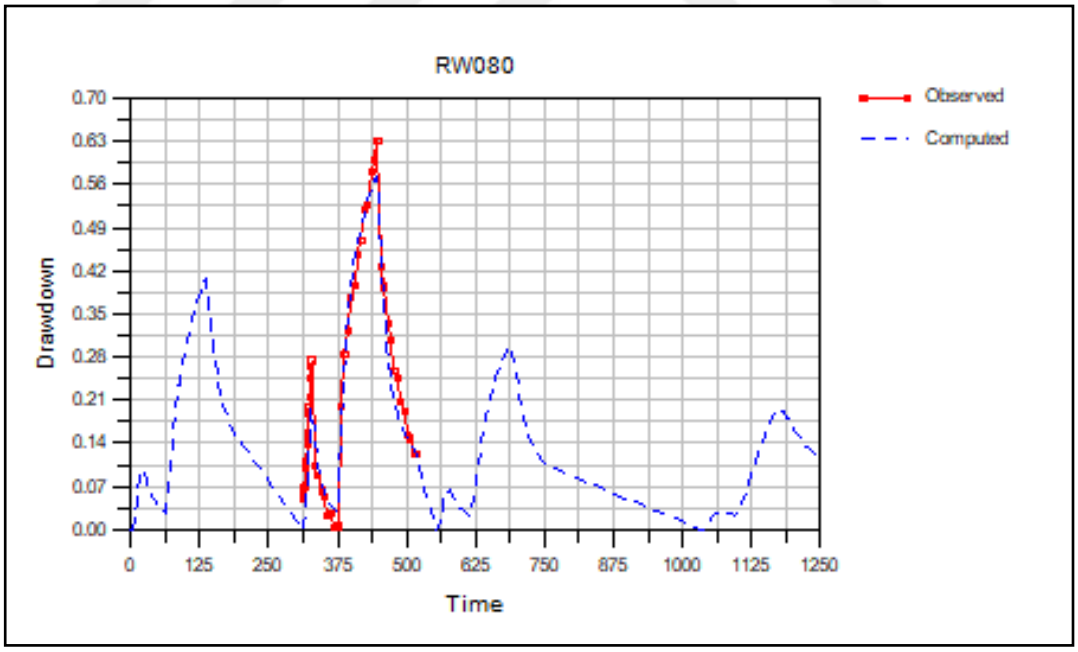

Figure 0.15. Observed vs Computed drawdown plot of RW080.

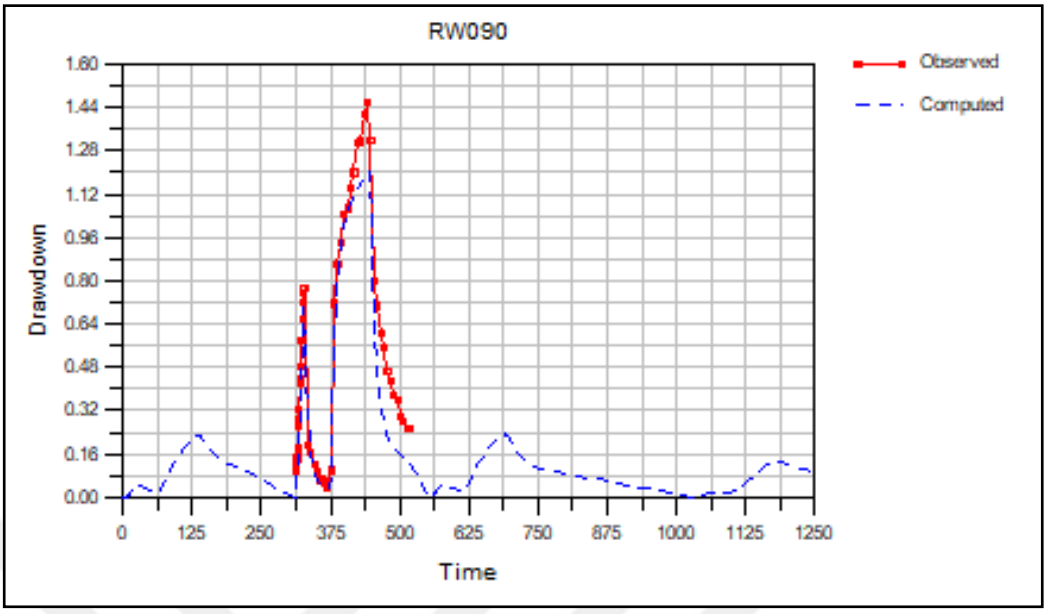

Figure 0.16. Observed vs Computed drawdown plot of RW090.

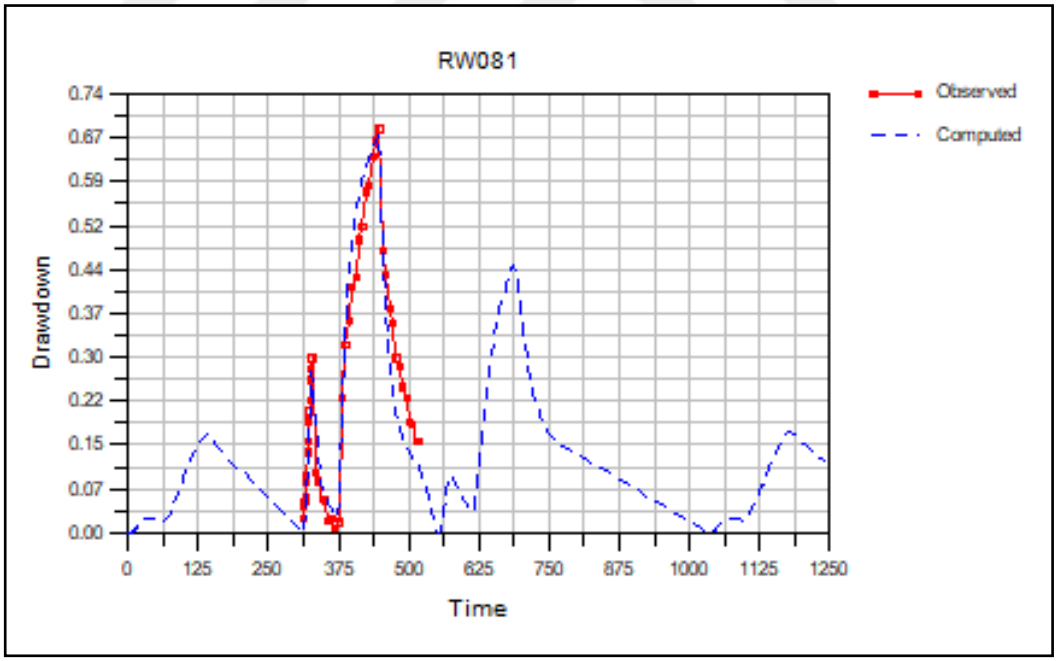

Figure 0.17. Observed vs Computed drawdown plot of RW081.

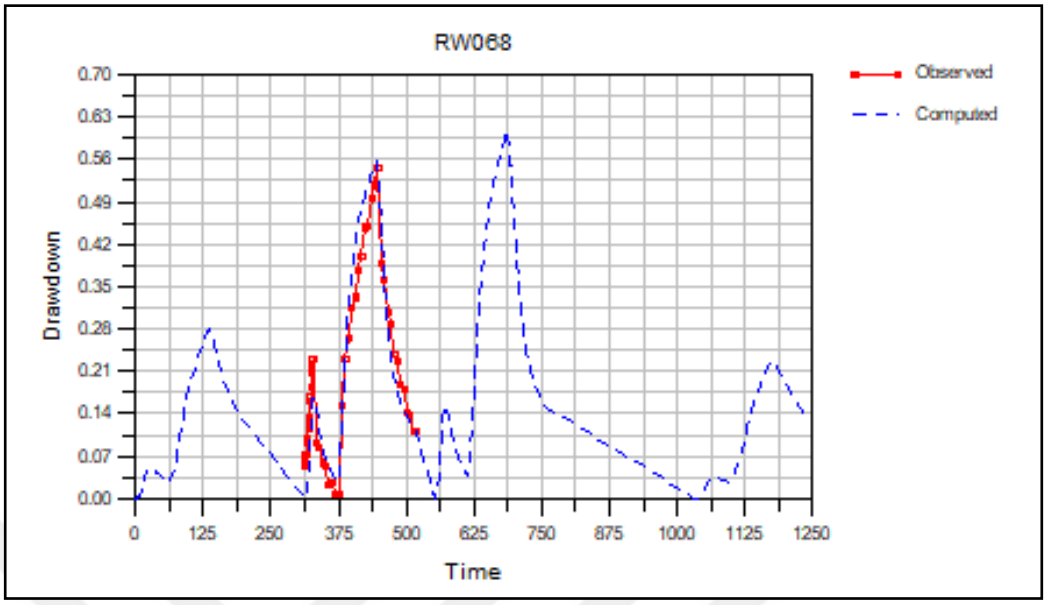

Figure 0.18. Observed vs Computed drawdown plot of RW068.

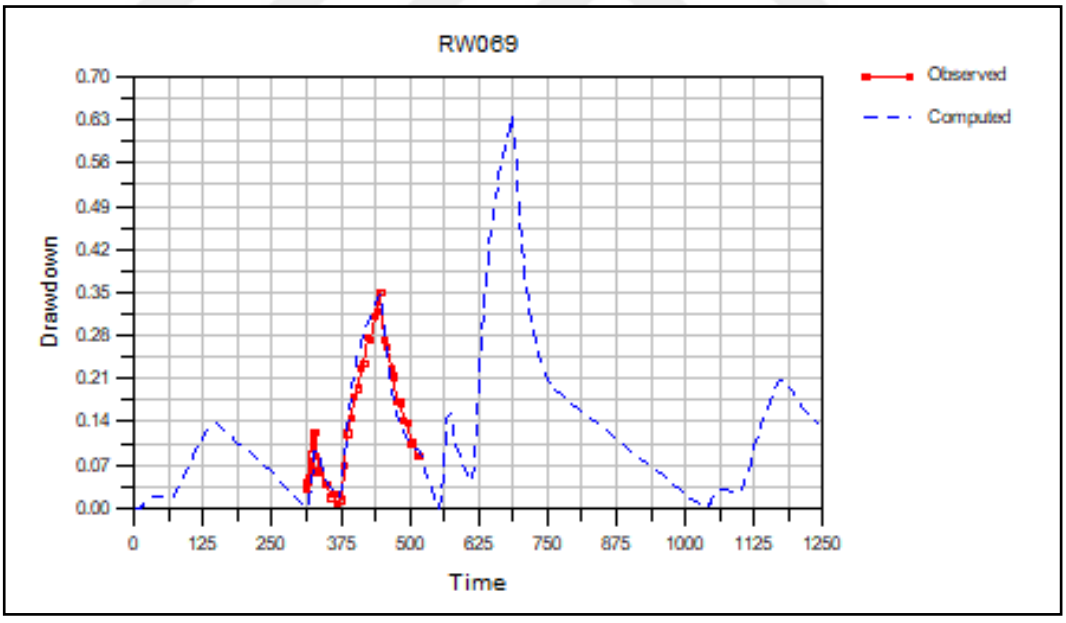

Figure 0.19. Observed vs Computed drawdown plot of RW069.

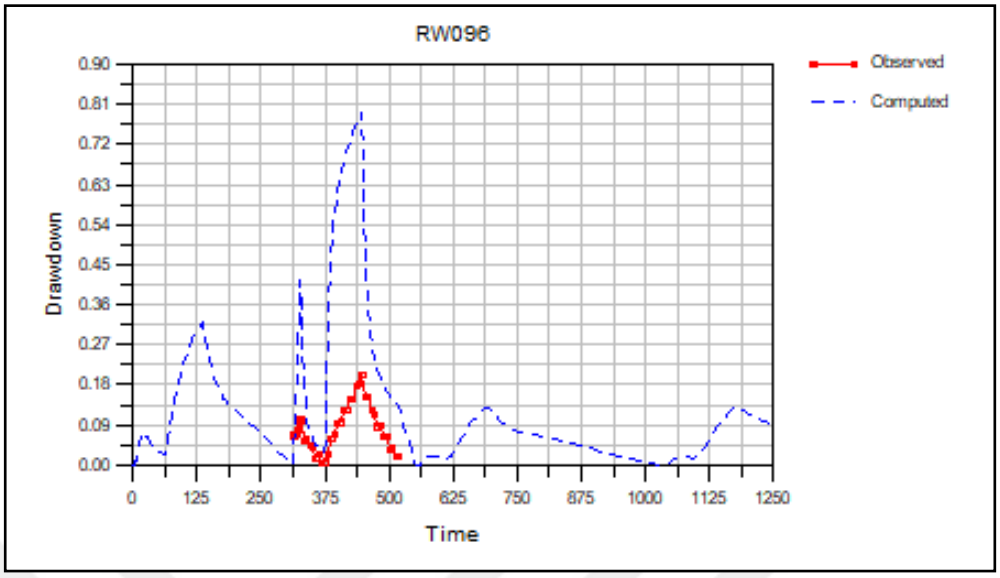

Figure 0.20. Observed vs Computed drawdown plot of RW096.

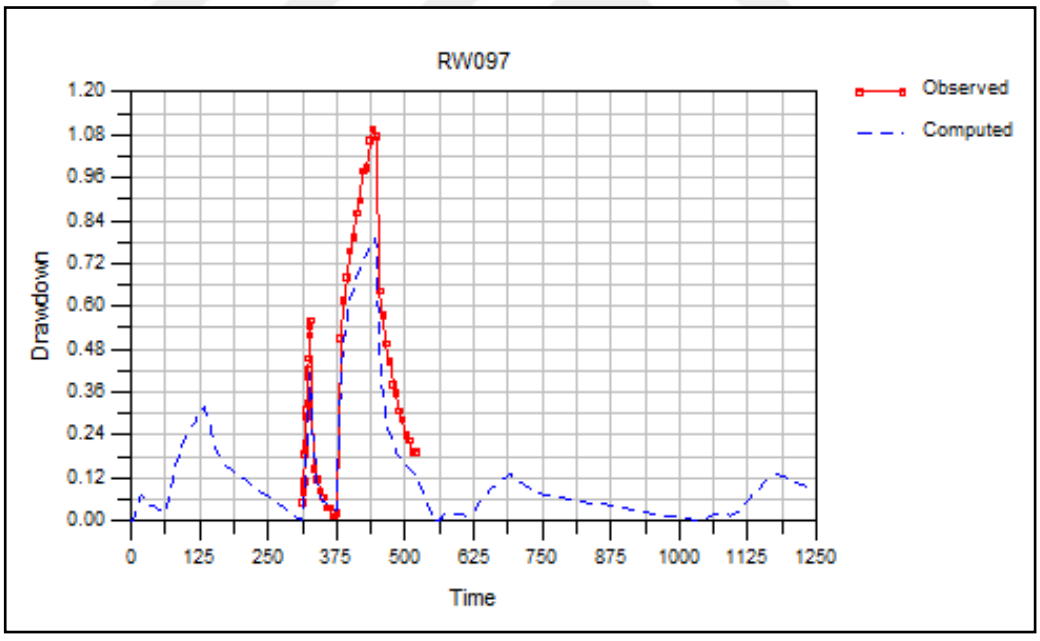

Figure 0.21. Observed vs Computed drawdown plot of RW097.

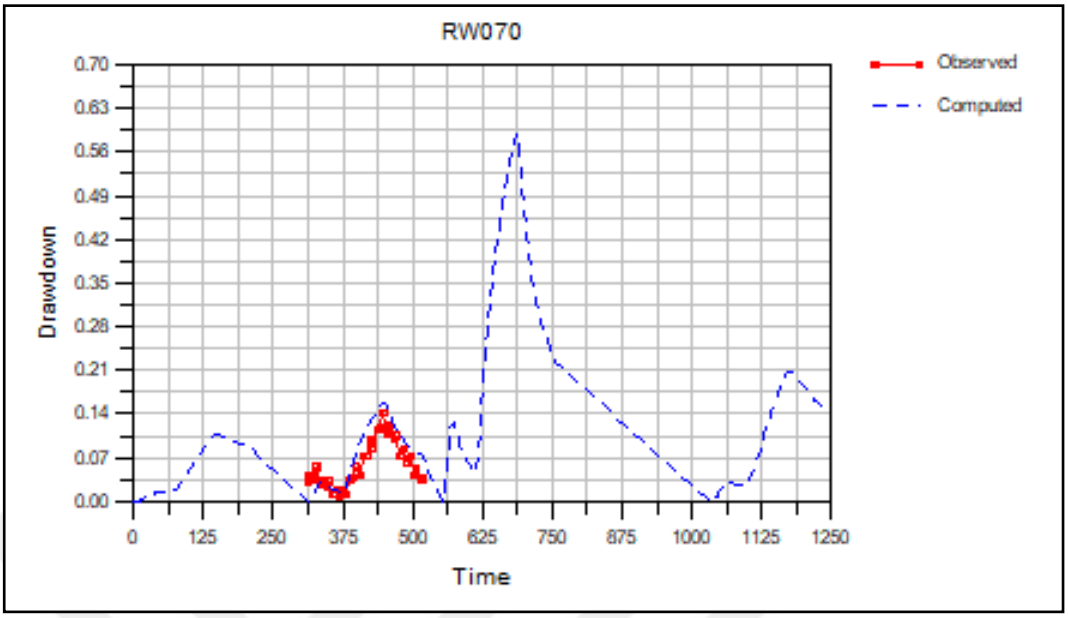

Figure 0.22. Observed vs Computed drawdown plot of RW070.

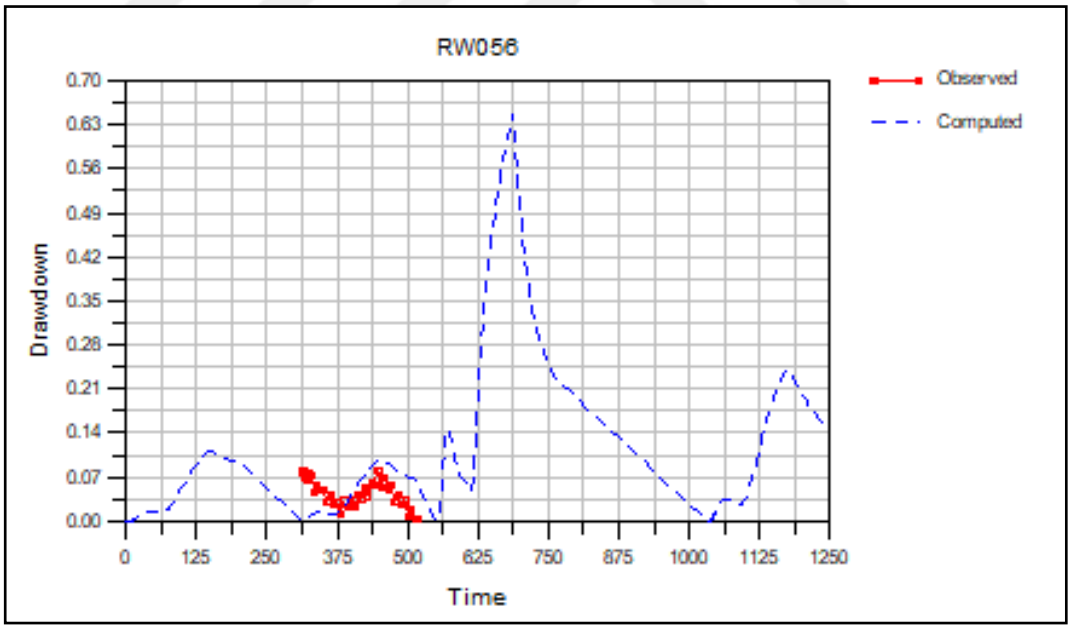

Figure 0.23. Observed vs Computed drawdown plot of RW056.

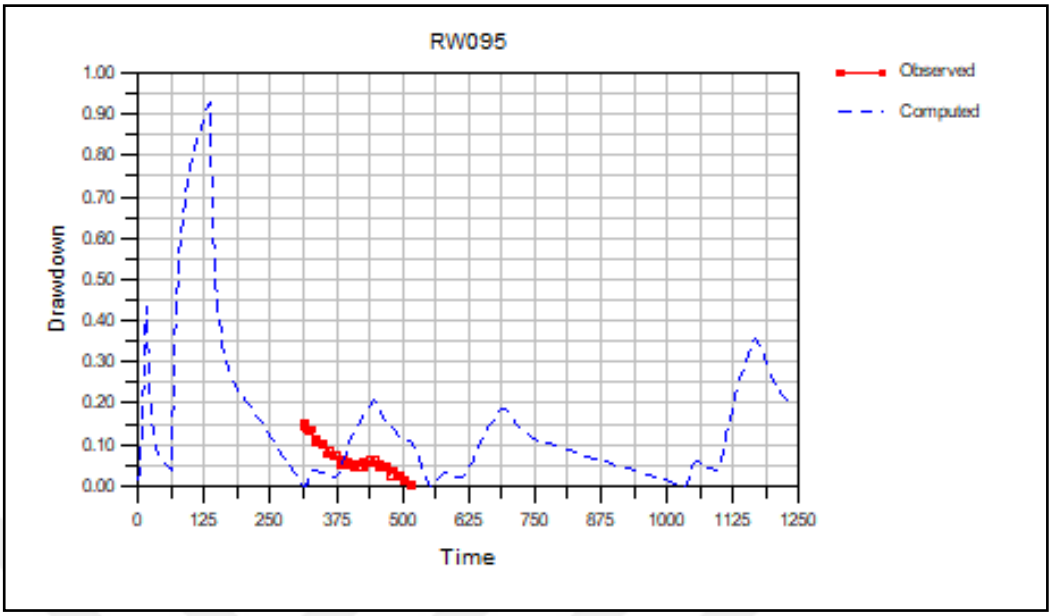

Figure 0.24. Observed vs Computed drawdown plot of RW095.

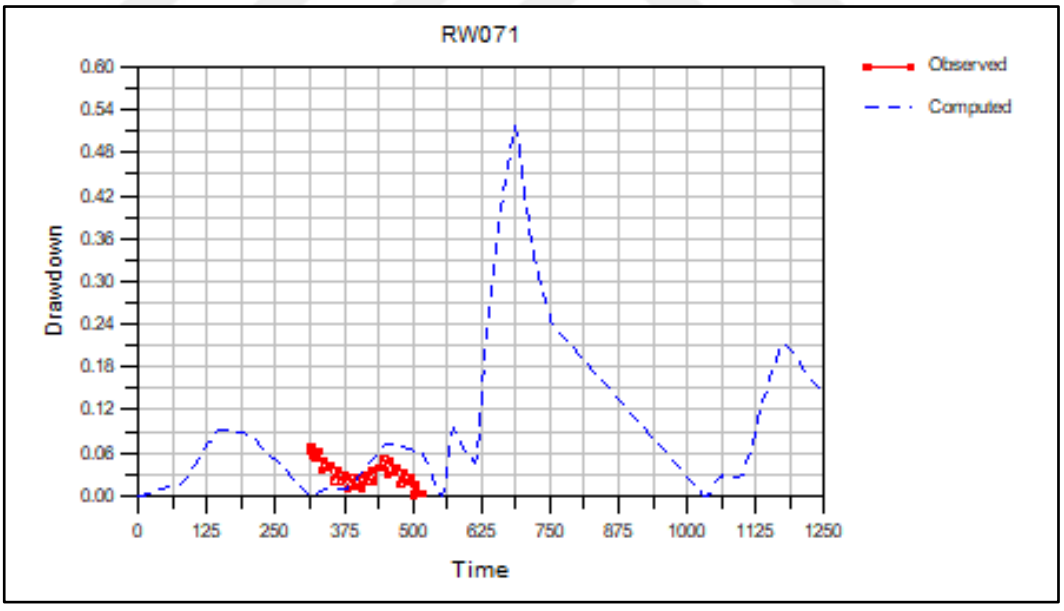

Figure 0.25. Observed vs Computed drawdown plot of RW071.

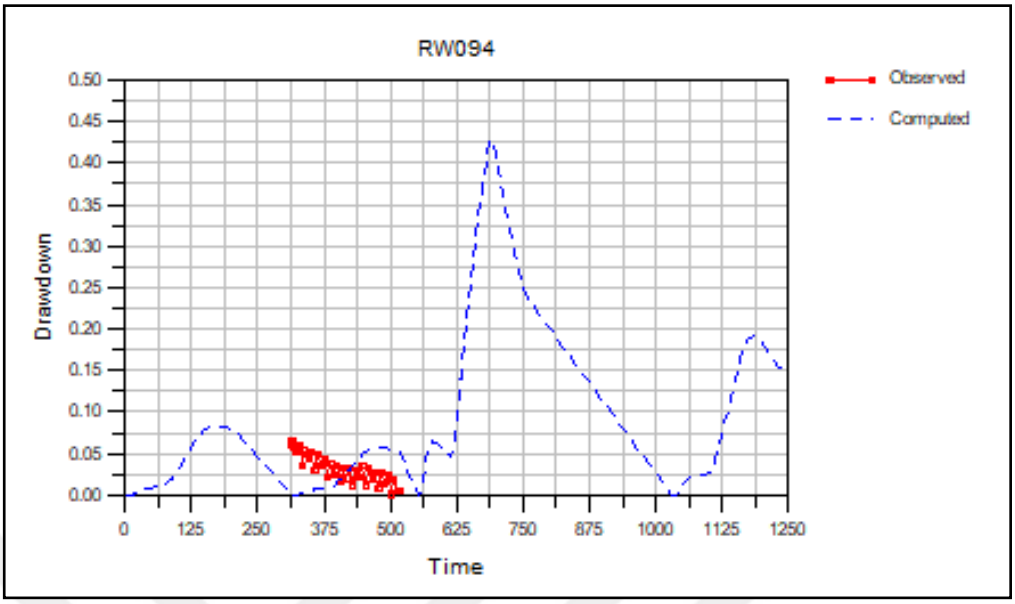

Figure 0.26. Observed vs Computed drawdown plot of RW094.

Appendix C. Observation Wells of RW008

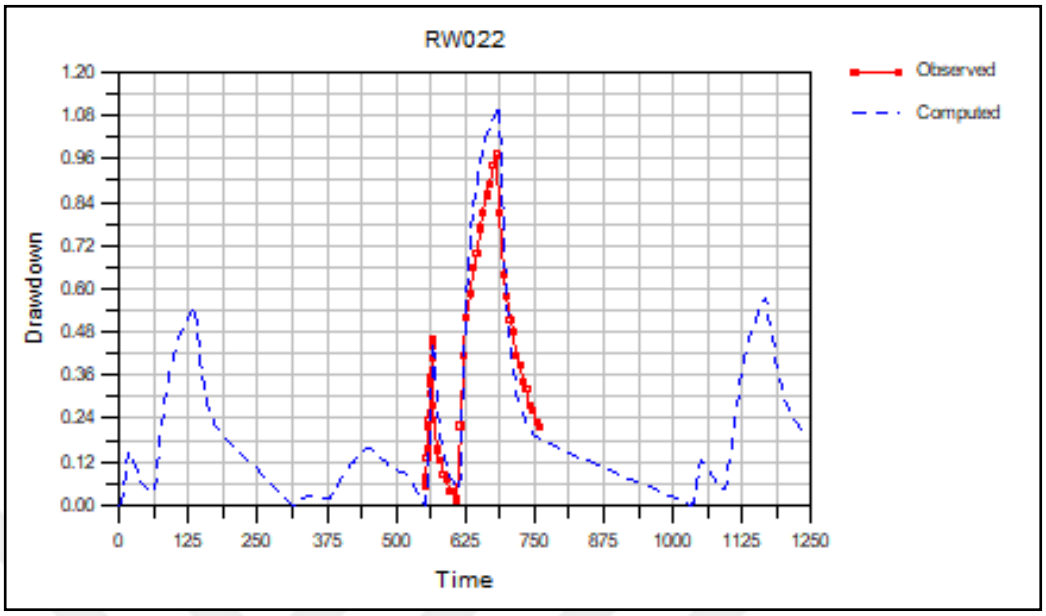

Figure 0.27. Observed vs Computed drawdown plot of RW022.

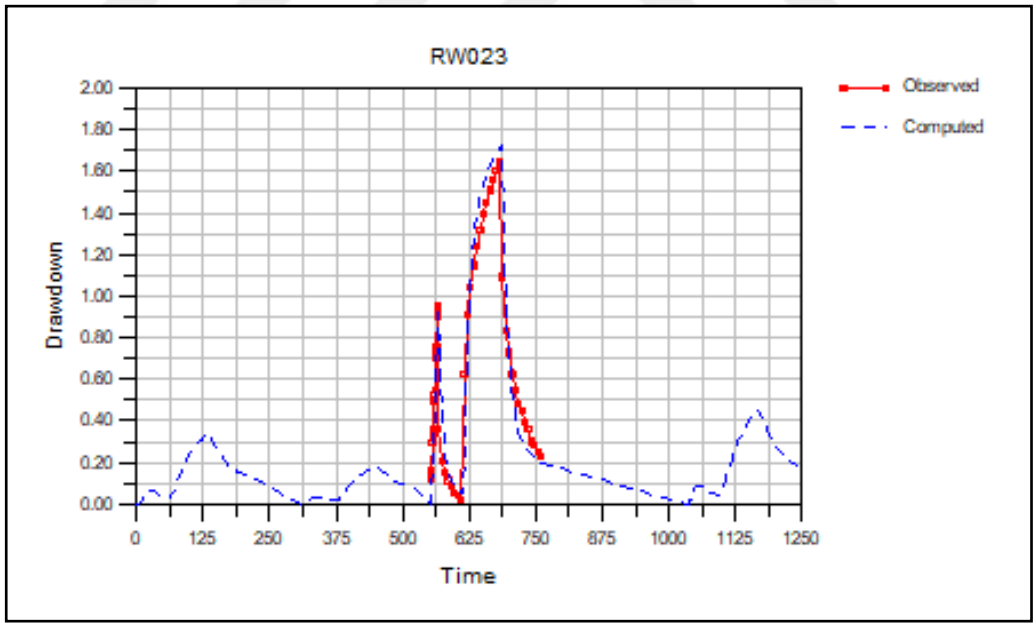

Figure 0.28. Observed vs Computed drawdown plot of RW023.

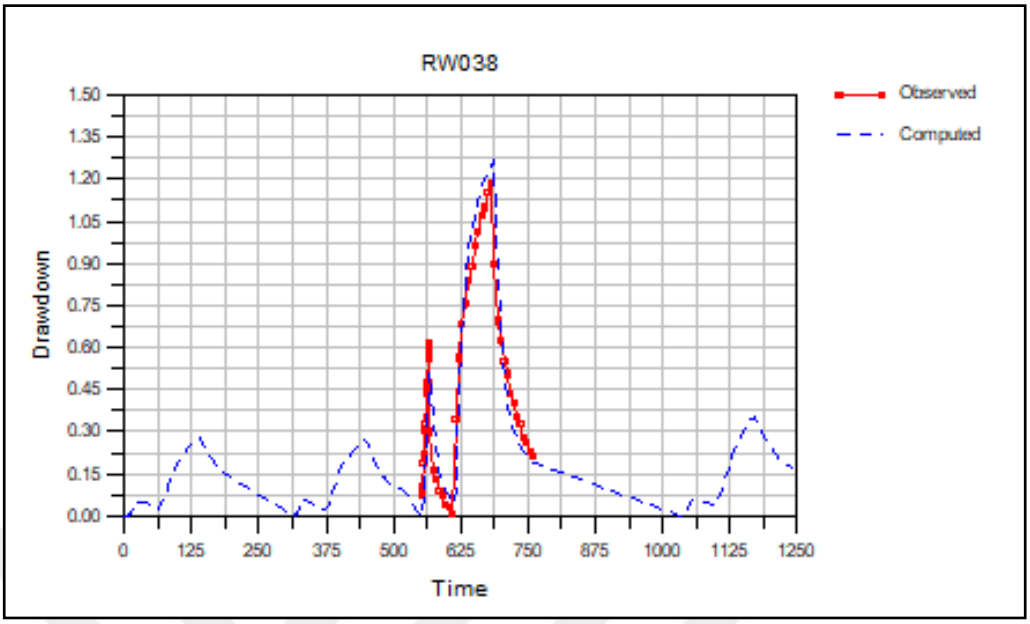

Figure 0.29. Observed vs Computed drawdown plot of RW038.

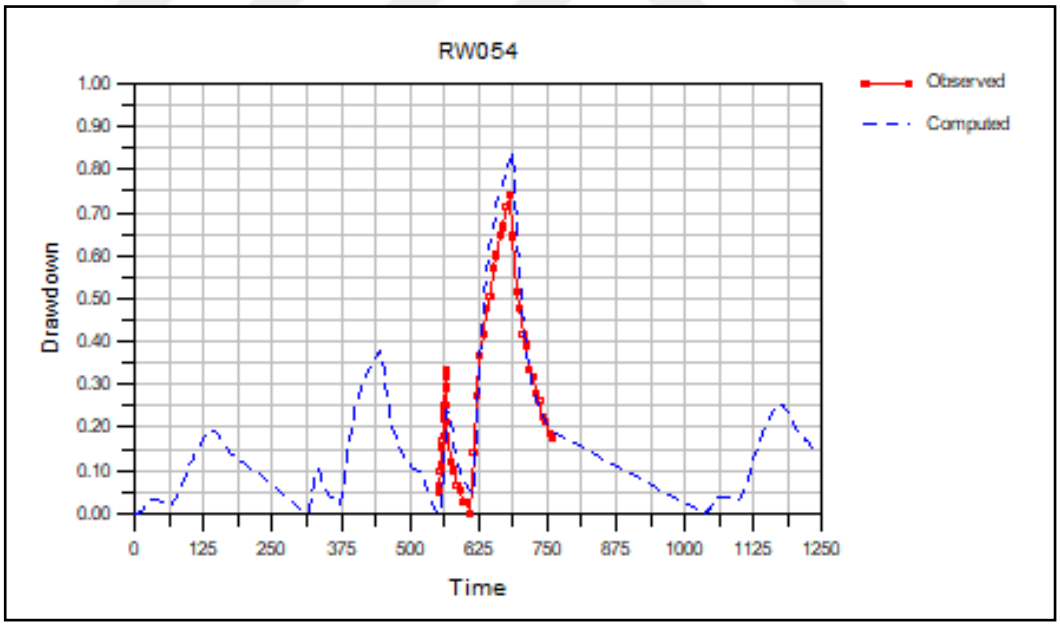

Figure 0.30. Observed vs Computed drawdown plot of RW054.

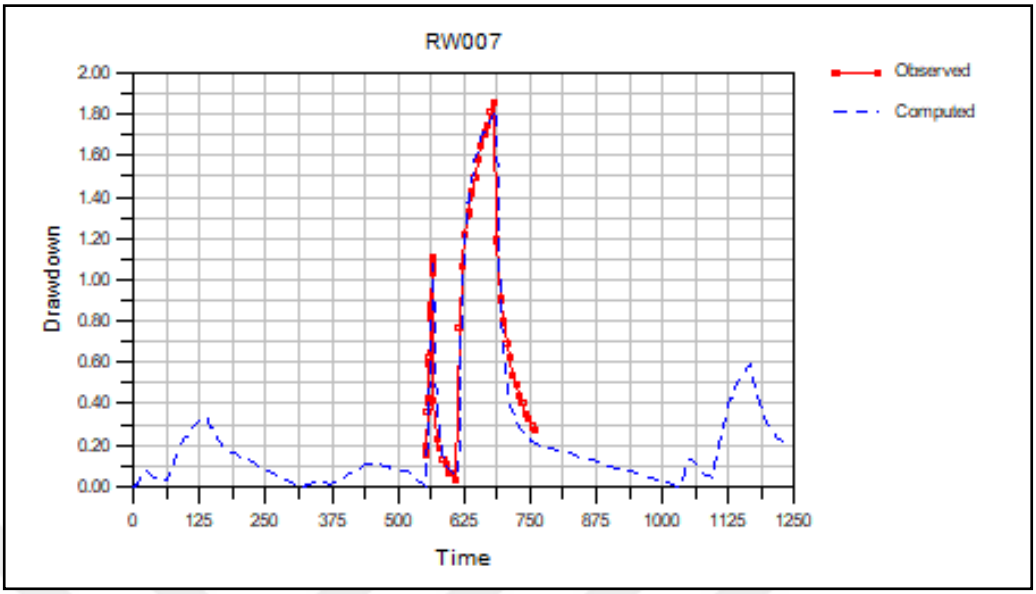

Figure 0.31. Observed vs Computed drawdown plot of RW007.

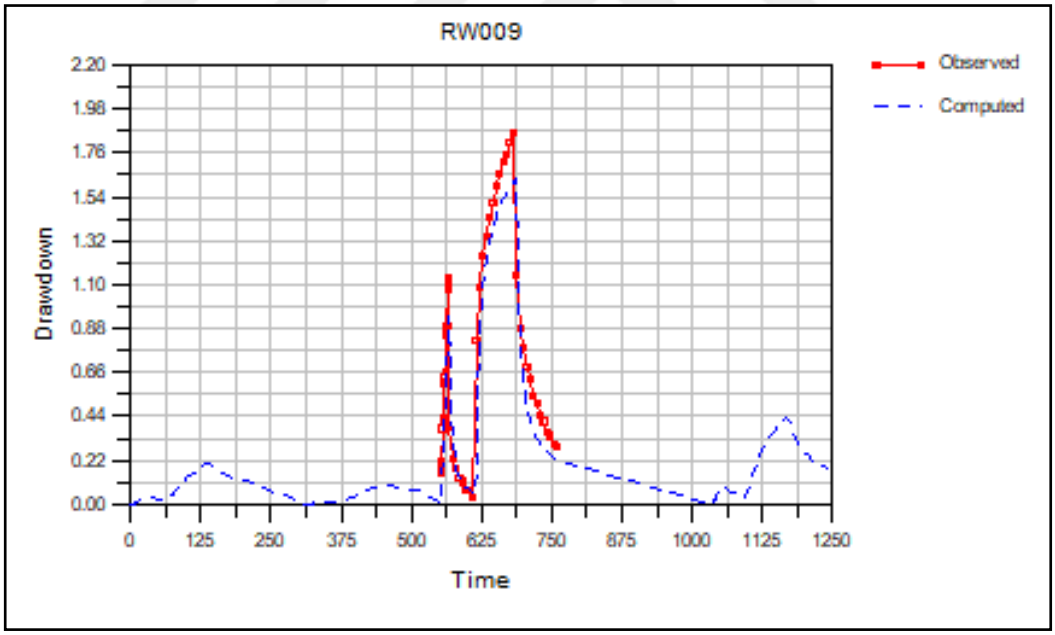

Figure 0.32. Observed vs Computed drawdown plot of RW009.

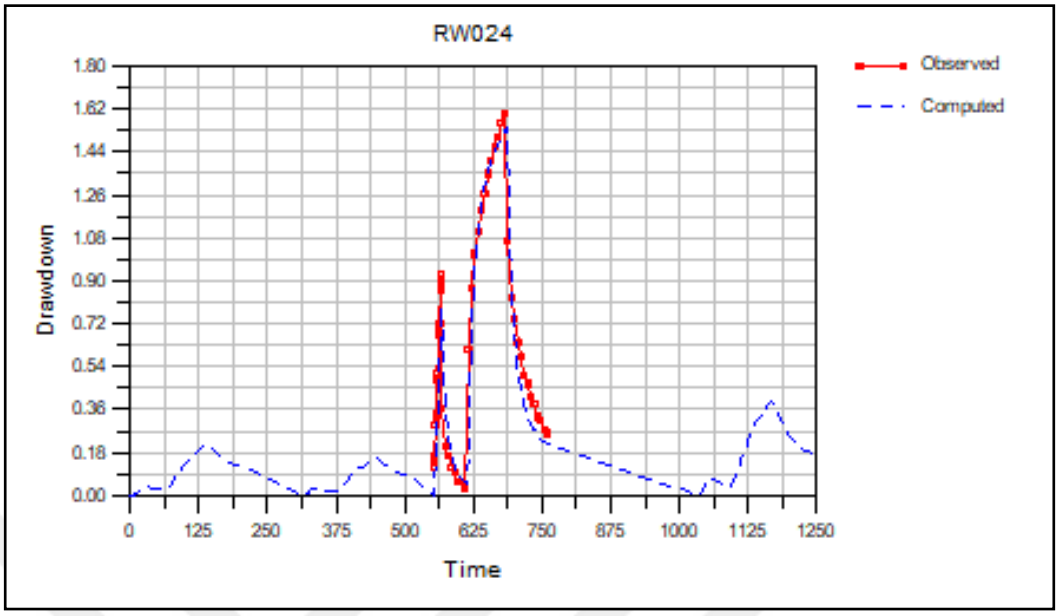

Figure 0.33. Observed vs Computed drawdown plot of RW024.

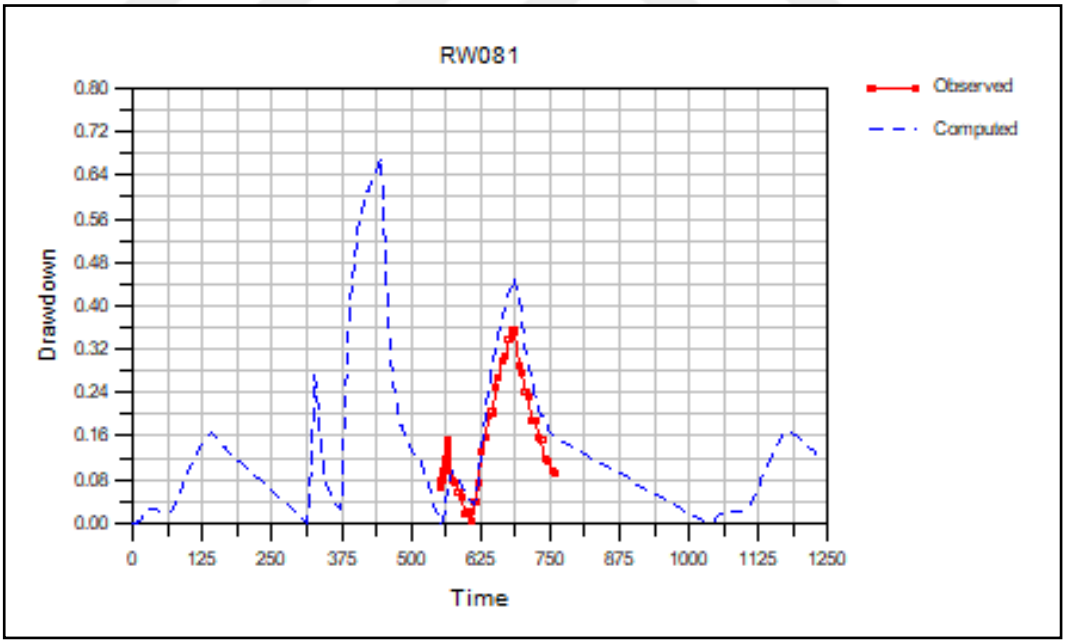

Figure 0.34. Observed vs Computed drawdown plot of RW081.

Appendix D. Observation Wells of RW033

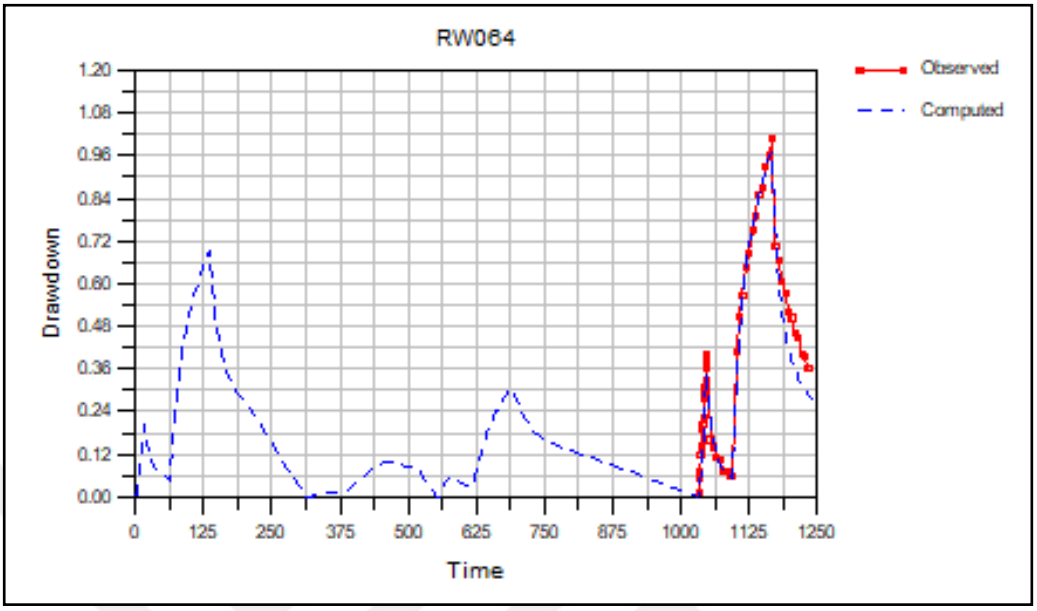

Figure 0.35. Observed vs Computed drawdown plot of RW064.

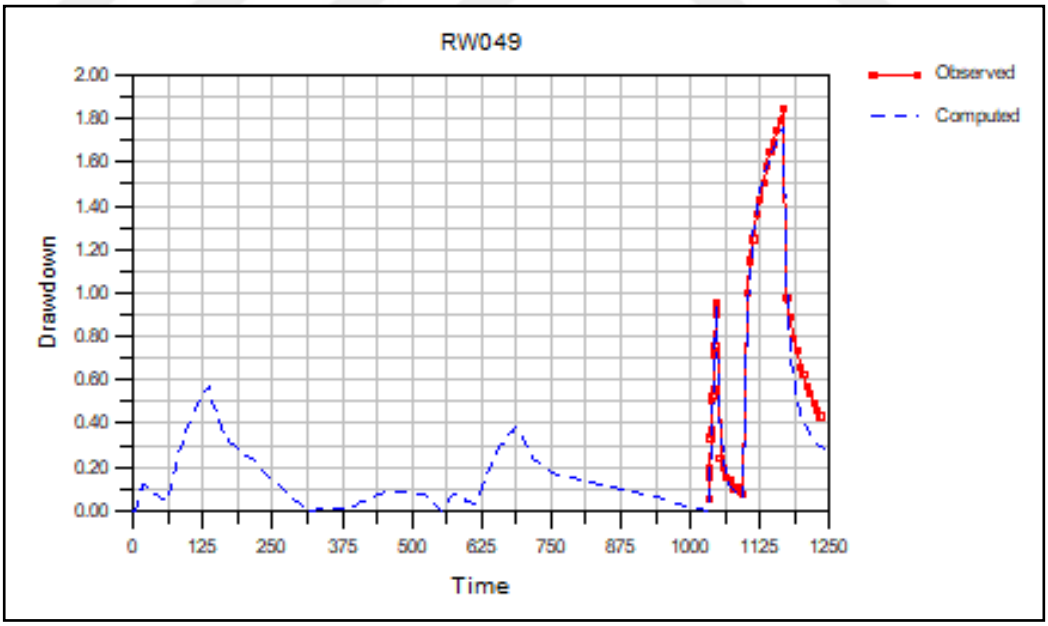

Figure 0.36. Observed vs Computed drawdown plot of RW049.

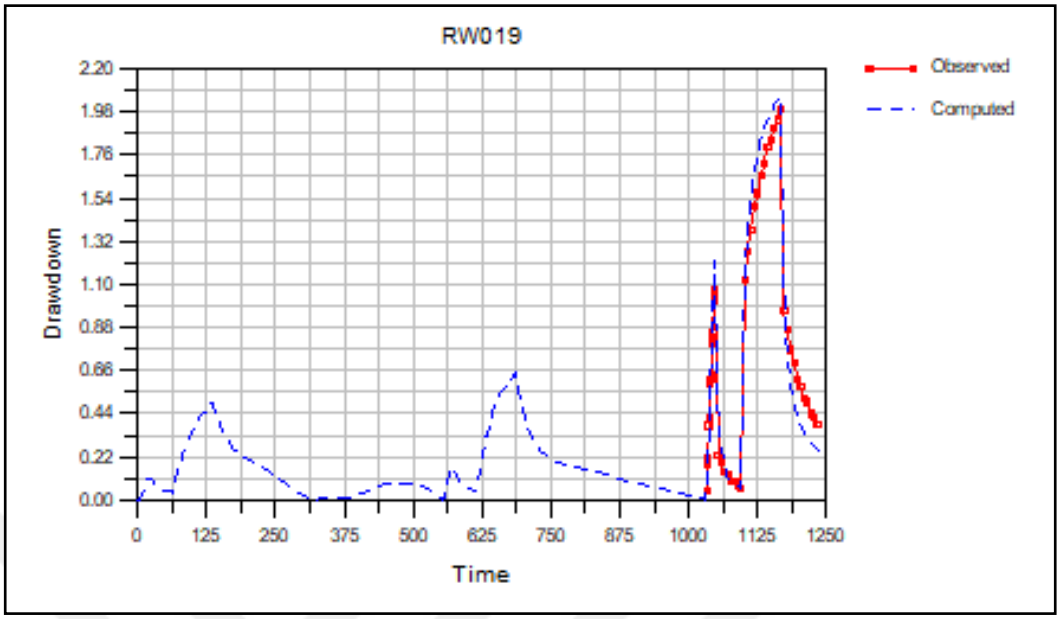

Figure 0.37. Observed vs Computed drawdown plot of RW019.

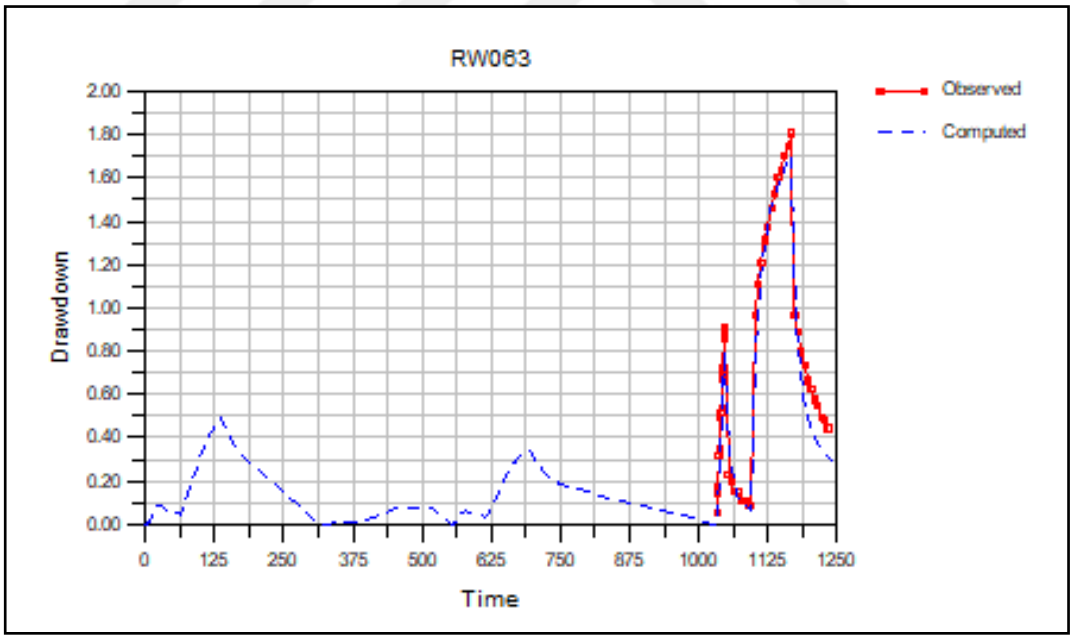

Figure 0.38. Observed vs Computed drawdown plot of RW063.

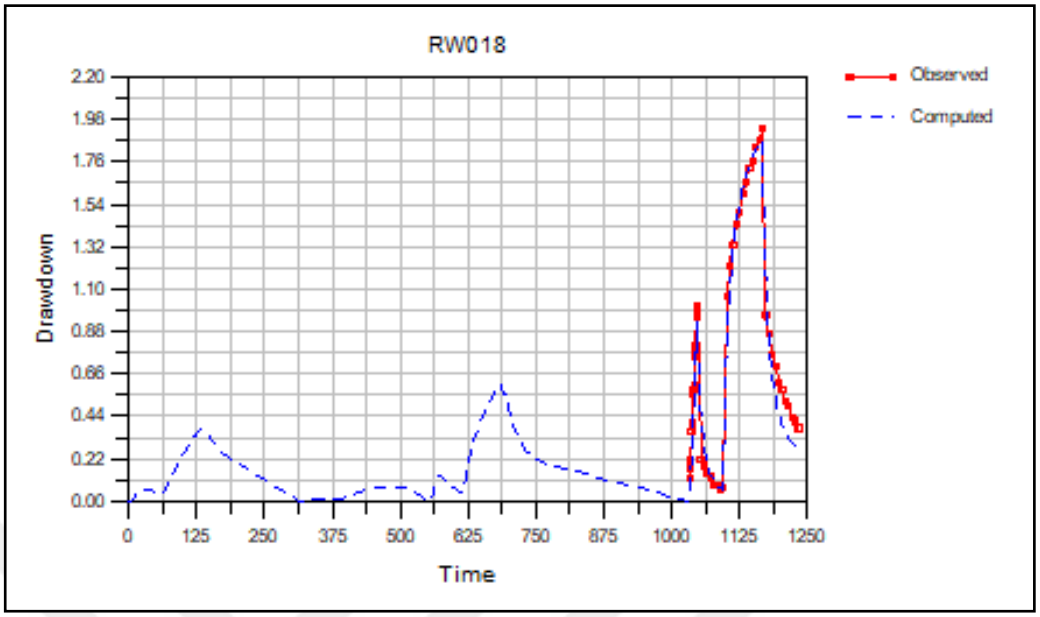

Figure 0.39. Observed vs Computed drawdown plot of RW018.

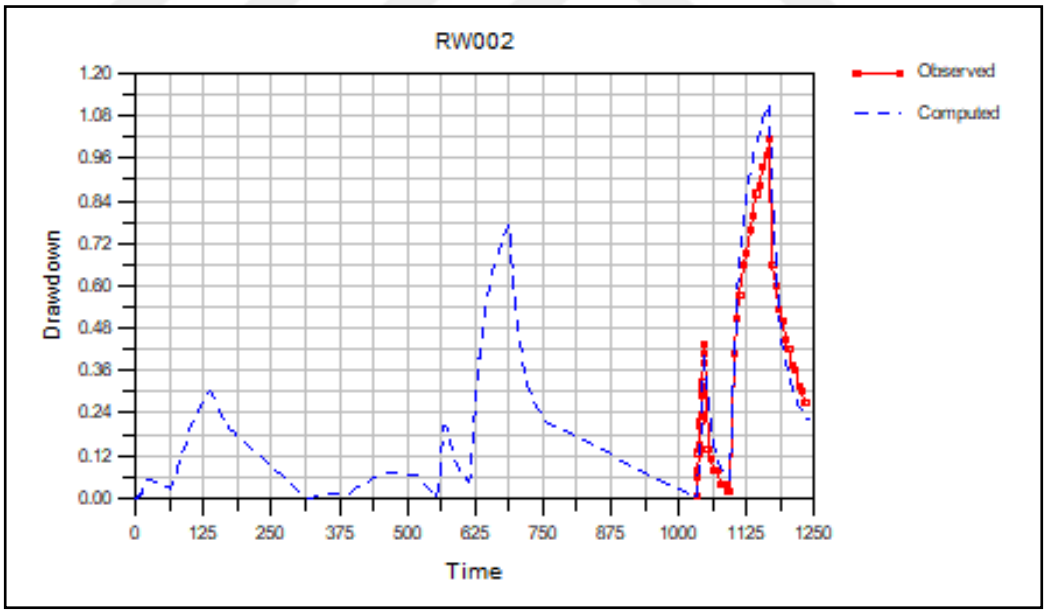

Figure 0.40. Observed vs Computed drawdown plot of RW002.

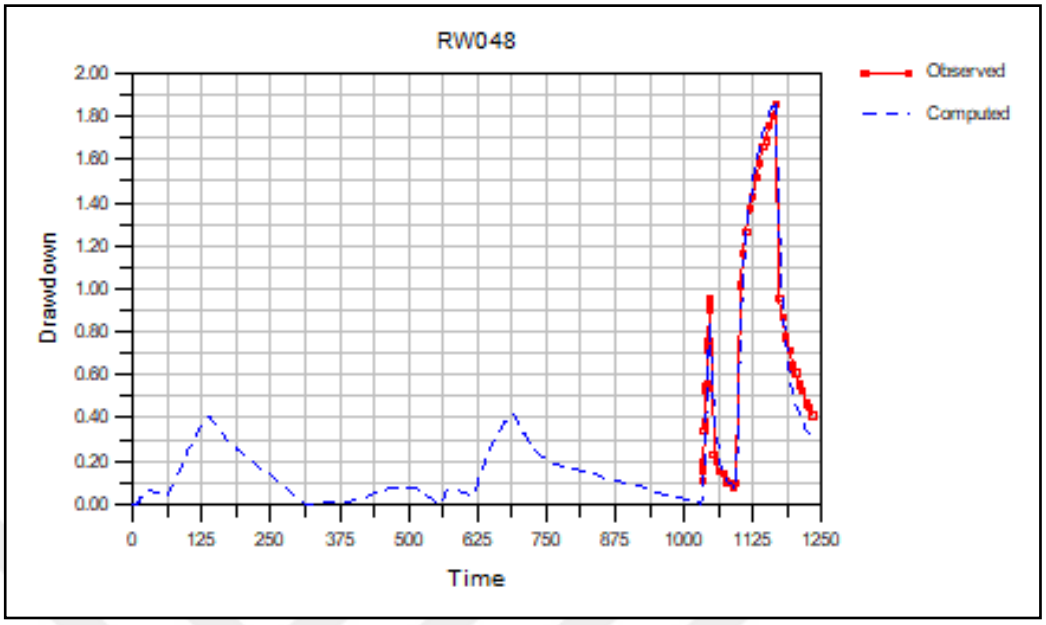

Figure 0.41. Observed vs Computed drawdown plot of RW048.

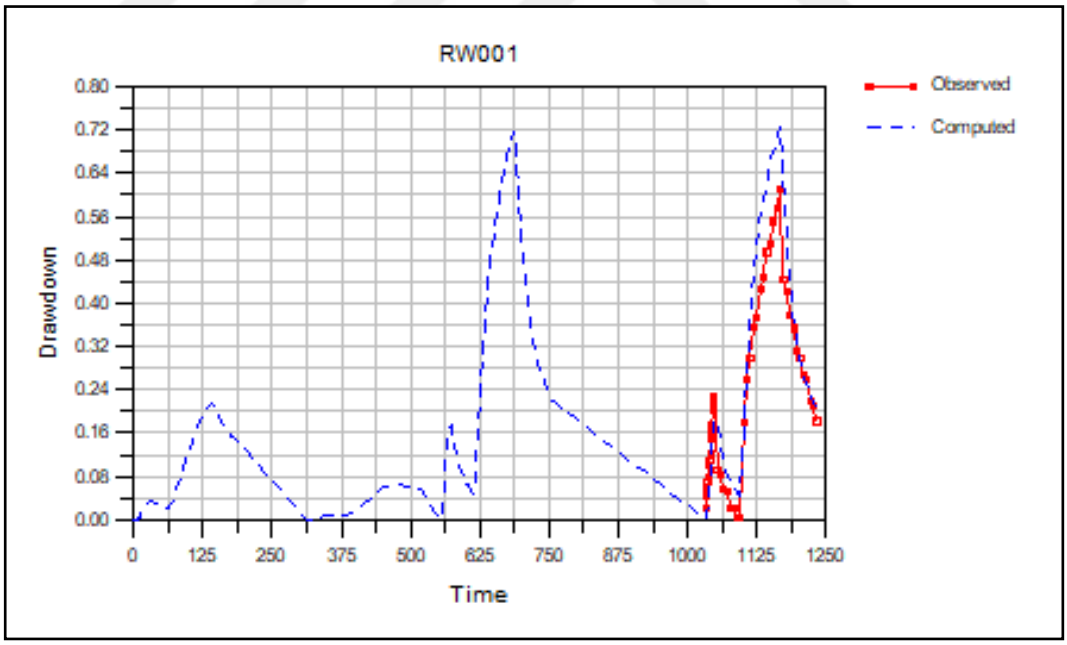

Figure 0.42. Observed vs Computed drawdown plot of RW001.

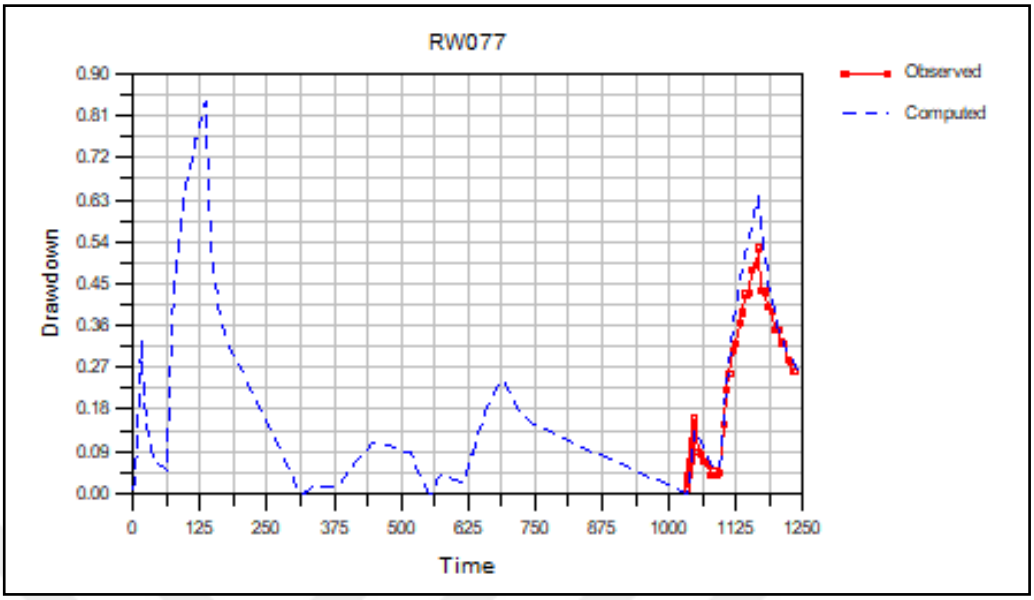

Figure 0.43. Observed vs Computed drawdown plot of RW077.

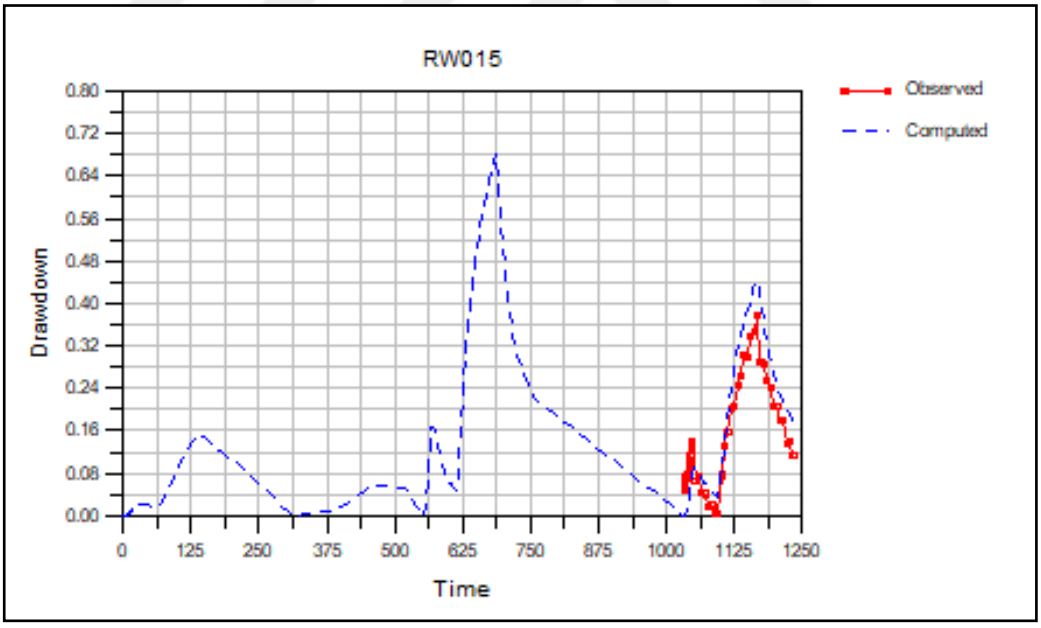

Figure 0.44. Observed vs Computed drawdown plot of RW015.

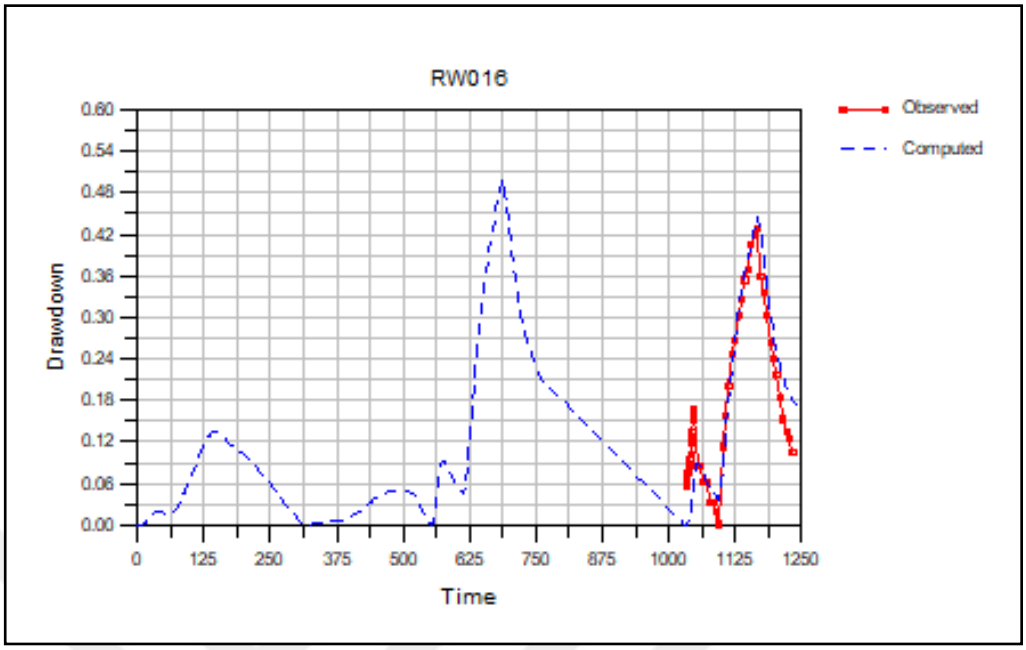

Figure 0.45. Observed vs Computed drawdown plot of RW016.

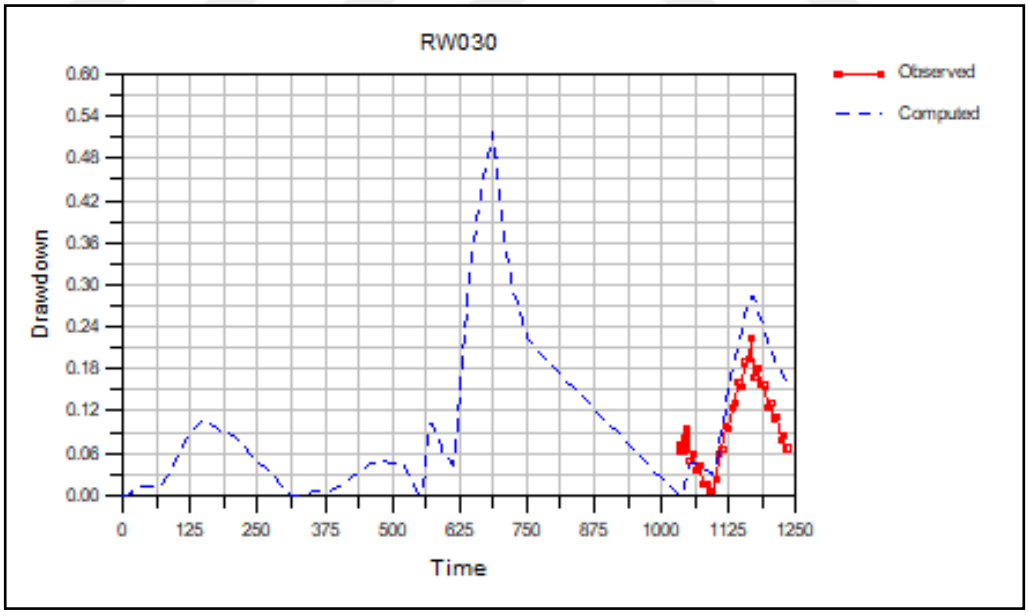

Figure 0.46. Observed vs Computed drawdown plot of RW030.

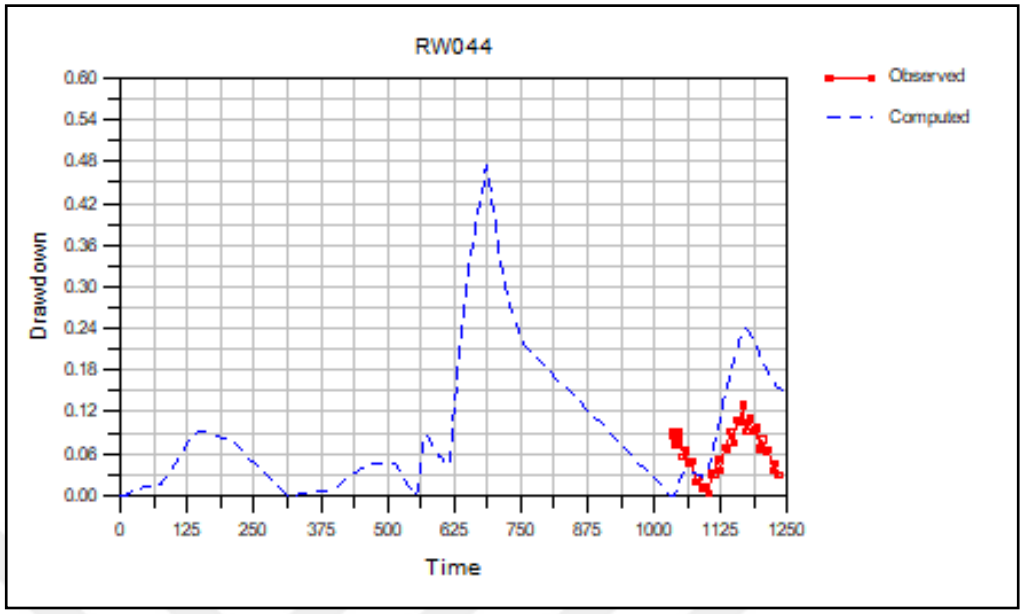

Figure 0.47. Observed vs Computed drawdown plot of RW044.

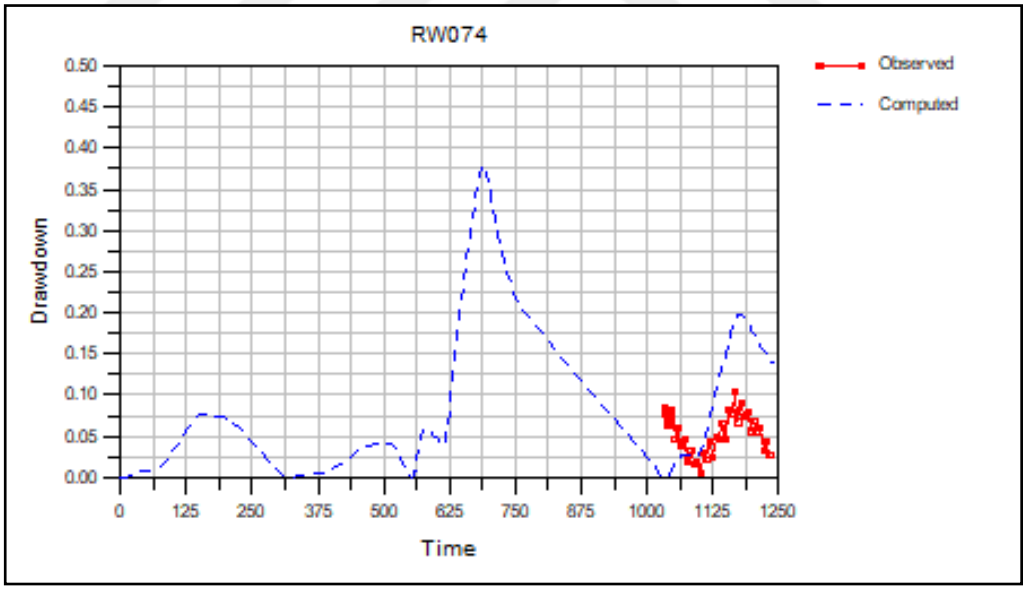

Figure 0.48. Observed vs Computed drawdown plot of RW074.

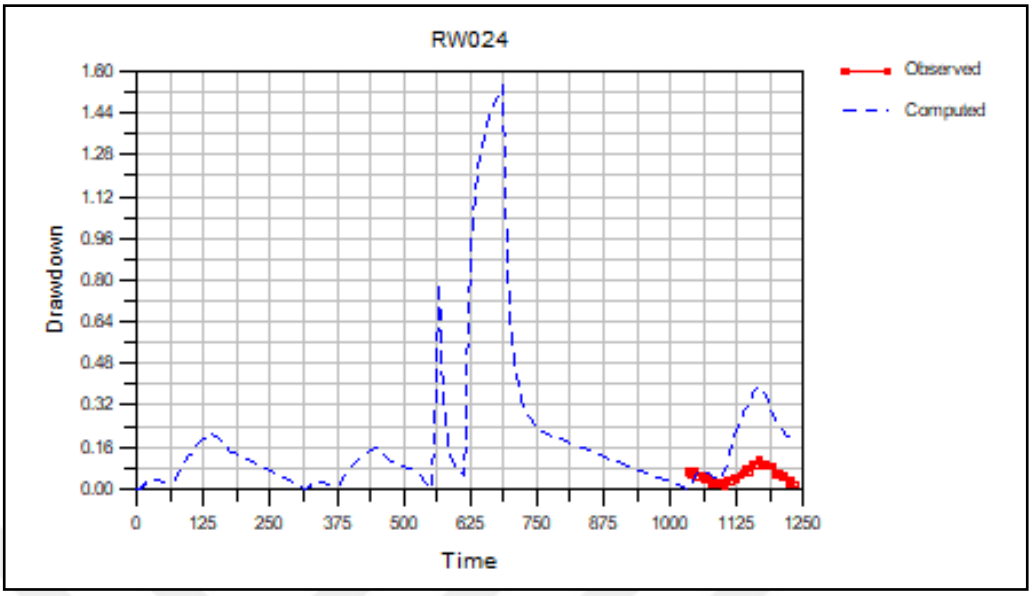

Figure 0.49. Observed vs Computed drawdown plot of RW024.

CURRICULUM VITAE

GONCA AVŞAR

21 Rue Jean Richard Bloch, Cité Marie Curie

Batiment A – 309, 86000 Poitiers, FRANCE

+33 641824507

gonca.avsar@etu.univ-poitiers.fr

EDUCATION

2016 – 2017: MSc. – University of Poitiers, France – Hydrogeology and Associated Transferts & Muğla Sıtkı Koçman University – Geological Engineering

2009 – 2016: B.Sc. – Middle East Technical University/METU – Geological Engineering

2004 – 2008: High School – Bornova Anatolian High School

INTERNSHIPS

2013 July – August: **Demirexport Inc., Turkey** – Worked as an intern at Mining Exploration Department; meanwhile, occupied in the workshop and the field survey. Learned geological and geotechnical well logging, how geochemical analysis and quartering method of sampling are done. Moreover, attended the field survey in Sivas and visited drilling wells for a week.

2015 July: **Güney Yıldızı Petroleum Inc., Turkey** – Worked as an intern at Petroleum Exploration Department.

PROJECTS

2015 January – May: **Middle East Technical University, Department of Geological Engineering** – *The Role of Oil and Gas Seepage in Petroleum Exploration, Case Study: Haymana, Turkey.*

FOREIGN LANGUAGES

English (Advanced)

French (Intermediate)

SCHOLARSHIPS

Embassy of France & Sıtkı Koçman Foundation Scholarship, Turkey.

COMPUTER SKILLS

MS Office (Word, Excel, Powerpoint), Groundwater Vistas (MODFLOW), GMS (MODFLOW&MT3DMS), AUTOCAD, MapInfo, Freehand, Surfer 8, HYDRUS-1D.

HOBBIES

Archeology, traveling, folk dancing, tracking, cinema, theatre.